



Search for the non-resonant production of Higgs boson pairs via gluon fusion and vector-boson fusion in the $b\bar{b}\tau^+\tau^-$ final state in proton–proton collisions at $\sqrt{s} = 13$ TeV with the ATLAS detector

The ATLAS Collaboration

A search for the non-resonant production of Higgs boson pairs in the $HH \rightarrow b\bar{b}\tau^+\tau^-$ channel is performed using 140 fb^{-1} of proton–proton collisions at a centre-of-mass energy of 13 TeV recorded by the ATLAS detector at the CERN Large Hadron Collider. The analysis strategy is optimised to probe anomalous values of the Higgs boson self-coupling modifier κ_λ and of the quartic $HHVV$ ($V = W, Z$) coupling modifier κ_{2V} . No significant excess above the expected background from Standard Model processes is observed. An observed (expected) upper limit $\mu_{HH} < 5.9$ (3.3) is set at 95% confidence-level on the Higgs boson pair production cross-section normalised to its Standard Model prediction. The coupling modifiers are constrained to an observed (expected) 95% confidence interval of $-3.1 < \kappa_\lambda < 9.0$ ($-2.5 < \kappa_\lambda < 9.3$) and $-0.5 < \kappa_{2V} < 2.7$ ($-0.2 < \kappa_{2V} < 2.4$), assuming all other Higgs boson couplings are fixed to the Standard Model prediction. The results are also interpreted in the context of effective field theories via constraints on anomalous Higgs boson couplings and Higgs boson pair production cross-sections assuming different kinematic benchmark scenarios.

Contents

1	Introduction	2
2	ATLAS detector	4
3	Data and simulated event samples	5
4	Event selection and categorisation	6
4.1	Preselection	7
4.2	Event categorisation	9
4.3	Multivariate discriminants	12
5	Systematic uncertainties	14
6	Results	16
7	Effective field theory interpretation	21
8	Conclusion	25

1 Introduction

After the discovery of the Higgs boson (H) in 2012 [1, 2], the ATLAS [3] and CMS [4] Collaborations at the Large Hadron Collider [5] (LHC) have been focusing on the measurement of its properties [6–12]. All features probed so far for this new particle are consistent with the Standard Model (SM) predictions [13–18] for a Higgs boson with an observed mass m_H near 125 GeV [19, 20].

In this extensive measurement programme, the properties of interactions involving multiple Higgs bosons remain to be verified. In the SM, these can be characterised by the trilinear and quartic self-couplings λ_{HHH} and λ_{HHHH} , which are both equal to the coefficient λ of the quartic term of the Higgs field potential $V(\phi) = \mu^2|\phi|^2 + \lambda|\phi|^4$. The quartic couplings g_{HHVV} ($V = W, Z$) characterise the interactions between two Higgs bosons and two W or Z bosons, and are related in the SM to the HWW and HZZ couplings g_{HVV} through the relation $g_{HHVV} = g_{HVV}/2v$, where v is the vacuum expectation value of the Higgs field. Significant deviations from the SM predictions for these couplings would provide a strong sign of beyond the Standard Model (BSM) physics [21].

The most sensitive test of Higgs boson self-interactions comes from processes of Higgs boson pair production (HH) such as gluon fusion (ggF) and vector-boson fusion (VBF) HH production. Measuring the cross-section of these processes offers a direct probe of the values of these couplings, through their scale factors with respect to the SM predictions: $\kappa_\lambda = \lambda_{HHH}/\lambda_{HHH}^{SM}$, affecting both ggF and VBF production, and $\kappa_V = g_{HVV}/g_{HVV}^{SM}$ and $\kappa_{2V} = g_{HHVV}/g_{HHVV}^{SM}$, which only impact VBF production.

The dominant mode for HH production is ggF, with a cross-section of $\sigma_{\text{ggF}}^{\text{SM}} = 31.1_{-7.2}^{+2.1}$ fb [22–29], calculated at next-to-next-to-leading order (NNLO) including finite top-quark-mass effects for $m_H = 125$ GeV at $\sqrt{s} = 13$ TeV, resulting from the destructive interference between the leading-order (LO) Feynman diagrams shown in Figure 1. The second most common HH production mechanism at the LHC is VBF, with a total

cross-section of $\sigma_{\text{VBF}}^{\text{SM}} = 1.73 \pm 0.04$ fb [30–34] calculated at next-to-next-to-next-to-leading order (N³LO) for $m_H = 125$ GeV at $\sqrt{s} = 13$ TeV. The LO diagrams for this process are shown in Figure 2.

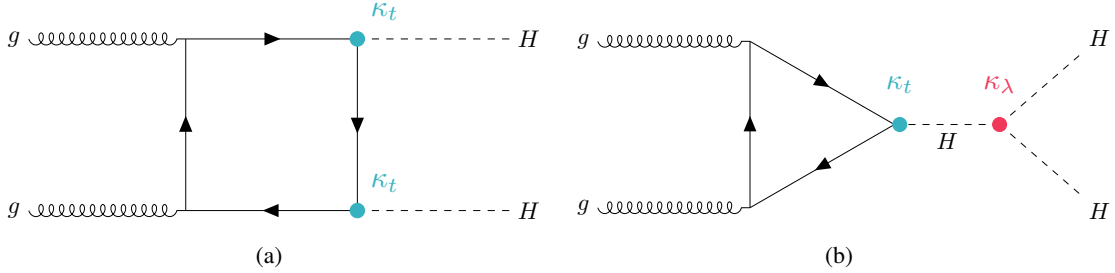


Figure 1: Leading-order Feynman diagrams of the ggF HH production process: (a) box and (b) triangle diagrams. The Higgs self-coupling modifier is shown as κ_λ , while the modifier for the coupling of the Higgs boson to the top quark is shown as κ_t .

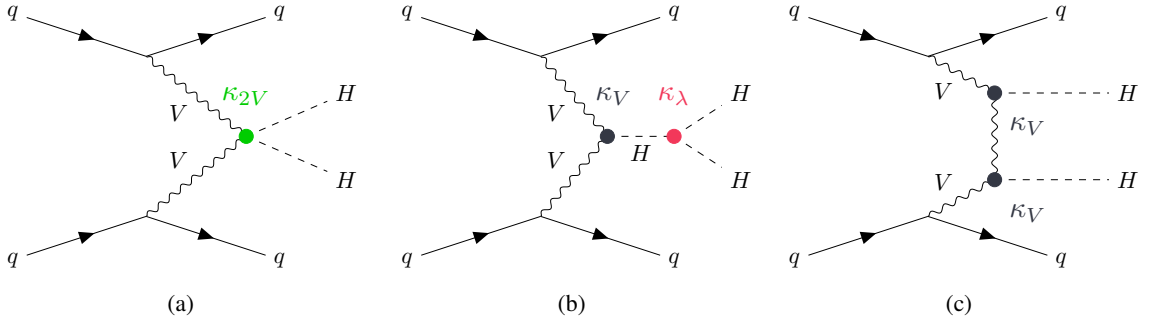


Figure 2: Leading-order Feynman diagrams of the VBF HH production process. The $g_{HHV}V$ coupling modifier is shown as κ_{2V} , the Higgs self-coupling modifier as κ_λ , and the modifier for the coupling of the Higgs boson to the SM vector bosons V as κ_V .

The most stringent constraints on SM HH production by the ATLAS Collaboration were obtained through a statistical combination [35] of the results in the $b\bar{b}\gamma\gamma$ [36], $b\bar{b}\tau^+\tau^-$ [37] and $b\bar{b}b\bar{b}$ [38] final states, exploiting the entire sample of proton–proton (pp) collisions provided by the LHC during its second phase (Run 2, 2015–2018). The 95% confidence level (CL) observed (expected) upper limit on the HH production signal strength $\mu_{HH} = (\sigma_{\text{ggF}} + \sigma_{\text{VBF}})/(\sigma_{\text{ggF}}^{\text{SM}} + \sigma_{\text{VBF}}^{\text{SM}})$ from the combination is 2.4 (2.9) with respect to the case $\mu_{HH} = 0$, which is later referred to as the *background-only hypothesis*. Using the values of the combination test statistic as a function of either κ_λ or κ_{2V} , when all other coupling modifiers are set to unity, the observed (expected with respect to the SM prediction) 95% confidence intervals (CIs) are $\kappa_\lambda \in [-0.6, 6.6]$ ($[-2.1, 7.8]$) and $\kappa_{2V} \in [0.1, 2.0]$ ($[0.0, 2.1]$). The CMS Collaboration also performed a combination of HH analyses in multiple final states, based on their full Run 2 dataset [12]. The observed (expected) 95% CL upper limit on μ_{HH} is 2.5 (3.4). The observed allowed ranges of κ_λ and κ_{2V} are restricted to $\kappa_\lambda \in [-1.24, 6.49]$ and $\kappa_{2V} \in [0.67, 1.38]$. No significant excess over the background-only hypothesis is observed by any of these analyses.

The $b\bar{b}\tau^+\tau^-$ final state captures 7.3% of all HH final states and provides a compromise between expected signal event yield and background contamination. This leads to a sensitivity similar to that of the $b\bar{b}b\bar{b}$ and $b\bar{b}\gamma\gamma$ decay modes. The latest ATLAS results for $HH \rightarrow b\bar{b}\tau^+\tau^-$ with the full LHC Run 2 dataset are documented in Ref. [37]. They result in an observed (expected) 95% CL upper limit on the total

HH production cross-section of 4.7 (3.9) times the SM prediction with respect to the background-only hypothesis. Moreover, observed (expected) 95% CIs on κ_λ and κ_{2V} are $\kappa_\lambda \in [-2.7, 9.5]$ ($[-3.1, 10.2]$) and $\kappa_{2V} \in [-0.6, 2.7]$ ($[-0.5, 2.7]$), respectively [35]. Recent results from the CMS Collaboration [39] set an observed (expected) upper limit of 3.3 (5.2) times the SM production cross-section at 95% CL over the background-only hypothesis. Additionally, constraints are set on κ_λ and κ_{2V} with respect to the background-only hypothesis, leading to the observed (expected) 95% CL constraints $\kappa_\lambda \in [-1.7, 8.7]$ ($[-2.9, 9.8]$) and $\kappa_{2V} \in [-0.4, 2.6]$ ($[-0.6, 2.8]$).

In this paper, an updated search for non-resonant Higgs boson pair production in the $b\bar{b}\tau^+\tau^-$ final state with the full Run 2 ATLAS dataset is presented, superseding and expanding upon the non-resonant results of Ref. [37]. Compared with the previous publication, the overall object identification, trigger strategy and event selection in the signal-enriched regions is unchanged, but an optimised classification of the selected events is implemented to enhance the sensitivity to κ_λ and to the VBF production mode. Improved multivariate classifiers are used to exploit the kinematic features of SM VBF HH production to define a dedicated VBF category, which improves the sensitivity to anomalous values of the coupling modifiers κ_λ and κ_{2V} . Updated Monte Carlo (MC) predictions are used for describing the main backgrounds of top-quark pair production ($t\bar{t}$) and Z boson production in association with heavy-flavour quarks, leading to a more accurate modelling of these processes and enhancing the statistical power of the simulation. The event selection for the auxiliary measurement of the background from Z boson production in association with heavy-flavour quarks is adapted to improve the consistency of the kinematic properties of this process with the signal-enriched regions. Finally, the obtained results are reinterpreted in the context of effective field theories (EFTs). These changes in analysis set-up and strategy lead to an improvement of the expected 95% CL limit on μ_{HH} of 15%. The widths of the 95% CIs on κ_λ and κ_{2V} with respect to the SM expectation are reduced by 11% and 19%, respectively, compared with the analysis described in Ref. [37].

This paper is organised as follows. Section 2 describes the ATLAS detector. The collected dataset and the simulated event samples are covered in Section 3. The event selection and categorisation, along with the description of the multivariate classifiers, are described in Section 4. Section 5 lists the systematic uncertainties. Finally, Section 6 summarises the results, Section 7 covers the conducted EFT interpretations, and the study is concluded in Section 8.

2 ATLAS detector

The ATLAS experiment at the LHC is a multipurpose particle detector with a forward–backward symmetric cylindrical geometry and a near 4π coverage in solid angle.¹ It consists of an inner tracking detector surrounded by a thin superconducting solenoid providing a 2 T axial magnetic field, electromagnetic and hadron calorimeters, and a muon spectrometer. The inner tracking detector covers the pseudorapidity range $|\eta| < 2.5$. It consists of silicon pixel, silicon microstrip, and transition radiation tracking detectors. Lead/liquid-argon (LAr) sampling calorimeters provide electromagnetic (EM) energy measurements with high granularity. A steel/scintillator-tile hadron calorimeter covers the central pseudorapidity range ($|\eta| < 1.7$). The endcap and forward regions are instrumented with LAr calorimeters for both the EM and hadronic energy measurements up to $|\eta| = 4.9$. The muon spectrometer surrounds the calorimeters and is

¹ ATLAS uses a right-handed coordinate system with its origin at the nominal interaction point (IP) in the centre of the detector and the z -axis along the beam pipe. The x -axis points from the IP to the centre of the LHC ring, and the y -axis points upwards. Polar coordinates (r, ϕ) are used in the transverse plane, ϕ being the azimuthal angle around the z -axis. The pseudorapidity is defined in terms of the polar angle θ as $\eta = -\ln \tan(\theta/2)$. Angular distance is measured in units of $\Delta R \equiv \sqrt{(\Delta\eta)^2 + (\Delta\phi)^2}$.

based on three large superconducting air-core toroidal magnets with eight coils each. The field integral of the toroids ranges between 2.0 and 6.0 T m across most of the detector. The muon spectrometer includes a system of precision tracking chambers and fast detectors for triggering. A two-level trigger system is used to select events. The first-level trigger is implemented in hardware and uses a subset of the detector information to accept events at a rate below 100 kHz. This is followed by a software-based trigger that reduces the accepted event rate to 1 kHz on average depending on the data-taking conditions. An extensive software suite [40] is used in simulation, in the reconstruction and analysis of real and simulated events, in detector operations, and in the trigger and data acquisition systems of the experiment.

3 Data and simulated event samples

The search presented in this paper uses the pp collision dataset collected by the ATLAS experiment during the LHC Run 2 at a centre-of-mass energy of $\sqrt{s} = 13$ TeV. After data quality requirements [41], the integrated luminosity of the dataset is $140.1 \pm 1.2 \text{ fb}^{-1}$ [42, 43].

The samples of simulated events used for this study are summarised in Table 1, and they correspond to those already employed in the previous publication [37], with a few important updates aimed at improving the statistical power of the simulated samples for the main background processes providing a more accurate simulation of the HH signal. All generated samples are passed through a detailed simulation of the ATLAS detector response [44] based on GEANT4 [45].

The production of $t\bar{t}$ events, and of single-top-quark events in the Wt -, s - and t -channels is simulated using the POWHEG BOX v2 [46] generator together with the NNPDF3.0_{NLO} parton distribution functions (PDF) set [47]. The simulated events are interfaced to PYTHIA 8.230 [48] for parton showering and hadronisation using the A14 tune [49] together with the NNPDF2.3_{LO} [50] PDF set. The setup of the MC event generator for these production processes is unchanged with respect to Ref. [37]. For $t\bar{t}$ processes the size of the sample is increased by including two statistically independent sets of events. The first sample is simulated with the requirement of at least one top quark decaying into a leptonic final state, while in the second sample both top quarks are forced to decay leptonically. The combination of these samples results in a decrease in the statistical uncertainty related to the $t\bar{t}$ simulation by a factor of approximately two in the selected phase space compared to using only the first sample, as was done in Ref. [37].

For events containing a W or a Z boson produced in association with jets, new samples are produced with the SHERPA 2.2.11 generator [51]. Events are simulated using NLO matrix elements for up to two partons, and LO matrix elements for up to five partons calculated using the OPENLOOPS [52–55] and Comix [56] matrix-element generators. For these samples, the NNPDF3.0_{NNLO} PDF set is used with dedicated parton shower, matched to the matrix element via the MEPS@NLO prescription [57]. The electroweak input scheme is updated compared to the previous version, along with corrected heavy-flavour hadron production fractions. The SHERPA 2.2.11 generator allows faster per-event generation time, with significant reduction of the negative weight fraction. Using a sample generated with SHERPA 2.2.11 instead of the sample generated with SHERPA 2.2.1 that was used in Ref. [37] results in a reduction of the MC statistical uncertainty ranging from 30% to 60%, depending on the flavour composition of the events and the analysis region.

Diboson (WW , WZ and ZZ) and $t\bar{t}Z$ production processes are simulated with the SHERPA 2.2.1 generator, whereas the $t\bar{t}W$ production process is simulated with the SHERPA 2.2.8 generator. These samples use the NNPDF3.0_{NNLO} PDF set with dedicated parton shower tuning developed by the SHERPA authors. Single Higgs boson production is considered as part of the background in this search, and its production modes are

simulated using the POWHEG BOX v2 generator and either the PDF4LHC15_{NLO} [58] with the AZNLO [59] tune or the NNPDF3.0_{NLO} PDF sets with the A14 tune. The setup of the MC event generator for these production processes is unchanged with respect to Ref. [37].

Signal samples consist of simulated events from non-resonant ggF and VBF production of Higgs boson pairs, with one Higgs boson decaying into $b\bar{b}$ and the other one to $\tau^+\tau^-$. The simulated ggF events are generated with the POWHEG BOX v2 generator at NLO with finite top-quark mass, and using the PDF4LHC15_{NLO} PDF set. The VBF events are generated at LO using the MADGRAPH5_AMC@NLO 2.7.3 [60] generator with the NNPDF3.0_{NLO} PDF set. Parton shower and hadronisation are simulated using PYTHIA 8.244 with the A14 tune and the NNPDF2.3_{LO} PDF set. A reweighting technique based on the particle-level invariant mass m_{HH} of the Higgs boson pair is applied to the $\kappa_\lambda = 1$ sample to determine the ggF HH signal yield and kinematic distributions for any value of κ_λ [61]. The particle-level m_{HH} spectrum for any generic value of κ_λ is calculated from the m_{HH} distributions of three ggF HH samples generated for $\kappa_\lambda = 0, 1$ or 20. To determine the potential non-closure in the reweighting process from residual kinematic effects, an additional ggF HH sample is generated with the same settings as the nominal sample but with the non-SM value of the self-coupling modifier $\kappa_\lambda = 10$, and then passed through detector simulation and reconstruction algorithms. The reweighting procedure is validated by comparing the predicted event yields and kinematic distributions of the simulated sample generated with $\kappa_\lambda = 1$ and reweighted to $\kappa_\lambda = 10$ with those of the simulated sample generated under the hypothesis $\kappa_\lambda = 10$. Furthermore, 12 additional VBF HH samples are generated and simulated with the same setup as the nominal VBF sample, but using non-SM combinations of the coupling modifiers $\kappa_\lambda, \kappa_{2V}$ and κ_V . A basis for a linear combination is formed by the SM sample and five of the other 12 samples, corresponding to the combinations of the $\kappa_\lambda, \kappa_{2V}$ and κ_V couplings (1, 1.5, 1), (0, 1, 1), (10, 1, 1), (1, 3, 1), (-5, 1, 0.5). This approach is used to determine the expected VBF HH yields and distributions for any value of $\kappa_\lambda, \kappa_{2V}$ and κ_V . The remaining seven samples are compared to the corresponding predictions from the interpolation procedure for validation purposes. The same procedure was used in the measurements presented in Ref. [35]. For both the ggF and the VBF production mode, good closure between the simulated and reweighted samples for alternative κ_λ, κ_V and κ_{2V} values is observed within statistical uncertainties.

The Higgs boson mass is assumed to be 125 GeV in both the simulation and the analysis of the data. All samples are normalised to the same cross-section calculations detailed in Ref [37]. The impacts of the differences with respect to the best-fit values of the m_H measurements reported in Refs. [19, 20] and the effects of the corresponding experimental uncertainties on m_H , are negligible.

4 Event selection and categorisation

Events are selected in three separate signal regions (SRs), which remain unchanged with respect to Ref. [37]. The $\tau_{\text{had}}\tau_{\text{had}}$ signal region (SR) targets fully hadronic decay modes of the τ -lepton pair, where the presence of two oppositely charged hadronically decaying τ leptons (τ_{had}) is determined by detector signatures compatible with the expected visible decay products ($\tau_{\text{had-vis}}$). Two $\tau_{\text{lep}}\tau_{\text{had}}$ SRs target events with a leptonic decay of a τ lepton (τ_{lep}) into an electron or a muon, and an oppositely charged $\tau_{\text{had-vis}}$. The electron and muon channels are considered together. The decay channel with both τ leptons decaying leptonically is not studied in this paper but is instead covered in Ref. [62]. A control region (CR) is defined to constrain the background from Z bosons produced in association with two jets initiated by b or c quarks (referred to as $Z + \text{HF}$ in the following), and top-quark pair production processes. In all regions the presence of two b -jets is also required. These four regions are briefly summarised in Section 4.1. Selected events are split

Table 1: Generators used to simulate the signal and background processes. If not otherwise specified, the order of the cross-section calculation refers to the expansion in the strong coupling constant (α_S). The acronyms ME, PS and UE are used for matrix element, parton shower and underlying event, respectively. More details on the simulation of the signal and background samples are described in the text and in Ref. [37]. (†) The NNLO(QCD)+NLO(EW) cross-section calculation for the $pp \rightarrow ZH$ process already includes the $gg \rightarrow ZH$ contribution. The $qq \rightarrow ZH$ process is normalised to the NNLO(QCD)+NLO(EW) cross-section for the $pp \rightarrow ZH$ process, after subtracting the $gg \rightarrow ZH$ contribution.

Process	ME generator	ME QCD order	PDF set	PS and hadronisation	UE model tune	Cross-section order
Signal						
$gg \rightarrow HH$ (ggF)	POWHEG Box v2 [46]	NLO	PDF4LHC15 _{NLO} [58]	PYTHIA 8.244 [48]	A14 [49]	NNLO FTApprox
$qq \rightarrow qqHH$ (VBF)	MADGRAPH5_AMC@NLO 2.7.3 [60]	LO	NNPDF3.0 _{NLO} [47]	PYTHIA 8.244	A14	N ³ LO(QCD)
Top-quark						
$t\bar{t}$	POWHEG Box v2	NLO	NNPDF3.0 _{NLO}	PYTHIA 8.230	A14	NNLO+NNLL
t -channel	POWHEG Box v2	NLO	NNPDF3.0 _{NLO}	PYTHIA 8.230	A14	NLO
s -channel	POWHEG Box v2	NLO	NNPDF3.0 _{NLO}	PYTHIA 8.230	A14	NLO
Wt	POWHEG Box v2	NLO	NNPDF3.0 _{NLO}	PYTHIA 8.230	A14	NLO
$t\bar{t}Z$	SHERPA 2.2.1 [51]	NLO	NNPDF3.0 _{NLO}	SHERPA 2.2.1	-	NLO
$t\bar{t}W$	SHERPA 2.2.8	NLO	NNPDF3.0 _{NLO}	SHERPA 2.2.8	-	NLO
Vector boson + jets						
W/Z +jets	SHERPA 2.2.11	NLO(≤ 2 jets) LO(3, 4 jets)	NNPDF3.0 _{NNLO}	SHERPA 2.2.11	-	NNLO
Diboson						
WW, WZ, ZZ	SHERPA 2.2.1	NLO(≤ 1 jets) LO(2, 3 jets)	NNPDF3.0 _{NNLO}	SHERPA 2.2.1	-	NLO
Single Higgs boson						
ggF	POWHEG Box v2	NNLO	PDF4LHC15 _{NNLO}	PYTHIA 8.212	AZNLO [59]	N ³ LO(QCD)+NLO(EW)
VBF	POWHEG Box v2	NLO	PDF4LHC15 _{NLO}	PYTHIA 8.212	AZNLO	NNLO(QCD)+NLO(EW)
$qq \rightarrow WH$	POWHEG Box v2	NLO	PDF4LHC15 _{NLO}	PYTHIA 8.212	AZNLO	NNLO(QCD)+NLO(EW)
$qq \rightarrow ZH$	POWHEG Box v2	NLO	PDF4LHC15 _{NLO}	PYTHIA 8.212	AZNLO	NNLO(QCD)+NLO(EW) [†]
$gg \rightarrow ZH$	POWHEG Box v2	NLO	PDF4LHC15 _{NLO}	PYTHIA 8.212	AZNLO	NLO+NNL
$t\bar{t}H$	POWHEG Box v2	NLO	NNPDF3.0 _{NLO}	PYTHIA 8.230	A14	NLO(QCD)+NLO(EW)

into different categories to enhance the sensitivity to the coupling modifiers κ_λ and κ_{2V} , as described in Section 4.2. In each category a multivariate approach based on boosted decision trees (BDTs) is adopted to build the final discriminants, as detailed in Section 4.3. The identification and reconstruction of electrons, muons, $\tau_{\text{had-vis}}$, jets from the hadronisation of quarks and gluons, b -tagged jets, and missing transverse momentum (\vec{p}_T^{miss}) is identical to what was documented in Ref. [37].

4.1 Preselection

Events in the $\tau_{\text{had}}\tau_{\text{had}}$ SR are selected using a combination of single- $\tau_{\text{had-vis}}$ triggers (STTs) and di- $\tau_{\text{had-vis}}$ triggers (DTTs), and are required to have two $\tau_{\text{had-vis}}$ with opposite charge. An electron and muon veto is applied to ensure orthogonality with the $\tau_{\text{lep}}\tau_{\text{had}}$ SRs. In the $\tau_{\text{had}}\tau_{\text{had}}$ SR event selection, the offline² transverse momentum (p_T) thresholds for the $\tau_{\text{had-vis}}$ range between 100 GeV and 180 GeV for STT events depending on the data-taking period, while they are set at 40 GeV (30 GeV) for the (sub-)leading $\tau_{\text{had-vis}}$ for DTT events. For events selected by the STTs a second $\tau_{\text{had-vis}}$ -candidate is required, with an offline p_T threshold of 25 GeV. Additional offline requirements for the DTTs are that either one extra jet with an offline p_T threshold set to 80 GeV is in the event, and the $\tau_{\text{had-vis}}$ are reconstructed within $\Delta R = 2.5$ of each other, or that two extra jets with offline p_T thresholds set to 45 GeV are present in the event. For events that satisfy both the STTs and DTTs, the offline requirements used for the STTs are applied.

² In this paper, offline objects are those reconstructed after the data were collected, as opposed to trigger-level objects.

Events containing exactly an electron or muon and one $\tau_{\text{had-vis}}$ with opposite charge are split into two mutually exclusive SRs, depending on whether they satisfy a single-lepton trigger (SLT) or a lepton-plus- $\tau_{\text{had-vis}}$ trigger (LTT), named the $\tau_{\text{lep}}\tau_{\text{had}}$ SLT SR and the $\tau_{\text{lep}}\tau_{\text{had}}$ LTT SR, respectively. Only events failing the $\tau_{\text{lep}}\tau_{\text{had}}$ SLT SR selection are considered for the $\tau_{\text{lep}}\tau_{\text{had}}$ LTT SR. Depending on the data-taking period, the offline electron (muon) selected by the SLT is required to have $p_{\text{T}}^e > 25$ GeV or $p_{\text{T}}^e > 27$ GeV ($p_{\text{T}}^\mu > 21$ GeV or $p_{\text{T}}^\mu > 27$ GeV). Events selected in the $\tau_{\text{lep}}\tau_{\text{had}}$ LTT SR are required to contain either an electron or a muon with offline p_{T} thresholds set to $p_{\text{T}}^e > 18$ GeV and $p_{\text{T}}^\mu > 15$ GeV respectively, along with a $\tau_{\text{had-vis}}$ with an offline p_{T} threshold set to 30 GeV.

Events in all SRs are required to have $m_{\tau\tau}^{\text{MMC}} > 60$ GeV.³ To target $H \rightarrow b\bar{b}$ decays, events are required to contain exactly two b -tagged jets in the pseudorapidity region of $|\eta| < 2.5$, satisfying the criteria of the ‘DL1r’ b -tagging algorithm with a nominal efficiency of 77% for b jets [64]. The two selected b -tagged jets have to satisfy minimum p_{T} thresholds of 45 and 20 GeV respectively, in addition to any trigger-dependent requirements. In the $\tau_{\text{lep}}\tau_{\text{had}}$ SRs the invariant mass of the b -tagged jet pair (m_{bb}) is required to be lower than 150 GeV to reject background $t\bar{t}$ events, and a $\tau_{\text{had-vis}}$ with p_{T} of at least 20 GeV is required in the $\tau_{\text{lep}}\tau_{\text{had}}$ SLT SR, while $p_{\text{T}} > 30$ GeV is required in the $\tau_{\text{lep}}\tau_{\text{had}}$ LTT SR, in addition to any trigger-dependent requirements.

Events in the CR are required to contain exactly two electrons or two muons of opposite charge with a dilepton invariant mass ($m_{\ell\ell}$) within the range of $75 \text{ GeV} < m_{\ell\ell} < 110 \text{ GeV}$, and exactly two b -tagged jets. The m_{bb} is required to be less than 40 GeV or greater than 210 GeV to avoid overlap with other analyses targeting $H \rightarrow b\bar{b}$ decays. Compared with Ref. [37], the requirement on the transverse momentum of the selected leptons is raised to $p_{\text{T}} > 40$ GeV (from $p_{\text{T}} > 9$ GeV), while the leading b -tagged jet is required to have $p_{\text{T}} > 45$ GeV. This selection provides a closer alignment between the kinematic properties of events selected in the CR and the SRs. Figure 3 shows the predicted and observed $m_{\ell\ell}$ distributions in the CR, after the likelihood fit described in Section 6.

The main sources of background in the SRs after this preselection are from top-quark, Z +jets, W +jets, diboson, single Higgs boson and multi-jet production. Depending on the source, the background contamination is estimated by using data-driven or simulation-based techniques, or a combination of both. The normalisations of simulated $t\bar{t}$ and Z + HF backgrounds are determined from data in the likelihood fits of signal and control regions described in Section 6. A reconstructed $\tau_{\text{had-vis}}$ candidate in these background events can originate either from a τ_{had} decay (true- $\tau_{\text{had-vis}}$), or from a misidentified quark- or gluon-initiated jet (fake- $\tau_{\text{had-vis}}$). Events in which an electron or a muon is misidentified as a $\tau_{\text{had-vis}}$ represent a small additional background. The processes that contribute most to background events with fake- $\tau_{\text{had-vis}}$ candidate are $t\bar{t}$ and multi-jet production. In $t\bar{t}$ events, fake- $\tau_{\text{had-vis}}$ candidates typically originate from quark-initiated jets from the top-quark decay. In multi-jet events, both quark- and gluon-initiated jets are a source for fake- $\tau_{\text{had-vis}}$ candidates. Events with fake- $\tau_{\text{had-vis}}$ candidate in $t\bar{t}$ and multi-jet production are estimated from techniques relying on both simulated events and data, described in Ref. [37], which prove to provide an accurate modelling of the variables used for the event categorisation and multivariate techniques described in this Section. The estimate of this background relies on a good description of the fundamental properties of τ leptons in the three analysis SRs, which are unchanged compared to Ref. [37]. In the $\tau_{\text{lep}}\tau_{\text{had}}$ regions a combined fake-factor method is used to estimate $t\bar{t}$ and multi-jet events with fake- $\tau_{\text{had-vis}}$, by employing two groups of regions: the identification (ID) regions containing one identified $\tau_{\text{had-vis}}$, and the anti-identification (anti-ID) regions containing one reconstructed $\tau_{\text{had-vis}}$ with modified requirements (anti- $\tau_{\text{had-vis}}$), leading to an enriched fake- $\tau_{\text{had-vis}}$ contribution. Fake-factors are derived separately for

³ The invariant mass of the τ -lepton pair ($m_{\tau\tau}^{\text{MMC}}$) is estimated by using the Missing Mass Calculator (MMC) [63].

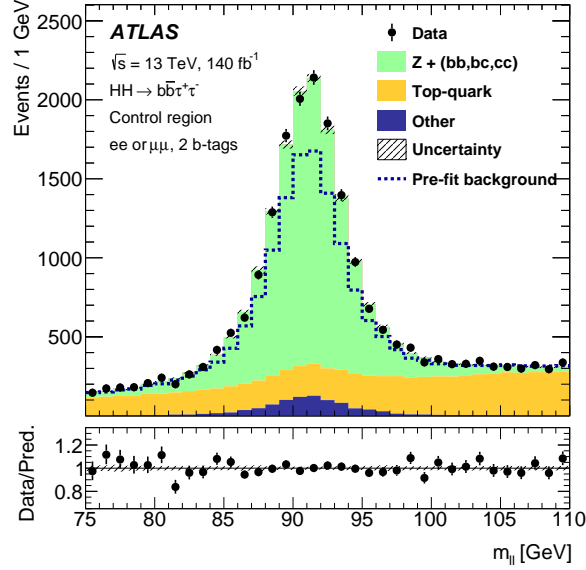


Figure 3: Predicted and observed $m_{\ell\ell}$ distributions in the CR, with the normalisation, shape and total uncertainty of the backgrounds as determined from the likelihood fit to data described in Section 6. The background processes named “Other” contain contributions from Z-boson production in association with less than two jets initiated by b or c quarks, W -boson production, vector boson pair production, $t\bar{t}W$ and $t\bar{t}Z$ production, and single Higgs boson production processes. The dashed histogram shows the total pre-fit background. The lower panel shows the ratio of data to the total post-fit background. The hatched bands in the upper and lower panels show the combined statistical and systematic uncertainties in the total background.

$t\bar{t}$ and multi-jet events in dedicated ID and anti-ID control regions, and are combined to scale events from the anti-ID SRs to obtain the fake- $\tau_{\text{had-vis}}$ background prediction in the $\tau_{\text{lep}}\tau_{\text{had}}$ SRs. In the $\tau_{\text{had}}\tau_{\text{had}}$ regions two separate methods are used to estimate the backgrounds with fake- $\tau_{\text{had-vis}}$ from $t\bar{t}$ and multi-jet production. Multi-jet events can only enter the SRs when both $\tau_{\text{had-vis}}$ are fake, and their contribution is estimated by using a fake-factor method. Fake-factors are derived for the multi-jet background in a dedicated set of ID control regions, defined for events with two identified $\tau_{\text{had-vis}}$, and anti-ID control regions for events with one identified $\tau_{\text{had-vis}}$ and one anti- $\tau_{\text{had-vis}}$ candidate. The fake-factors are applied to scale events from the anti-ID SRs to obtain the multi-jet fake- $\tau_{\text{had-vis}}$ background prediction in the $\tau_{\text{had}}\tau_{\text{had}}$ SRs. Background events with fake- $\tau_{\text{had-vis}}$ from $t\bar{t}$ production in the $\tau_{\text{had}}\tau_{\text{had}}$ SRs are estimated using simulation, while correcting the fake- $\tau_{\text{had-vis}}$ misidentification efficiencies with scale factors derived from data in the $t\bar{t}$ control region defined for the fake-factor estimate in the $\tau_{\text{lep}}\tau_{\text{had}}$ channel. The modelling of events with a fake- $\tau_{\text{had-vis}}$ candidate from background processes other than $t\bar{t}$ and multi-jet production is performed using MC simulation, as they represent a minor contribution to the total background. Simulated event samples are used to model background events containing true- $\tau_{\text{had-vis}}$ and events with an electron or a muon misidentified as a $\tau_{\text{had-vis}}$ candidate. The changes introduced to the MC simulation detailed in Section 3 are found to have a negligible impact on the data-driven estimate of the background.

4.2 Event categorisation

Events selected in each SR described in Section 4.1 are split into three separate categories. To enhance the sensitivity to the coupling modifier κ_{2V} , a dedicated VBF category is defined with a multivariate approach,

defining a dedicated BDT to select events with characteristic features of VBF HH production, separately for each analysis SR. These are referred to as *categorisation BDTs* in the following. The distribution of the invariant mass of the HH system (m_{HH}) in ggF HH events is significantly affected by the value of κ_λ . Hence, events not falling in the VBF category are split into two m_{HH} categories, targeting ggF HH production with κ_λ values close to the SM expectation (ggF high- m_{HH}) or significantly different from it (ggF low- m_{HH}). The three categories are mutually exclusive, and they are defined separately for each SR following the procedure outlined in Figure 4, leading to a total of nine event categories. First,

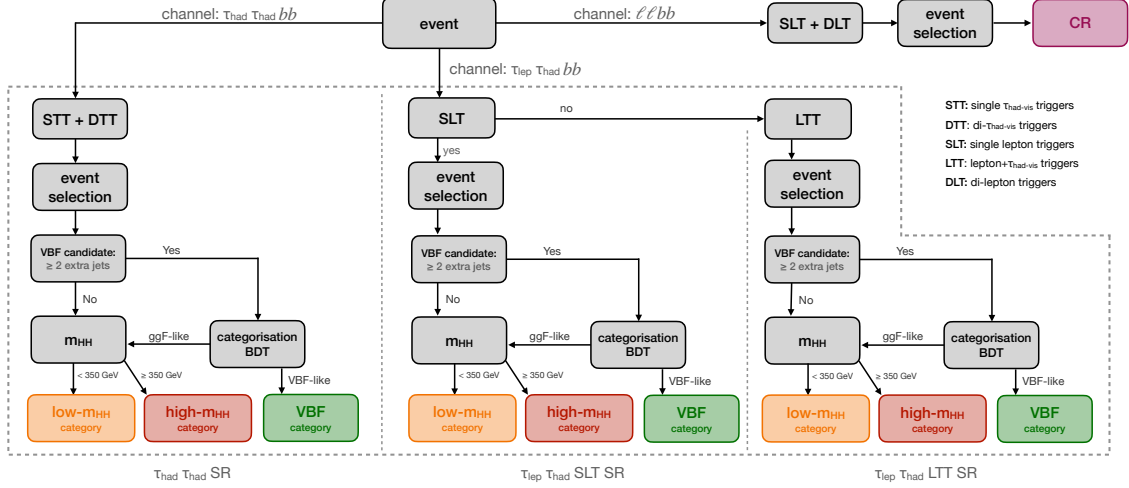


Figure 4: Flowchart summarizing the definition of the $\tau_{had} \tau_{had}$ SR, the $\tau_{lep} \tau_{had}$ SLT SR, the $\tau_{lep} \tau_{had}$ LTT SR and the dedicated CR defined in Section 4. The flowchart shows the selection criteria applied to define the corresponding ggF low- m_{HH} , ggF high- m_{HH} and VBF categories for each analysis SR, leading to a total number of nine analysis categories and an additional CR.

VBF candidate events are identified by requiring the presence of at least two jets in addition to the ones associated with the $H \rightarrow b\bar{b}$ decay. These events are used to train the categorisation BDTs to separate ggF and VBF HH production modes in event topologies with additional jets. Events satisfying a SR-dependent selection on the output of these BDTs are assigned to the VBF category. Events failing the VBF selection are assigned to the ggF categories, together with events not selected as VBF candidates.

The categorisation BDTs are built using the Toolkit for Multivariate Data Analysis (TMVA [65]) using ggF HH events as signal and VBF HH events as background, scaled such that the total event yield is the same for both processes. A dedicated version of the BDT is trained in each SR respectively. To make use of the complete set of simulated events for the BDT training, optimisation and evaluation, the events are split into three samples of equal size, A, B and C. The performance of the BDTs trained on sample A (respectively B, C), is optimised using sample B (C, A) and evaluated with sample C (A, B), ensuring an unbiased estimate of the performance of the BDTs. The selected data events are split into three samples, each analysed with one of the three separately trained BDTs. The output distributions of the BDTs evaluated on samples A, B and C are merged for both simulated and data events to produce the final discriminant. The number of trees and their depth are chosen to maximise the BDT separation power, quantified by the value of the number-counting significance z [66] computed from the binned distribution of the BDT discriminant.

The minimal set of training variables that optimises the BDT separation power is determined starting from a small set and iteratively adding variables one at a time from a pre-defined list of candidate variables.

The variable leading to the largest increase (or minimal decrease⁴) in significance z is included, until no changes are observed. The starting set of variables comprises the invariant mass of the VBF jets (m_{jj}^{VBF}), defined as the two jets with the highest p_T not associated with the $H \rightarrow b\bar{b}$ decay, and their pseudorapidity gap ($\Delta\eta_{jj}^{\text{VBF}}$). The final set of variables for the categorisation BDTs in each SR is summarised in Table 2. It includes the product of VBF jet pseudorapidities (VBF $\eta_0 \times \eta_1$), their angular separations ($\Delta\phi_{jj}^{\text{VBF}}$ and $\Delta R_{jj}^{\text{VBF}}$) and m_{HH} . In addition, the Fox-Wolfram moments f_i of i -th order [67] and their modified definitions for usage in hadron collider experiments h_i [68] can further increase the separation power, together with the centrality⁵ (C) and the invariant mass (m_{Eff}) of the system composed by the selected τ leptons, the missing transverse momentum vector \vec{p}_T^{miss} and the selected jets. The predicted and observed distributions of the resulting BDT scores are shown in Figure 5 for all three SRs. VBF candidate events are assigned to the VBF category if their BDT score is evaluated below a certain threshold. The value of this threshold is optimised to achieve the best upper limits on HH production for ggF and VBF production modes separately and combined, along with the best exclusion limits for the coupling modifiers κ_λ and κ_{2V} from the likelihood fit described in Section 6. The categorisation BDT cut values are set to 0.1, -0.13 and -0.1 for the $\tau_{\text{had}}\tau_{\text{had}}$, $\tau_{\text{lep}}\tau_{\text{had}}$ SLT and $\tau_{\text{lep}}\tau_{\text{had}}$ LTT SRs, respectively.

Table 2: Input variables for the categorisation BDTs in each of the three SRs. The superscripts a and c specify the selection of jets that are taken into account for the calculation in addition to the two τ -lepton candidates and the \vec{p}_T^{miss} vector. For variables with a c , only the four-momenta of central jets, i.e., jets with $|\eta| < 2.5$, are included, while an a indicates that all available jets are included.

Variable	$\tau_{\text{had}}\tau_{\text{had}}$	$\tau_{\text{lep}}\tau_{\text{had}}$ SLT	$\tau_{\text{lep}}\tau_{\text{had}}$ LTT
m_{jj}^{VBF}	✓	✓	✓
$\Delta\eta_{jj}^{\text{VBF}}$	✓	✓	✓
VBF $\eta_0 \times \eta_1$	✓	✓	
$\Delta\phi_{jj}^{\text{VBF}}$	✓		
$\Delta R_{jj}^{\text{VBF}}$		✓	✓
$\Delta R_{\tau\tau}$	✓		
m_{HH}	✓		
f_2^a	✓		
C^a		✓	✓
m_{Eff}^a		✓	✓
f_0^c		✓	
f_0^a			✓
h_3^a			✓

Events not retained in the VBF category are split into low- m_{HH} and high- m_{HH} categories targeting ggF

⁴ Variables showing minimal decrease of the z significance are retained to mitigate the impact of statistical fluctuations on the optimisation, potentially leading to prematurely terminating the iterative procedure. In the final selection only variables improving the BDT sensitivity are retained.

⁵ The centrality of a set of four-momenta of index i is defined as $C = \frac{\sum_i p_T(i)}{\sum_i E(i)}$

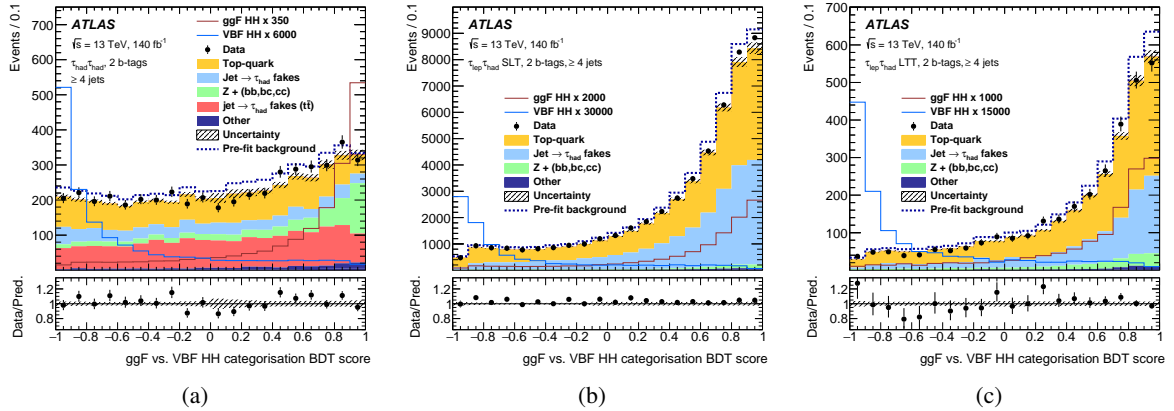


Figure 5: Predicted and observed distributions of the categorisation BDT scores in (a) the $\tau_{\text{had}}\tau_{\text{had}}$, (b) the $\tau_{\text{lep}}\tau_{\text{had}}$ SLT and (c) the $\tau_{\text{lep}}\tau_{\text{had}}$ LTT SRs, for all candidate VBF events. The background distributions are shown as obtained from the combined likelihood fit to data described in Section 6. The background processes named “Other” contain contributions from Z -boson production in association with less than two jets initiated by b or c quarks, W -boson production, vector boson pair production, $t\bar{t}W$ and $t\bar{t}Z$ production, and single Higgs boson production processes. The ggF and VBF HH signal distributions are overlaid and scaled to the factor indicated in the legend times the SM expectation. The dashed histogram shows the total pre-fit background. The lower panels show the ratio of data to the total post-fit sum of signal and background. The hatched bands in the upper and lower panels show the combined statistical and systematic uncertainties in the total prediction.

HH production. While the ggF HH cross-section increases for κ_λ values larger than the SM expectation and close to the current experimental sensitivity ($\kappa_\lambda \sim 6$ [35]), the softer m_{HH} spectrum leads to smaller detector acceptance and selection efficiency. The event split into different regions of m_{HH} allows to partially disentangle these effects, improving the sensitivity to higher κ_λ values. The splitting value is chosen to be 350 GeV since the effect of the interference between the box and triangle diagrams on the differential ggF HH production cross-section is maximal there.

4.3 Multivariate discriminants

Based on the event categorisation described in Section 4.2, an additional set of multivariate discriminants making use of BDTs is trained and evaluated in each of the analysis SRs separately to achieve optimal separation between the HH signal and the background. One dedicated BDT is trained for each analysis SR ($\tau_{\text{had}}\tau_{\text{had}}$, $\tau_{\text{lep}}\tau_{\text{had}}$ SLT, $\tau_{\text{lep}}\tau_{\text{had}}$ LTT) and each category (ggF low- m_{HH} , ggF high- m_{HH} and VBF), leading to nine separate BDTs. In the ggF high- m_{HH} and VBF categories, the signal corresponds to the ggF and VBF SM production of HH pairs, respectively. In the ggF low- m_{HH} category the signal is defined as ggF HH production with $\kappa_\lambda = 10$. During training, the sum of all backgrounds normalised to their respective cross-sections is used, which is scaled such that the total background yield matches that of the corresponding signal sample. The backgrounds containing $\tau_{\text{had-vis}}$ from misidentified quark- or gluon-initiated jets are modelled using simulation, except for the multi-jet background in the $\tau_{\text{had}}\tau_{\text{had}}$ category, where the data-driven estimate introduced in Section 4.1 is used. The BDTs evaluated in the low- m_{HH} and high- m_{HH} categories are trained on the event samples selected in the respective categories. The BDTs evaluated in the VBF categories are trained on events from both the VBF and ggF categories to maximise the available sample size.

To make use of the complete set of simulated events for the BDT training, optimisation and evaluation, the events are split into three samples, following the same procedure described in Section 4.2. The number of trees and their depth are chosen to maximise the BDT separation power, quantified by the value of the signal significance z computed from the binned distribution of the BDT output.

The input variables used for the BDTs are chosen to maximise the BDT separation power, separately for each trained BDT. A list of variables is built for each BDT, ordered according to their impact on the signal significance z , following the same procedure as described in Section 4.2. In each analysis SR and category the starting set comprises the following variables: the invariant mass of the two selected b -jets (m_{bb}), the invariant mass of the τ -lepton pair ($m_{\tau\tau}^{\text{MMC}}$), the m_{HH} reconstructed from the selected b -jet and τ -lepton pairs, the angular separation between b -jets (ΔR_{bb}) and between τ -leptons ($\Delta R_{\tau\tau}$). In the $\tau_{\text{lep}}\tau_{\text{had}}$ LTT high- m_{HH} category ΔR_{bb} is not included, and in the $\tau_{\text{lep}}\tau_{\text{had}}$ LTT VBF category both ΔR_{bb} and $\Delta R_{\tau\tau}$ are removed. The additional variables included in the BDT training through a z -based optimisation as described in Section 4.2 can be grouped in several categories. Variables that require the presence of a charged lepton are not included for the $\tau_{\text{had}}\tau_{\text{had}}$ SR. Higgs boson candidates H are reconstructed from either b -jet or τ -lepton pairs. For the low- m_{HH} and high- m_{HH} categories, variables describing the kinematic properties of the selected b -jets and τ leptons are included: the transverse momentum of the leading and subleading b -jets and τ leptons, along with the pseudorapidity of the τ leptons and the transverse mass of each of the τ leptons and \vec{p}_T^{miss} . The angular separation between the (sub)leading b -jet and the (sub)leading τ lepton is included, along with the angular separation between the leading b -jet and the subleading τ lepton, the pseudorapidity separation and the transverse momentum difference between the selected τ -lepton candidate and the charged lepton. Variables related to the reconstructed H candidate topologies include: the azimuthal angular separation between the b -jet pair and the τ -lepton pair, and between either the b -jet or the τ -lepton pair and the magnitude E_T^{miss} of \vec{p}_T^{miss} , the azimuthal angle of the selected b -jet (or τ -lepton) pair relative to the H candidate rest frame, along with the transverse momentum of the b -jet and τ -lepton pairs. The separation power is further increased by including variables describing the hadronic activity in candidate events, such as the number of selected hadronic jets, the scalar sum of jet transverse momenta (H_T), the effective mass of the τ -lepton pair and all jets with $|\eta| < 2.5$, the E_T^{miss} , the transverse mass [69] (M_{T2}), the azimuthal angular separation between the selected charged lepton and the \vec{p}_T^{miss} . Additional variables are included to characterise event properties, such as the transverse mass of the W boson candidate in the $\tau_{\text{lep}}\tau_{\text{had}}$ SRs (defined as the transverse mass of the selected lepton and the \vec{p}_T^{miss}), the topness variable [70] as defined in Ref. [71] assuming either $\sigma_t = 5 \text{ GeV}$, $\sigma_W = 5 \text{ GeV}$ (T_1) or $\sigma_t = 15 \text{ GeV}$, $\sigma_W = 5 \text{ GeV}$ (T_2), the reduced invariant mass of the HH system (defined as $m_{HH}^* = m_{HH} - m_{bb} - m_{\tau\tau}^{\text{MMC}} + 250 \text{ GeV}$), the scaled invariant mass of the HH system (defined by scaling the four-momenta of both H candidates by the ratio $125 \text{ GeV}/m_H$, where m_H is the H candidate invariant mass), the transverse momentum of the reconstructed HH system and the effective mass of the HH decay products. To construct the E_T^{miss} centrality, the transverse plane is transformed such that the directions of the $\tau_{\text{had-vis}}$ candidates or leptons are orthogonal, and that the smaller ϕ angle between them defines the positive quadrant of the transformed plane. Then the E_T^{miss} centrality is defined as the sum of the x and y components of the \vec{p}_T^{miss} unit vector in this transformed plane. Dedicated variables describing characteristic event configurations are included via a selection of Fox-Wolfram moments (as defined in Section 4.2), circularity, sphericity, thrust and planar flow variables reconstructed from the HH decay products. Finally, the b -tagging information is provided by the quantile distribution of the DL1r tagger output for the selected b -jets, which is included as a training variable. For the VBF categories the first five variables listed in Table 2 are also included, along with circularity, sphericity and planar flow variables reconstructed from the τ -lepton pair and all selected jets, to target the specific features of VBF HH events.

5 Systematic uncertainties

While the largest source of uncertainty in this analysis comes from the limited number of data events, systematic uncertainties can affect the signal and background estimates. Uncertainties originating from the detector response in the selection and reconstruction of the used objects are included as documented in Ref. [37]. Statistical uncertainties in the predicted background processes are modelled using a simplified version of the Beeston-Barlow technique [72], in which only the uncertainty in the total background contribution in each bin is considered. An uncertainty in the full Run 2 integrated luminosity of 0.83% [42], from measurements using the LUCID-2 [43] detector and a complementary measurement using the inner detector and calorimeters, is assigned to physics processes whose normalisations are taken from simulation.

For all processes whose estimation relies on MC simulation, the impact of various sources of theoretical uncertainties in their cross-section, on the fractional contribution to each analysis category within each SR, as well as on the shape of the BDTs introduced in Section 4.3 is considered. The total normalisation of $t\bar{t}$ and $Z + \text{HF}$ backgrounds is determined via the likelihood fit described in Section 6; therefore, no uncertainty is included for their cross-section calculation. For $t\bar{t}$ and $Z + \text{HF}$ backgrounds, the uncertainty in the fractional contribution in each analysis category is computed as the relative variation in acceptance with respect to the dedicated CR introduced in Section 4, while for other processes this is evaluated as the absolute acceptance variation in each analysis category. To assess an uncertainty in the shape of the BDT output, a dedicated rebinning algorithm is applied to ensure that only statistically significant shape variations are considered. In the signal-enriched region of the BDT distribution, the statistical uncertainty of each bin is required to be below a process- and variation-dependent threshold (ranging from 5% to 15%), while in the background-enriched region of the distribution the fraction of total events per bin is required to be larger than 5%. For each process, the impact of each source of uncertainty in the fractional contribution in each analysis category is correlated with the uncertainty in the shape of the BDT score in the corresponding category, in the likelihood fit described in Section 6. All sources of uncertainty are evaluated separately and correlated across the three analysis SRs. The uncertainties in the SM cross-section calculations for all processes are unchanged with respect to Ref. [37], along with the full uncertainty estimate for smaller background processes including $Z + \text{light-flavour jets}$, $W + \text{jets}$, diboson and single-top-quark production in the s - and t -channels.

The $t\bar{t}$ hard-scatter and parton-shower uncertainties are evaluated by comparing the nominal sample with samples generated using MADGRAPH5_AMC@NLO +PYTHIA 8 and POWHEG BOX v2 +HERWIG 7.04 [73, 74], respectively. The hard-scatter uncertainty also accounts for uncertainties in the matching and merging of the matrix-element calculation with the parton-shower algorithm. The uncertainty in missing higher-order QCD corrections and the modelling of initial-state QCD radiation is assessed via independent variations of the renormalisation and factorisation scales in the hard-scatter calculation, of the showering tune VAR3c parameter [49] and of the h_{damp} ⁶ parameter, while for the modelling of final state QCD radiation alternative choices of factorisation and renormalisation scales in the showering algorithm are considered. Finally, uncertainties in the PDF and the value of the strong coupling constant α_S are also evaluated. All sources of uncertainty have an impact on the shape of the BDT score and the $t\bar{t}$ fractional contribution in each analysis category. The largest effect on the latter is due to parton-shower variations and ranges between 1% and 10% of the nominal values, depending on the analysis category and SR.

⁶ The h_{damp} parameter regulates the p_T of the first additional emission beyond the Born configuration in the POWHEG BOX generator, controlling the matching of the matrix element to the parton shower.

For $Z + \text{HF}$ processes the uncertainty in the modelling of the hard scatter and the parton shower are evaluated by comparing the nominal sample with a `MADGRAPH5_AMC@NLO+PYTHIA8` sample with up to three additional partons in the final state at NLO accuracy in the QCD coupling, in which additional jet multiplicities are merged together with the `FxFx` NLO matrix-element and parton-shower merging prescription [75]. The A14 parton-shower tune and the NNPDF2.3LO PDF set are used for this alternative sample. Uncertainties from missing higher-order QCD corrections are evaluated with renormalisation and factorisation scale variations from the nominal samples, along with PDF and α_S variations. The effect of higher-order electroweak corrections for $Z + \text{HF}$ processes is found to be negligible, and thus not included. Uncertainties in the matching between matrix element calculation and parton shower are considered via variations of the `SHERPA` matching parameter (CKKW) and the resummation scale (QSF). All sources of uncertainty have an impact on the $Z + \text{HF}$ fractional contribution in each analysis category, with the largest effect due to renormalisation and factorisation scale variations ranging up to 13% of the nominal values depending on the analysis category and SR. The uncertainty in the modelling of the hard scatter and the parton shower, from the comparison with the alternative `MADGRAPH5_AMC@NLO+PYTHIA8`, is the only source of uncertainty with a significant impact on the shape of the BDT score in the analysis SRs. The same source of uncertainty is found to have a non-negligible impact on the shape of the $m_{\ell\ell}$ variable in the CR, which is included as a dedicated uncertainty uncorrelated from the BDT score shape uncertainty in the likelihood fit. Finally, an additional systematic uncertainty is included to cover the residual difference between data and MC simulation in the dedicated CR, as a function of the transverse momentum of the selected lepton pair. This uncertainty is applied in all analysis SRs as a function of the transverse momentum of the τ -lepton pair selected from the MC truth record.

For single-top-quark processes only uncertainties related to the Wt -channel are considered, as it is found to be dominant compared with s - and t - channel contributions. The hard-scatter and the parton-shower uncertainties are evaluated by comparing the nominal sample with alternative `MADGRAPH5_AMC@NLO+PYTHIA8` and `POWHEG BOX v2+HERWIG7` samples. The uncertainty in the modelling of QCD radiation is evaluated by varying the showering tune `VAR3C`, along with independent variations of the renormalisation and factorisation scales in the hard-scatter and parton-shower calculations. The uncertainty related to the interference between the $t\bar{t}$ and the Wt -channel single-top-quark processes is evaluated by comparing the nominal Wt -channel sample produced with the diagram removal scheme to an alternative sample produced with the diagram subtraction scheme [76]. Finally, uncertainties in the PDF are also evaluated. All sources of uncertainty have an impact on the Wt -channel single-top-quark fractional contribution in each analysis category. Variations due to the uncertainty in the Wt -channel interference scheme range from 1% to 7% in the low- m_{HH} categories, from 23% to 29% in the high- m_{HH} categories and from 14% to 34% in VBF categories. Uncertainties in the Wt -channel interference scheme are also evaluated on the shape of the BDT score, rather than on the p_T of the b -tagged jet pair as in Ref. [37]. The hard-scatter and parton-shower uncertainties range from 15% to 36% on the Wt -channel fractional contribution, depending on the analysis category and SR. Uncertainties in the modelling of QCD radiation are found to have a significant impact on the shape of the BDT score.

An uncertainty of 100% is applied on the normalisation of single Higgs boson in the ggF, VBF and associated production WH mechanisms where the Higgs boson decays into a τ -lepton pair, to account for difficulties in the modelling of these processes in association with heavy-flavour jets [77, 78]. Uncertainties from missing higher-order QCD corrections are evaluated with independent variations of the renormalisation and factorisation scales from the nominal samples, along with PDF and α_S variations. Parton-shower uncertainties are evaluated by comparing the nominal sample to alternative `POWHEG BOX v2+HERWIG7` samples for associated production ZH and $t\bar{t}H$ processes. For $t\bar{t}H$ processes the hard-scatter uncertainties are derived by comparing the nominal samples to `MADGRAPH5_AMC@NLO+PYTHIA8` predictions, and

uncertainties in the modelling of QCD radiation are assessed via variations of the showering tune VAR3c, along with independent variations of the renormalisation and factorisation scales in the parton-shower algorithm. All sources of uncertainty have an impact on the single-Higgs-boson fractional contribution in each analysis category, while only parton-shower uncertainties are included as variations of the BDT score for the ZH and $t\bar{t}H$ processes.

For the SM ggF and VBF HH signal processes, uncertainties from missing higher-order QCD corrections are assessed via independent variations of the renormalisation and factorisation scales in the hard-scatter calculation, along with PDF and α_S variations. Parton-shower uncertainties are evaluated by comparing the nominal samples with alternative POWHEG BOX v2+HERWIG7 samples. All sources of uncertainty have an impact on the signal fractional contribution in each analysis category, while only parton-shower uncertainties are included as variations of the BDT score. Cross-section uncertainties for single-Higgs-boson and HH processes [29] follow the same approach detailed in Ref. [37], along with uncertainties in the $H \rightarrow b\bar{b}$ and $H \rightarrow \tau^+\tau^-$ branching ratios [79].

A dedicated uncertainty in the reweighting method applied to the ggF HH samples to model alternative κ_λ hypotheses, described in Section 3, is defined via a comparison of the SM ggF HH samples with an alternative sample generated assuming $\kappa_\lambda = 10$. The SM sample and the $\kappa_\lambda = 10$ sample are reweighted to a wide range of κ_λ values and the acceptance values of both predictions are compared independently in each category. The maximum of the obtained deviations is taken as an uncertainty and applied to the $\kappa_\lambda = 0$ and $\kappa_\lambda = 20$ templates used for the linear combination of signal samples in the fit. These deviations range from 2% to 4% in the ggF categories and from 20% to 40% in the VBF categories. The uncertainty in the VBF categories arises from the m_{HH} -based reweighting method not accounting for additional radiation produced with the HH pair, to which the categorisation BDTs are highly sensitive. The linear combination of VBF HH samples described in Section 3 is found to accurately model alternative κ_λ and κ_{2V} hypothesis; therefore, no dedicated uncertainty is considered.

The estimate of systematic uncertainties affecting the data-driven background follows the approach described in Ref. [37]. Uncertainties in the fractional contribution of the data-driven background and on the shape of the BDT score are derived in all the analysis SRs and categories.

6 Results

The statistical procedures applied for extracting results are the same as in Refs. [35, 37]. The global likelihood function $L(\alpha, \theta)$ is constructed from the binned distribution of the BDT output score for signal, background and data distributions in the nine orthogonal analysis categories described in Section 4, together with the $m_{\ell\ell}$ distribution in the dedicated CR. The set α contains the parameters of interest (POI) of the measurement, while θ is the ensemble of nuisance parameters, corresponding to systematic uncertainties constrained by auxiliary measurements in control regions or by theoretical predictions, or to parameters such as the $t\bar{t}$ and $Z + \text{HF}$ background yields, which are *a priori* unconstrained.

A dedicated procedure is applied to transform the BDT discriminant to obtain a smoother distribution for the background processes and a finer binning in the regions with the largest signal contribution, while preserving a sufficiently large number of background events in each bin, similarly to Ref. [37]. Starting from finely binned histograms, bins are iteratively merged starting from the most signal-enriched bins until they satisfy the condition of $10f_s + 5f_b > 1$, where f_s and f_b are the fractions of signal and background contained in the bin, respectively. The relative statistical uncertainty in the predicted background contribution has to

be below 20%, and at least three expected background events are required per bin. The $m_{\ell\ell}$ distribution in the CR is binned uniformly with a width of 1 GeV.

The constraints on the coupling modifiers are determined using a profile likelihood ratio $\Lambda(\alpha, \theta)$ as the test statistic, computed from the likelihood function in the asymptotic approximation [66], where the POI α are the coupling modifiers κ . The procedure adopted in Ref. [35] is used to set constraints on κ_λ and κ_{2V} , expressed as 68% and 95% CIs. Signal strength upper limits are derived using the CL_s method [80] with the procedure described in Ref. [37]. Upper limits are set on the overall μ_{HH} and on the separate signal strength parameters $\mu_{\text{ggF}} = \sigma_{\text{ggF}}/\sigma_{\text{ggF}}^{\text{SM}}$ and $\mu_{\text{VBF}} = \sigma_{\text{VBF}}/\sigma_{\text{VBF}}^{\text{SM}}$. The expected results are obtained with Asimov datasets [66] generated from the likelihood function after setting all nuisance parameters to their maximum-likelihood estimate in the fit to the data and fixing the POIs to the values corresponding to the hypothesis under test. The asymptotic results are found to agree within 7% with the upper limits obtained using pseudo-experiments. Figure 6 shows the BDT score distribution in the nine orthogonal categories, after performing the maximum-likelihood fit to data for the $L(\mu_{HH}, \theta)$ function. Good agreement between the data and the prediction is found within the assessed uncertainties.

The maximum-likelihood estimator for the total HH production signal strength is found to be $\hat{\mu}_{HH} = 2.2 \pm 1.7$ by the combined fit to data. The uncertainty in the fitted signal strength is obtained from the variation of log-likelihood-based test statistic Λ by one unit, and includes both statistical and systematic uncertainties. The maximum-likelihood estimator for the unconstrained normalisation factor of the $t\bar{t}$ and $Z + \text{HF}$ backgrounds are measured at 0.96 ± 0.03 and 1.34 ± 0.08 , respectively, by the combined fit to data. An observed 95% CL upper limit of 5.9 is set on μ_{HH} , to be compared with an expected limit of 3.3 in the background-only hypothesis ($\mu_{HH} = 0$), corresponding to an observed (expected) significance with respect to the background-only hypothesis of 1.4 (0.75) σ . From the simultaneous fit of μ_{ggF} and μ_{VBF} , observed (expected) 95% CL upper limits are $\mu_{\text{ggF}} < 5.8$ (3.4) and $\mu_{\text{VBF}} < 91$ (73), respectively, for each production mode, assuming that the signal strength parameters can vary independently for each production mode. If μ_{VBF} is fixed to the SM prediction, the observed (expected) 95% CL upper limit is $\mu_{\text{ggF}} < 5.9$ (3.4). Similarly, if μ_{ggF} is fixed to the SM prediction, the observed (expected) 95% upper limit is $\mu_{\text{VBF}} < 93$ (72).

Expected upper limits for the separate production mode signal strengths are derived with respect to the background-only hypothesis. The signal strength upper limits are summarised in Table 3 and Figure 7, in each SR individually along with the combined fit. The results for the individual SRs are obtained from the combined likelihood fit of the BDT score distributions in the categories of a single SR with the $m_{\ell\ell}$ distribution from the dedicated CR. The observed limit on μ_{HH} from the combined fit is looser than the expected one as a result of an excess in the $\tau_{\text{lep}}\tau_{\text{had}}$ SLT SR, in the high- m_{HH} category. This excess corresponds to a local significance of 2.3 σ with respect to the SM hypothesis ($\mu_{HH} = 1$), and a local significance of 2.7 σ with respect to the background-only hypothesis, as obtained from the individual fit of the $\tau_{\text{lep}}\tau_{\text{had}}$ SLT SR.

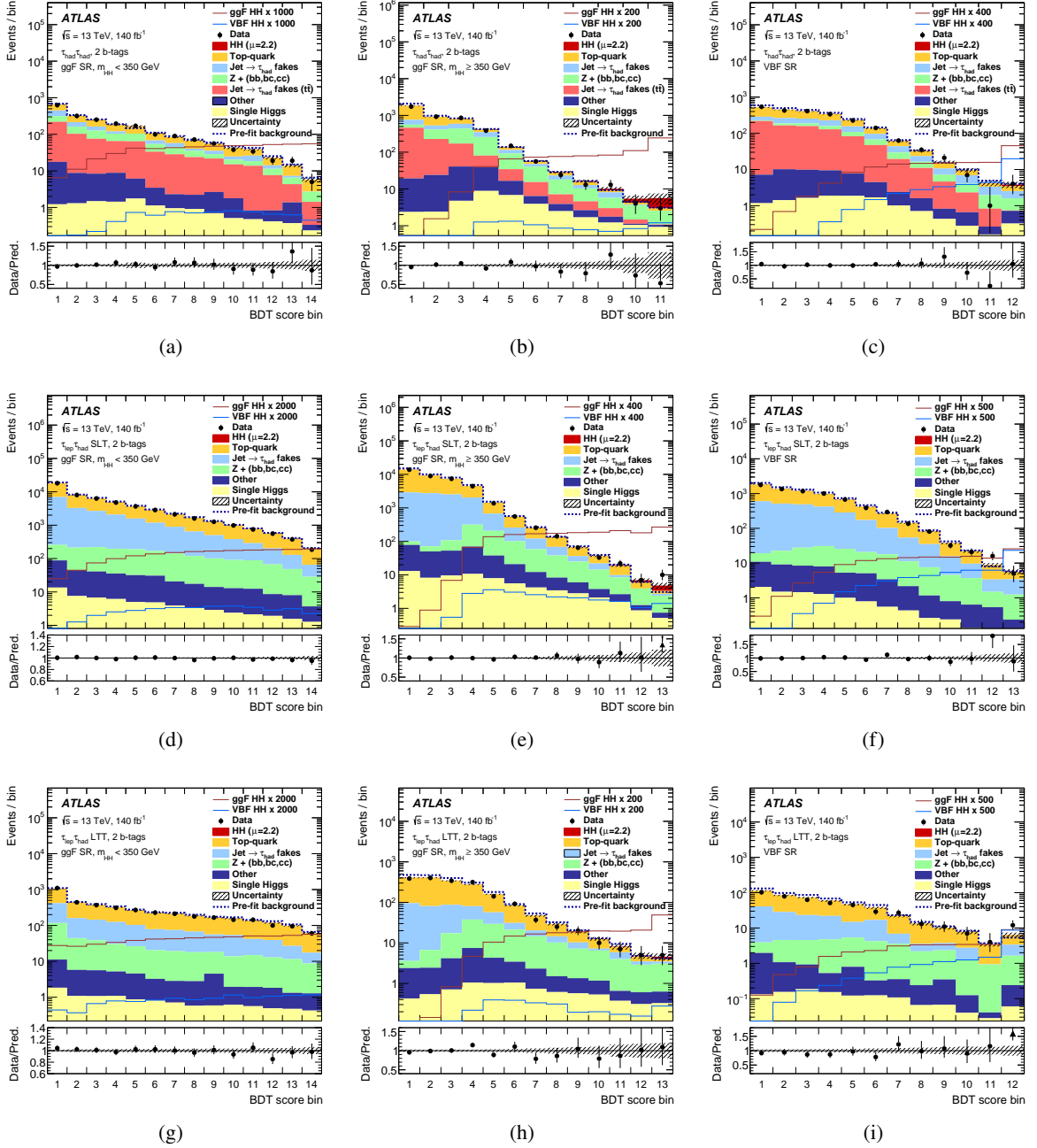


Figure 6: Predicted and observed distribution of the BDT score in (left) the low- m_{HH} , (middle column) the high- m_{HH} and (right) the VBF categories of (top) the $\tau_{had}\tau_{had}$, (middle row) the $\tau_{lep}\tau_{had}$ SLT and (bottom) the $\tau_{lep}\tau_{had}$ LTT SRs. The signal and background distributions are shown at post-fit level as obtained from the combined likelihood fit to data described in Section 6. The background processes named ‘Other’ contain contributions from Z -boson production in association with less than two jets initiated by b or c quarks, W -boson production, vector boson pair production, $t\bar{t}W$ and $t\bar{t}Z$ production processes. The ‘HH’ signal contribution is scaled to the fitted signal strength μ_{HH} from the combined likelihood fit times the SM expectation. The ggF and VBF HH signal distributions are overlaid and scaled to the factor indicated in the legend times the SM expectation. The dashed histograms show the total pre-fit background. The lower panels show the ratio of data to the total post-fit sum of signal and background, where the hatched bands show the statistical and systematic uncertainties of this prediction. The BDT score distributions are shown with the binning used in the likelihood fit. For visualisation purposes each bin is displayed with uniform width and an index labeling it.

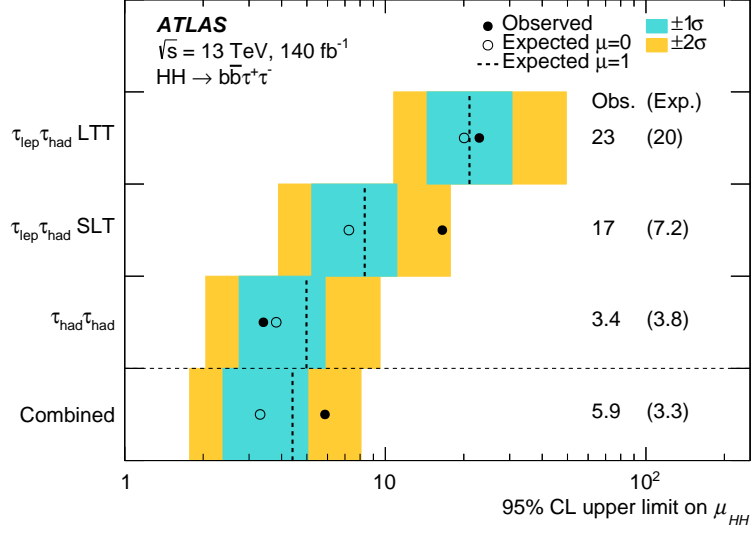


Figure 7: Summary of observed (filled circles) and expected (open circles) 95% CL upper limits on μ_{HH} from the fit of each individual channel and the combined fit in the background-only ($\mu_{HH} = 0$) hypothesis. The dashed lines indicate the expected 95% CL upper limits on μ_{HH} in the SM hypothesis ($\mu_{HH} = 1$). The inner and outer bands indicate the $\pm 1\sigma$ and $\pm 2\sigma$ variations, respectively, on the expected limit with respect to the background-only hypothesis due to statistical and systematic uncertainties.

Table 3: Observed and expected 95% CL upper limits on μ_{HH} , μ_{ggF} and μ_{VBF} from the individual SR likelihood fits as well as the combined results. The μ_{ggF} and μ_{VBF} limits are quoted both from the results of the simultaneous fit of both signal strengths (central column), and from independent fits for the individual production modes, assuming the other to be as predicted by the SM. The uncertainties quoted on the combined expected upper limits correspond to the 1σ uncertainty band.

		μ_{HH}	μ_{ggF}	μ_{VBF}	$\mu_{ggF} (\mu_{VBF}=1)$	$\mu_{VBF} (\mu_{ggF}=1)$
$\tau_{had}\tau_{had}$	observed	3.4	3.6	87	3.5	80
	expected	3.8	3.9	102	3.9	99
$\tau_{lep}\tau_{had}$ SLT	observed	17	17	136	17	158
	expected	7.2	7.4	129	7.4	127
$\tau_{lep}\tau_{had}$ LTT	observed	23	18	765	22	733
	expected	20	21	359	20	350
Combined	observed	5.9	5.8	91	5.9	93
	expected	$3.3^{+1.7}_{-0.9}$	$3.4^{+1.8}_{-1.0}$	73^{+32}_{-21}	$3.4^{+1.8}_{-0.9}$	72^{+32}_{-20}

The observed and expected values of $-2 \ln \Lambda$ as a function of the coupling modifiers κ_λ and κ_{2V} are shown in Figure 8, under the hypothesis that all other coupling modifiers are equal to their SM predictions. The combined fit allows to set observed (expected) 95% CIs of $\kappa_\lambda \in [-3.1, 9.0]$ ($[-2.5, 9.3]$) (assuming $\kappa_{2V} = 1$) and $\kappa_{2V} \in [-0.5, 2.7]$ ($[-0.2, 2.4]$) (assuming $\kappa_\lambda = 1$). Additional constraints are set on κ_λ and κ_{2V} assuming that both coupling modifiers can vary simultaneously. The resulting observed and expected two-dimensional 68% and 95% contours are shown in Figure 9. The observed and expected constraints on

κ_λ reported in this paper are affected by the issue concerning the ggF HH prediction for BSM scenarios in POWHEG reported in the erratum of Ref. [81] and do not include the changes to resolve this issue described in Ref. [82]. If the ggF HH signal yields in the analysis categories are scaled based on the ratio of the predicted differential ggF HH cross-sections with and without the changes described in Ref. [82], the width of the 95% CI on κ_λ changes by less than 5%.

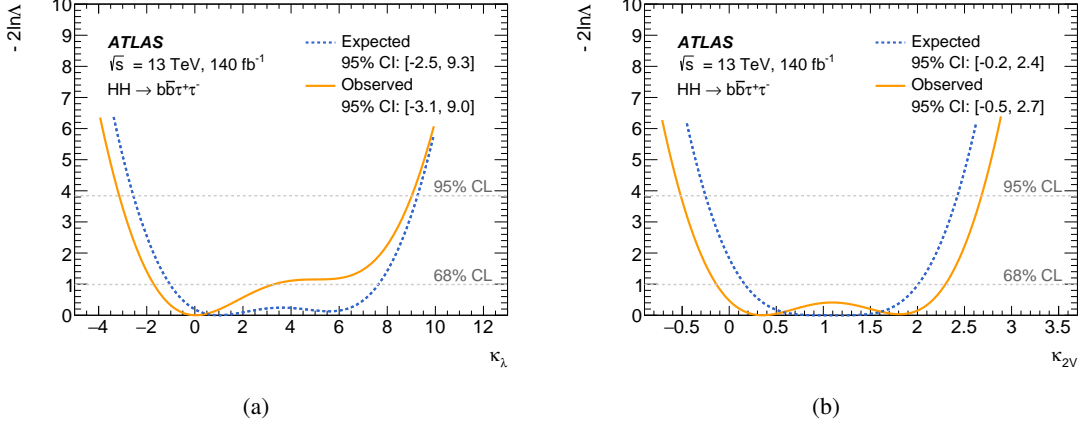


Figure 8: Values of $-2 \ln \Lambda$ for different (a) κ_λ and (b) κ_{2V} hypotheses obtained from fits to the data (solid orange) and an Asimov dataset (dashed blue) constructed under the SM hypothesis. In each case, all coupling modifiers but the scanned parameter are fixed to their SM values.

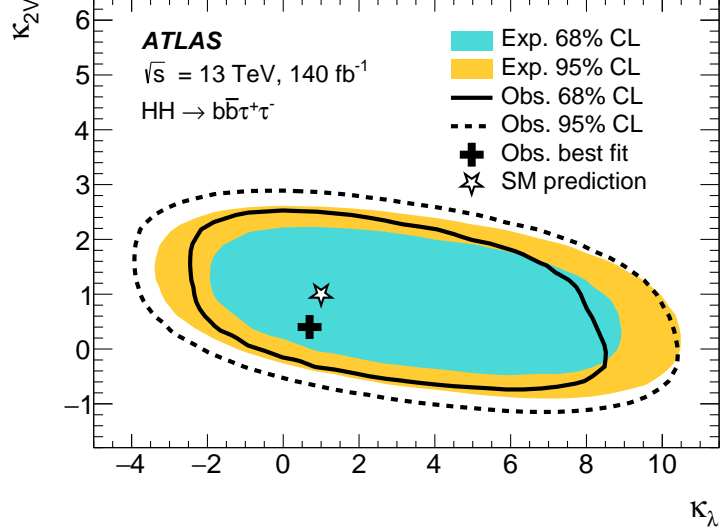


Figure 9: Likelihood contours at 68% (solid line) and 95% (dashed line) CL in the $(\kappa_\lambda, \kappa_{2V})$ parameter space, when all other coupling modifiers are fixed to one. The corresponding expected contours are shown by the inner and outer shaded regions. The SM prediction is indicated by the star, while the best-fit value is denoted by the black cross.

As in Ref. [37], the analysis sensitivity is primarily limited by the statistical uncertainty of the data. The leading systematic uncertainty in the measurement of μ_{HH} is the uncertainty in the ggF HH production cross-section arising from variations of the QCD scales and the top-quark mass scheme. The next leading sources of uncertainty are the statistical precision of the background MC samples and the uncertainty related

to the interference between the Wt and $t\bar{t}$ processes. The combined impact of all sources of systematic uncertainties leads to an increase in the expected upper limits on the signal strength μ_{HH} by 23% and to a widening of the expected 95% CI for κ_λ and κ_{2V} by 9% and 2%, respectively, with respect to the case in which systematic uncertainties are neglected (excluding the $t\bar{t}$ and $Z + \text{HF}$ floating normalisation and MC statistical uncertainties).

Based on a consistent statistical procedure for evaluating the 95% CIs and upper limits as described at the beginning of this section, these results can be compared with the previous analysis of Ref. [37]. The approach presented in this paper leads to an increase (reduction) of the observed (expected) upper limit on the signal strength μ_{HH} by 25% (15%), along with new results for the upper limits on the separate ggF and VBF HH production mode signal strengths. The width of the observed (expected) CI for κ_λ is reduced by < 1% (11%) and the width of the observed (expected) CI for κ_{2V} is reduced by 2% (19%) compared with the previous analysis.

The compatibility, considering statistical and systematic uncertainties, between the upper limit at 95% CL on the signal strength μ_{HH} from this study and that of Ref. [37] is evaluated using a bootstrap technique [83] separately for the independent SR fits and for the combined fit. The compatibility between the two results is at the level of 1σ for the individual fit of the $\tau_{\text{had}}\tau_{\text{had}}$ SR, of 2.5σ for the individual fit of the $\tau_{\text{lep}}\tau_{\text{had}}$ SLT SR, and of 0.1σ for the individual fit of the $\tau_{\text{lep}}\tau_{\text{had}}$ LTT SR. The compatibility is at the level of 0.8σ for the combined fit.

7 Effective field theory interpretation

Effective field theory approaches can be employed to parameterise effects of new particles and anomalous couplings on the HH production rates and Higgs boson decay rates, assuming that the energy scale of the underlying BSM processes is far too high to be probed directly. Interpretations of the results in the context of the Higgs Effective Field Theory (HEFT) and SM Effective Field Theory (SMEFT) are presented in this section, following closely the procedure in Refs. [38, 84].

The SMEFT interpretation is based on the effective Lagrangian

$$\mathcal{L}_{\text{SMEFT}} = \mathcal{L}_{\text{SM}} + \frac{1}{\Lambda_{\text{EFT}}^2} \sum_k c_k^{(6)} O_k^{(6)},$$

where \mathcal{L}_{SM} is the SM Lagrangian and Λ_{EFT} is the energy scale of the new physics phenomena, which is set to 1 TeV. The $c_k^{(6)}$ are the Wilson coefficients corresponding to an operator $O_k^{(6)}$ of mass dimension 6. The Warsaw basis [85] is chosen for the dimension-6 operators, and constraints are placed on the Wilson coefficients c_H and $c_{H\Box}$. They correspond to the operators $(\phi^\dagger\phi)^3$ and $(\phi^\dagger\phi)\Box(\phi^\dagger\phi)$, respectively. While the VBF HH contribution is affected by variations of c_H and $c_{H\Box}$, the SMEFT preserves the Higgs doublet structure of the SM, which implies cancellations between the LO diagrams 2(a) and 2(c). Therefore, the change in the expected VBF HH contribution is small, and the process is ignored for the SMEFT interpretations, as it is dominated by the ggF HH contribution in all considered coupling scenarios.

For the HEFT interpretation, two studies are conducted. First, cross-section limits are placed on the seven m_{HH} shape benchmark scenarios defined in Ref. [86]. As described in Ref. [87], these benchmark scenarios have been determined using a clustering algorithm that identifies distinct shapes of the m_{HH} spectrum that can be obtained by varying five Wilson coefficients in the HEFT framework. In addition to the study of these benchmark scenarios, the Wilson coefficients c_{tthh} and c_{gghh} are considered, which

quantify the strengths of the effective $t\bar{t}HH$ and $ggHH$ couplings, respectively. The Wilson coefficient of the only considered anomalous coupling that affects VBF HH production at NLO precision is c_{hhh} , which is equivalent to κ_λ . Due to the much smaller overall expected yield compared with ggF HH production, and the decorrelation of the two production modes through the event categorisation, the impact of VBF HH contribution on the m_{HH} shape benchmark limits is expected to be negligible, even when taking c_{hhh} variations into account. Hence, it is ignored in the following, i.e., μ_{VBF} is set to 0.

Signal predictions for ggF HH production assuming different effective coupling strengths are obtained from the SM sample. For this purpose, a reweighting method is used that assigns each event a weight corresponding to the ratio of the differential NLO cross-section (in m_{HH}) predicted by the SM and the hypothesis of interest. These weights are taken from Ref. [86]. Possible effects of the anomalous couplings on the Higgs boson branching fractions are neglected. The SMEFT coefficients can also affect single Higgs boson processes. To take these effects on production cross-sections and branching fractions into account, the procedure in Ref. [88] is adopted.

For a continuous parameterisation of the effect of the Wilson coefficients on the predicted ggF HH distributions, the linear combination method described in Ref. [61] is applied to the ggF HH cross-section dependence on the respective Wilson coefficients. The basis samples for the Wilson coefficients are chosen to be close to the 95% CL limits in order to reduce the effect of large cancellations between the basis samples on the obtained results. The values of the couplings ($c_{gg hh}, c_{t\bar{t} hh}, c_{hhh}$) that define the ten samples making up the basis for measuring the HEFT Wilson coefficients are (0, 0, 1), (-0.3, 0, 1), (0.4, 0, 1), (0, -0.2, 1), (0, 0.7, 1), (0, 0, -2.5), (0, 0, 9), (0.4, 0, -2.5), (0, 1, -10), (0.4, -0.2, 1). The six values of ($c_H, c_{H\Box}$) used for the SMEFT interpretation are (0, 0), (-17, 0), (7, 0), (0, -7), (0, 13), (7, -7).

Uncertainties on the ggF HH event yield from the reweighting procedure are derived using comparisons to alternative MC samples generated with different assumed coupling values. They are produced for the seven HEFT m_{HH} shape benchmarks and for $c_{gg hh/t\bar{t} hh} \in \{-0.5, 0.5, 1\}$ using POWHEG Box v2 interfaced with PYTHIA 8.244 for parton showering and hadronisation. The uncertainty assessment for variations in c_H is based on the LO relation $\kappa_\lambda = 1 - 2\frac{v^4}{m_H^2 \Lambda_{\text{EFT}}^2} c_H + 3\frac{v^2}{\Lambda_{\text{EFT}}^2} \left(c_{H\Box} - \frac{1}{4} c_{HD} \right)$ [86], which allows for a comparison to a $\kappa_\lambda = 10$ sample. Here, c_{HD} is the Wilson coefficient corresponding to the dimension-6 operator $(\phi^\dagger D_\mu \phi)^* (\phi^\dagger D^\mu \phi)$. For $c_{H\Box}$, alternative samples with $c_{H\Box} \in \{-9.5, 7\}$ are used. Additionally, the signal modelling uncertainties are evaluated for each signal configuration, as described in Section 5. For scans of Wilson coefficients, the modelling uncertainties are computed for all signal configurations used in the linear combination approach. The maximal obtained deviation is taken as the final value for each source of uncertainty.

The 95% CL upper limits on the ggF HH cross-section assuming the different benchmark m_{HH} shapes are summarised in Figure 10. The following changes are made in the fit model with respect to the measurement of signal strength limits described in Section 6. The ggF HH prediction is replaced depending on the benchmark scenario, while the contribution from VBF HH production is neglected. Moreover, as this is a cross-section measurement, no uncertainties in the ggF HH production cross-section are taken into account. Overall, it is observed that lower average signal m_{HH} values, as represented by benchmarks 1 and 2, lead to weaker constraints.

The Wilson coefficients are probed with the same profile likelihood ratio scan as for κ_λ and κ_{2V} in Section 6. The one-dimensional constraints on the HEFT and SMEFT Wilson coefficients are summarised in Table 4.

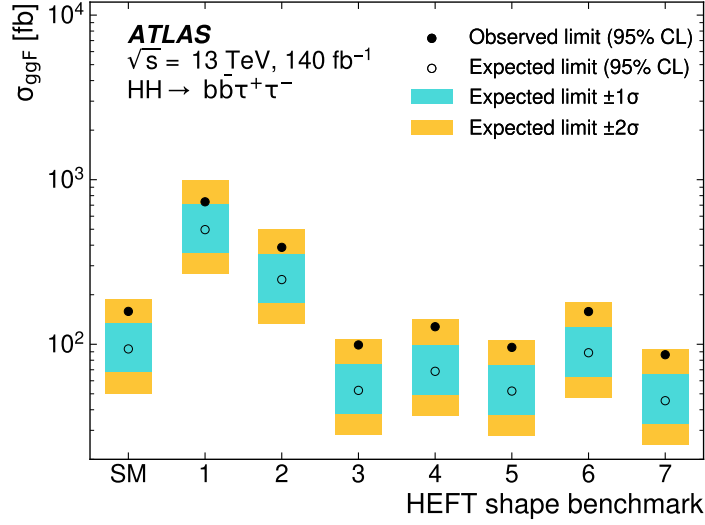


Figure 10: Observed (filled circles) and expected (open circles) 95% CL upper limits on the ggF HH production cross-section with respect to the background-only hypothesis in the SM and each of the seven HEFT shape benchmarks obtained from the combined fit. The inner and outer bands show the $\pm 1\sigma$ and $\pm 2\sigma$ variations on the expected upper limit. The contribution from VBF HH production is neglected for this result.

The observed and expected constraints on the ggF HH cross-section limits assuming the HEFT shape benchmarks shown in Figure 10 and the CIs on individual Wilson coefficients reported in Table 4 are affected by the issue concerning the ggF HH prediction for BSM scenarios in POWHEG reported in the erratum of Ref. [81] and do not include the changes to resolve this issue described in Ref. [82]. If the ggF HH signal yields in the analysis categories are scaled based on the ratio of the predicted differential ggF HH cross-sections with and without the changes described in Ref. [82], the expected limits and CIs changes by less than 10%.

Table 4: Observed and expected 95% CIs on HEFT and SMEFT Wilson coefficients, obtained from one-dimensional scans of $-2 \ln \Lambda$ in fits to the observed data and an Asimov dataset constructed under the SM hypothesis. In each case, only the scanned Wilson coefficient is varied while all others are fixed to their respective SM predicted value. The contribution from VBF HH production is neglected for this result. The SM value for all considered Wilson coefficients is 0, hence no sign of BSM physics is found.

Wilson coefficient	Observed 95% CI	Expected 95% CI
c_{gghh}	[-0.51, 0.58]	[-0.42, 0.44]
c_{tthh}	[-0.40, 0.84]	[-0.32, 0.72]
c_H	[-19.4, 10.0]	[-19.1, 8.6]
$c_{H\Box}$	[-12.6, 11.6]	[-8.5, 11.1]

Two-dimensional 68% and 95% CL likelihood contours are measured for the HEFT Wilson coefficients c_{gghh} and c_{tthh} , respectively, as a function of c_{hhh} . They are shown in Figure 11. In addition, two-dimensional contours are measured for the SMEFT coefficients c_H and $c_{H\Box}$, as shown in Figure 12. The observed non-parabolic features in the two-dimensional contours, such as the double-minimum structure

in Figure 11(b), stem from different best-fit Wilson coefficient values in the $\tau_{\text{lep}}\tau_{\text{had}}$ SLT and $\tau_{\text{had}}\tau_{\text{had}}$ high- m_{HH} categories, which drive the sensitivity of the combined fit. The excess in the SLT high- m_{HH} category leads to a 68% CL rejection of the region between the two 68% CL contours, as those Wilson coefficient combinations correspond to the lowest signal yields. The tighter 68% CL contour at $c_{gghh} \approx 0$ in Figure 11(a) can also be attributed to this excess. As the signal yield is minimal around $c_{hhh} = 3$, for higher c_{hhh} the $-2 \ln \Lambda$ value will decrease in the $\tau_{\text{lep}}\tau_{\text{had}}$ SLT high- m_{HH} category, while it increases in the $\tau_{\text{had}}\tau_{\text{had}}$ high- m_{HH} category that does not feature an excess. Hence, the slope of the combined $-2 \ln \Lambda$ function is small in that region of the parameter space, leading to the observed behaviour. The same effect can also be seen in Figure 8(a).

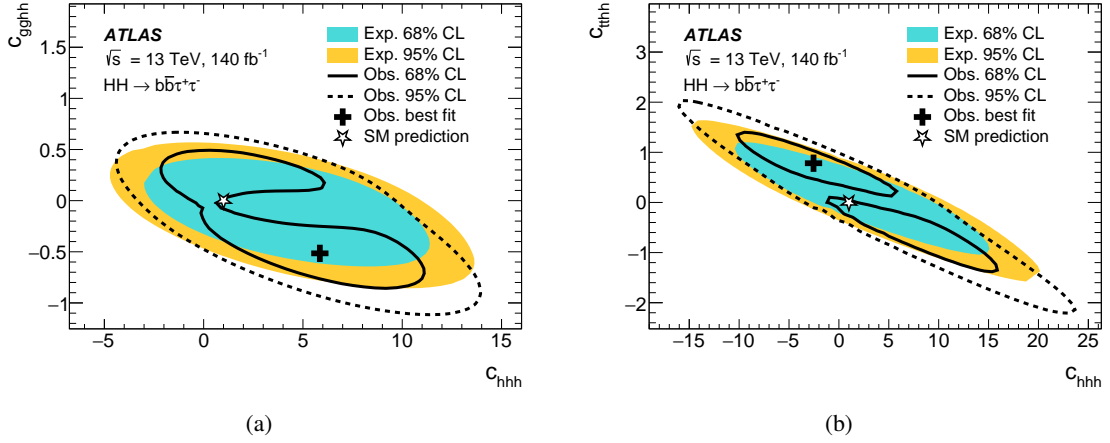


Figure 11: Likelihood contours at 68% (solid line) and 95% (dashed line) CL in (a) the (c_{hhh}, c_{gghh}) and (b) the (c_{hhh}, c_{tthh}) parameter space, when all other Wilson coefficients are fixed to their SM values. The corresponding expected contours are shown by the inner and outer shaded regions. The SM prediction is indicated by the star, while the best-fit value is denoted by the black cross.

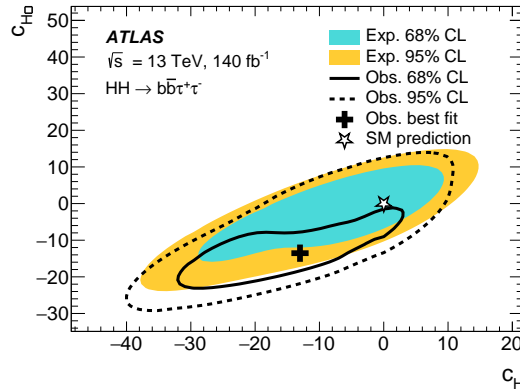


Figure 12: Likelihood contours at 68% (solid line) and 95% (dashed line) CL in the $(c_H, c_{H\Box})$ parameter space, when all other Wilson coefficients are fixed to their SM values. The corresponding expected contours are shown by the inner and outer shaded regions. The SM prediction is indicated by the star, while the best-fit value is denoted by the black cross.

8 Conclusion

An updated search for non-resonant Higgs boson pair production in the $b\bar{b}\tau^+\tau^-$ final state has been performed using the full Run 2 ATLAS dataset, corresponding to 140 fb^{-1} of proton–proton collisions at a centre-of-mass energy of 13 TeV. The results supersede and expand on those of a previous search based on the same dataset described in Ref. [37]. Compared with the previous publication, the event classification has been reoptimised to enhance the sensitivity to κ_λ and to the VBF production mode. Improved multivariate classifiers are used to build the final discriminants, increasing the sensitivity to SM HH production and to anomalous values of the coupling modifiers κ_λ and κ_{2V} . The analysis sensitivity is improved by 11% to 19%, depending on the parameter of interest. Results interpreted in terms of ggF and VBF production modes have been added, compared with the results of Ref. [37]. The statistical procedure for the interpretation of the observed yields in terms of the signal coupling modifiers has been updated from scans of cross-section limits to profile likelihood ratio scans.

No evidence of HH signal is found. An observed 95% CL upper limit of 5.9 is set on the HH production signal strength μ_{HH} , to be compared with an expected limit of 3.3 in the background-only ($\mu_{HH} = 0$) hypothesis. The observed limit on μ_{HH} is looser than the expected one as a result of a mild excess in the $\tau_{\text{lep}}\tau_{\text{had}}$ SLT SR, in the high- m_{HH} category. The corresponding observed (expected) 95% confidence intervals for the self-coupling modifier κ_λ and the quartic coupling modifier κ_{2V} are $-3.1 < \kappa_\lambda < 9.0$ ($-2.5 < \kappa_\lambda < 9.3$) and $-0.5 < \kappa_{2V} < 2.7$ ($-0.2 < \kappa_{2V} < 2.4$), respectively. Based on these improvements, 95% CL upper limits are set on the HH production cross-section in the seven shape benchmark scenarios proposed in Ref. [86]. Moreover, one-dimensional constraints are set on the Wilson coefficients c_H and $c_{H\Box}$ in the SMEFT framework as well as on c_{gghh} and c_{tthh} in the HEFT framework.

Acknowledgements

We thank CERN for the very successful operation of the LHC and its injectors, as well as the support staff at CERN and at our institutions worldwide without whom ATLAS could not be operated efficiently.

The crucial computing support from all WLCG partners is acknowledged gratefully, in particular from CERN, the ATLAS Tier-1 facilities at TRIUMF/SFU (Canada), NDGF (Denmark, Norway, Sweden), CC-IN2P3 (France), KIT/GridKA (Germany), INFN-CNAF (Italy), NL-T1 (Netherlands), PIC (Spain), RAL (UK) and BNL (USA), the Tier-2 facilities worldwide and large non-WLCG resource providers. Major contributors of computing resources are listed in Ref. [89].

We gratefully acknowledge the support of ANPCyT, Argentina; YerPhI, Armenia; ARC, Australia; BMWFW and FWF, Austria; ANAS, Azerbaijan; CNPq and FAPESP, Brazil; NSERC, NRC and CFI, Canada; CERN; ANID, Chile; CAS, MOST and NSFC, China; Minciencias, Colombia; MEYS CR, Czech Republic; DNRF and DNSRC, Denmark; IN2P3-CNRS and CEA-DRF/IRFU, France; SRNSFG, Georgia; BMBF, HGF and MPG, Germany; GSRI, Greece; RGC and Hong Kong SAR, China; ISF and Benozziyo Center, Israel; INFN, Italy; MEXT and JSPS, Japan; CNRST, Morocco; NWO, Netherlands; RCN, Norway; MEiN, Poland; FCT, Portugal; MNE/IFA, Romania; MESTD, Serbia; MSSR, Slovakia; ARRS and MIZŠ, Slovenia; DSI/NRF, South Africa; MICINN, Spain; SRC and Wallenberg Foundation, Sweden; SERI, SNSF and Cantons of Bern and Geneva, Switzerland; MOST, Taipei; TENMAK, Türkiye; STFC, United Kingdom; DOE and NSF, United States of America.

Individual groups and members have received support from BCKDF, CANARIE, CRC and DRAC, Canada; CERN-CZ, PRIMUS 21/SCI/017 and UNCE SCI/013, Czech Republic; COST, ERC, ERDF, Horizon 2020, ICSC-NextGenerationEU and Marie Skłodowska-Curie Actions, European Union; Investissements d’Avenir Labex, Investissements d’Avenir Idex and ANR, France; DFG and AvH Foundation, Germany; Herakleitos, Thales and Aristeia programmes co-financed by EU-ESF and the Greek NSRF, Greece; BSF-NSF and MINERVA, Israel; Norwegian Financial Mechanism 2014-2021, Norway; NCN and NAWA, Poland; La Caixa Banking Foundation, CERCA Programme Generalitat de Catalunya and PROMETEO and GenT Programmes Generalitat Valenciana, Spain; Göran Gustafssons Stiftelse, Sweden; The Royal Society and Leverhulme Trust, United Kingdom.

In addition, individual members wish to acknowledge support from CERN: European Organization for Nuclear Research (CERN PNAS); Chile: Agencia Nacional de Investigación y Desarrollo (FONDECYT 1190886, FONDECYT 1210400, FONDECYT 1230987); China: National Natural Science Foundation of China (NSFC - 12175119, NSFC 12275265); European Union: European Research Council (ERC - 948254, ERC 101089007), Horizon 2020 Framework Programme (MUCCA - CHIST-ERA-19-XAI-00), Italian Center for High Performance Computing, Big Data and Quantum Computing (ICSC, NextGenerationEU); France: Agence Nationale de la Recherche (ANR-20-CE31-0013, ANR-21-CE31-0013, ANR-21-CE31-0022), Investissements d’Avenir Labex (ANR-11-LABX-0012); Germany: Baden-Württemberg Stiftung (BW Stiftung-Postdoc Eliteprogramme), Deutsche Forschungsgemeinschaft (DFG - 469666862, DFG - CR 312/5-2); Italy: Istituto Nazionale di Fisica Nucleare (ICSC, NextGenerationEU); Japan: Japan Society for the Promotion of Science (JSPS KAKENHI 22H01227, JSPS KAKENHI 22KK0227, JSPS KAKENHI JP21H05085, JSPS KAKENHI JP22H04944); Netherlands: Netherlands Organisation for Scientific Research (NWO Veni 2020 - VI.Veni.202.179); Norway: Research Council of Norway (RCN-314472); Poland: Polish National Agency for Academic Exchange (PPN/PPO/2020/1/00002/U/00001), Polish National Science Centre (NCN 2021/42/E/ST2/00350, NCN OPUS nr 2022/47/B/ST2/03059, NCN UMO-2019/34/E/ST2/00393, UMO-2020/37/B/ST2/01043, UMO-2021/40/C/ST2/00187, UMO-2022/47/O/ST2/00148); Slovenia: Slovenian Research Agency (ARIS grant J1-3010); Spain: BBVA Foundation (LEO22-1-603), Generalitat Valenciana (Artemisa, FEDER, IDIFEDER/2018/048), La Caixa Banking Foundation (LCF/BQ/PI20/11760025), Ministry of Science and Innovation (RYC2019-028510-I, RYC2020-030254-I), PROMETEO and GenT Programmes Generalitat Valenciana (CIDEGENT/2019/023, CIDEGENT/2019/027); Sweden: Swedish Research Council (VR 2022-03845, VR 2022-04683), Knut and Alice Wallenberg Foundation (KAW 2017.0100, KAW 2018.0157, KAW 2019.0447, KAW 2022.0358); Switzerland: Swiss National Science Foundation (SNSF - PCEFP2_194658); United Kingdom: Leverhulme Trust (Leverhulme Trust RPG-2020-004); United States of America: Neubauer Family Foundation.

References

- [1] ATLAS Collaboration, *Observation of a new particle in the search for the Standard Model Higgs boson with the ATLAS detector at the LHC*, *Phys. Lett. B* **716** (2012) 1, arXiv: [1207.7214 \[hep-ex\]](#).
- [2] CMS Collaboration, *Observation of a new boson at a mass of 125 GeV with the CMS experiment at the LHC*, *Phys. Lett. B* **716** (2012) 30, arXiv: [1207.7235 \[hep-ex\]](#).
- [3] ATLAS Collaboration, *The ATLAS Experiment at the CERN Large Hadron Collider*, *JINST* **3** (2008) S08003.
- [4] CMS Collaboration, *The CMS Experiment at the CERN LHC*, *JINST* **3** (2008) S08004.
- [5] L. Evans and P. Bryant, *LHC Machine*, *JINST* **3** (2008) S08001.
- [6] ATLAS Collaboration, *Study of the spin and parity of the Higgs boson in diboson decays with the ATLAS detector*, *Eur. Phys. J. C* **75** (2015) 476, arXiv: [1506.05669 \[hep-ex\]](#),
Erratum: *Eur. Phys. J. C* **76** (2016) 152.
- [7] ATLAS Collaboration, *CP Properties of Higgs Boson Interactions with Top Quarks in the $t\bar{t}H$ and tH Processes Using $H \rightarrow \gamma\gamma$ with the ATLAS Detector*, *Phys. Rev. Lett.* **125** (2020) 061802, arXiv: [2004.04545 \[hep-ex\]](#).
- [8] CMS Collaboration, *Constraints on anomalous Higgs boson couplings to vector bosons and fermions in its production and decay using the four-lepton final state*, *Phys. Rev. D* **104** (2021) 052004, arXiv: [2104.12152 \[hep-ex\]](#).
- [9] ATLAS Collaboration, *Evidence of off-shell Higgs boson production from ZZ leptonic decay channels and constraints on its total width with the ATLAS detector*, *Phys. Lett. B* **846** (2023) 138223, arXiv: [2304.01532 \[hep-ex\]](#).
- [10] CMS Collaboration, *Measurement of the Higgs boson width and evidence of its off-shell contributions to ZZ production*, *Nature Phys.* **18** (2022) 1329, arXiv: [2202.06923 \[hep-ex\]](#).
- [11] ATLAS Collaboration, *A detailed map of Higgs boson interactions by the ATLAS experiment ten years after the discovery*, *Nature* **607** (2022) 52, arXiv: [2207.00092 \[hep-ex\]](#).
- [12] CMS Collaboration, *A portrait of the Higgs boson by the CMS experiment ten years after the discovery*, *Nature* **607** (2022) 60, arXiv: [2207.00043 \[hep-ex\]](#).
- [13] F. Englert and R. Brout, *Broken Symmetry and the Mass of Gauge Vector Mesons*, *Phys. Rev. Lett.* **13** (1964) 321.
- [14] P. Higgs, *Broken symmetries, massless particles and gauge fields*, *Phys. Lett.* **12** (1964) 132.
- [15] P. W. Higgs, *Broken Symmetries and the Masses of Gauge Bosons*, *Phys. Rev. Lett.* **13** (1964) 508.
- [16] G. S. Guralnik, C. R. Hagen and T. W. B. Kibble, *Global Conservation Laws and Massless Particles*, *Phys. Rev. Lett.* **13** (1964) 585.
- [17] P. W. Higgs, *Spontaneous Symmetry Breakdown without Massless Bosons*, *Phys. Rev.* **145** (1966) 1156.

- [18] T. W. B. Kibble, *Symmetry Breaking in Non-Abelian Gauge Theories*, [Phys. Rev. **155** \(1967\) 1554](#).
- [19] ATLAS and CMS Collaborations, *Combined Measurement of the Higgs Boson Mass in pp Collisions at $\sqrt{s} = 7$ and 8 TeV with the ATLAS and CMS Experiments*, [Phys. Rev. Lett. **114** \(2015\) 191803](#), arXiv: [1503.07589 \[hep-ex\]](#).
- [20] ATLAS Collaboration, *Combined Measurement of the Higgs Boson Mass from the $H \rightarrow \gamma\gamma$ and $H \rightarrow ZZ^* \rightarrow 4\ell$ Decay Channels with the ATLAS Detector Using $\sqrt{s} = 7, 8,$ and 13 TeV pp Collision Data*, [Phys. Rev. Lett. **131** \(2023\) 251802](#), arXiv: [2308.04775 \[hep-ex\]](#).
- [21] P. Agrawal, D. Saha, L.-X. Xu, J.-H. Yu and C.-P. Yuan, *Determining the shape of the Higgs potential at future colliders*, [Phys. Rev. D **101** \(2020\) 075023](#), arXiv: [1907.02078 \[hep-ph\]](#).
- [22] S. Dawson, S. Dittmaier and M. Spira, *Neutral Higgs-boson pair production at hadron colliders: QCD corrections*, [Phys. Rev. D **58** \(1998\) 115012](#), arXiv: [hep-ph/9805244](#).
- [23] S. Borowka et al., *Higgs Boson Pair Production in Gluon Fusion at Next-to-Leading Order with Full Top-Quark Mass Dependence*, [Phys. Rev. Lett. **117** \(2016\) 012001](#), arXiv: [1604.06447 \[hep-ph\]](#), Erratum: [Phys. Rev. Lett. **117** \(2016\) 079901](#).
- [24] J. Baglio et al., *Gluon fusion into Higgs pairs at NLO QCD and the top mass scheme*, [Eur. Phys. J. C **79** \(2019\) 459](#), arXiv: [1811.05692 \[hep-ph\]](#).
- [25] D. de Florian and J. Mazzitelli, *Higgs Boson Pair Production at Next-to-Next-to-Leading Order in QCD*, [Phys. Rev. Lett. **111** \(2013\) 201801](#), arXiv: [1309.6594 \[hep-ph\]](#).
- [26] D. Y. Shao, C. S. Li, H. T. Li and J. Wang, *Threshold resummation effects in Higgs boson pair production at the LHC*, [JHEP **07** \(2013\) 169](#), arXiv: [1301.1245 \[hep-ph\]](#).
- [27] D. de Florian and J. Mazzitelli, *Higgs pair production at next-to-next-to-leading logarithmic accuracy at the LHC*, [JHEP **09** \(2015\) 053](#), arXiv: [1505.07122 \[hep-ph\]](#).
- [28] M. Grazzini et al., *Higgs boson pair production at NNLO with top quark mass effects*, [JHEP **05** \(2018\) 059](#), arXiv: [1803.02463 \[hep-ph\]](#).
- [29] J. Baglio et al., *$gg \rightarrow HH$: Combined uncertainties*, [Phys. Rev. D **103** \(2021\) 056002](#), arXiv: [2008.11626 \[hep-ph\]](#).
- [30] J. Baglio et al., *The measurement of the Higgs self-coupling at the LHC: theoretical status*, [JHEP **04** \(2013\) 151](#), arXiv: [1212.5581 \[hep-ph\]](#).
- [31] R. Frederix et al., *Higgs pair production at the LHC with NLO and parton-shower effects*, [Phys. Lett. B **732** \(2014\) 142](#), arXiv: [1401.7340 \[hep-ph\]](#).
- [32] L.-S. Ling et al., *NNLO QCD corrections to Higgs pair production via vector boson fusion at hadron colliders*, [Phys. Rev. D **89** \(2014\) 073001](#), arXiv: [1401.7754 \[hep-ph\]](#).
- [33] F. A. Dreyer and A. Karlberg, *Fully differential vector-boson fusion Higgs pair production at next-to-next-to-leading order*, [Phys. Rev. D **99** \(2019\) 074028](#), arXiv: [1811.07918 \[hep-ph\]](#).

- [34] F. A. Dreyer and A. Karlberg, *Vector-boson fusion Higgs pair production at N^3LO* , *Phys. Rev. D* **98** (2018) 114016, arXiv: [1811.07906 \[hep-ph\]](#).
- [35] ATLAS Collaboration, *Constraints on the Higgs boson self-coupling from single- and double-Higgs production with the ATLAS detector using pp collisions at $\sqrt{s} = 13$ TeV*, *Phys. Lett. B* **843** (2023) 137745, arXiv: [2211.01216 \[hep-ex\]](#).
- [36] ATLAS Collaboration, *Search for Higgs boson pair production in the two bottom quarks plus two photons final state in pp collisions at $\sqrt{s} = 13$ TeV with the ATLAS detector*, *Phys. Rev. D* **106** (2022) 052001, arXiv: [2112.11876 \[hep-ex\]](#).
- [37] ATLAS Collaboration, *Search for resonant and non-resonant Higgs boson pair production in the $b\bar{b}\tau^+\tau^-$ decay channel using 13 TeV pp collision data from the ATLAS detector*, *JHEP* **07** (2023) 040, arXiv: [2209.10910 \[hep-ex\]](#).
- [38] ATLAS Collaboration, *Search for nonresonant pair production of Higgs bosons in the $b\bar{b}b\bar{b}$ final state in pp collisions at $\sqrt{s} = 13$ TeV with the ATLAS detector*, *Phys. Rev. D* **108** (2023) 052003, arXiv: [2301.03212 \[hep-ex\]](#).
- [39] CMS Collaboration, *Search for nonresonant Higgs boson pair production in final state with two bottom quarks and two tau leptons in proton–proton collisions at $\sqrt{s} = 13$ TeV*, *Phys. Lett. B* **842** (2023) 137531, arXiv: [2206.09401 \[hep-ex\]](#).
- [40] ATLAS Collaboration, *The ATLAS Collaboration Software and Firmware*, ATL-SOFT-PUB-2021-001, 2021, URL: <https://cds.cern.ch/record/2767187>.
- [41] ATLAS Collaboration, *ATLAS data quality operations and performance for 2015–2018 data-taking*, *JINST* **15** (2020) P04003, arXiv: [1911.04632 \[physics.ins-det\]](#).
- [42] ATLAS Collaboration, *Luminosity determination in pp collisions at $\sqrt{s} = 13$ TeV using the ATLAS detector at the LHC*, *Eur. Phys. J. C* **83** (2023) 982, arXiv: [2212.09379 \[hep-ex\]](#).
- [43] G. Avoni et al., *The new LUCID-2 detector for luminosity measurement and monitoring in ATLAS*, *JINST* **13** (2018) P07017.
- [44] ATLAS Collaboration, *The ATLAS Simulation Infrastructure*, *Eur. Phys. J. C* **70** (2010) 823, arXiv: [1005.4568 \[physics.ins-det\]](#).
- [45] S. Agostinelli et al., *GEANT4 – a simulation toolkit*, *Nucl. Instrum. Meth. A* **506** (2003) 250.
- [46] S. Alioli, P. Nason, C. Oleari and E. Re, *A general framework for implementing NLO calculations in shower Monte Carlo programs: the POWHEG BOX*, *JHEP* **06** (2010) 043, arXiv: [1002.2581 \[hep-ph\]](#).
- [47] NNPDF Collaboration, R. D. Ball et al., *Parton distributions for the LHC run II*, *JHEP* **04** (2015) 040, arXiv: [1410.8849 \[hep-ph\]](#).
- [48] T. Sjöstrand et al., *An introduction to PYTHIA 8.2*, *Comput. Phys. Commun.* **191** (2015) 159, arXiv: [1410.3012 \[hep-ph\]](#).
- [49] ATLAS Collaboration, *ATLAS Pythia 8 tunes to 7 TeV data*, ATL-PHYS-PUB-2014-021, 2014, URL: <https://cds.cern.ch/record/1966419>.
- [50] NNPDF Collaboration, R. D. Ball et al., *Parton distributions with LHC data*, *Nucl. Phys. B* **867** (2013) 244, arXiv: [1207.1303 \[hep-ph\]](#).
- [51] E. Bothmann et al., *Event generation with Sherpa 2.2*, *SciPost Phys.* **7** (2019) 034, arXiv: [1905.09127 \[hep-ph\]](#).

- [52] F. Buccioli et al., *OpenLoops 2*, *Eur. Phys. J. C* **79** (2019) 866, arXiv: [1907.13071 \[hep-ph\]](#).
- [53] F. Cascioli, P. Maierhöfer and S. Pozzorini, *Scattering Amplitudes with Open Loops*, *Phys. Rev. Lett.* **108** (2012) 111601, arXiv: [1111.5206 \[hep-ph\]](#).
- [54] F. Buccioli, S. Pozzorini and M. Zoller, *On-the-fly reduction of open loops*, *Eur. Phys. J. C* **78** (2018) 70, arXiv: [1710.11452 \[hep-ph\]](#).
- [55] A. Denner, S. Dittmaier and L. Hofer, *COLLIER: A fortran-based complex one-loop library in extended regularizations*, *Comput. Phys. Commun.* **212** (2017) 220, arXiv: [1604.06792 \[hep-ph\]](#).
- [56] T. Gleisberg and S. Höche, *Comix, a new matrix element generator*, *JHEP* **12** (2008) 039, arXiv: [0808.3674 \[hep-ph\]](#).
- [57] S. Höche, F. Krauss, M. Schönherr and F. Siegert, *QCD matrix elements + parton showers. The NLO case*, *JHEP* **04** (2013) 027, arXiv: [1207.5030 \[hep-ph\]](#).
- [58] J. Butterworth et al., *PDF4LHC recommendations for LHC Run II*, *J. Phys. G* **43** (2016) 023001, arXiv: [1510.03865 \[hep-ph\]](#).
- [59] ATLAS Collaboration, *Measurement of the Z/γ^* boson transverse momentum distribution in pp collisions at $\sqrt{s} = 7$ TeV with the ATLAS detector*, *JHEP* **09** (2014) 145, arXiv: [1406.3660 \[hep-ex\]](#).
- [60] J. Alwall et al., *The automated computation of tree-level and next-to-leading order differential cross sections, and their matching to parton shower simulations*, *JHEP* **07** (2014) 079, arXiv: [1405.0301 \[hep-ph\]](#).
- [61] ATLAS Collaboration, *Validation of signal Monte Carlo event generation in searches for Higgs boson pairs with the ATLAS detector*, ATL-PHYS-PUB-2019-007, 2019, URL: <https://cds.cern.ch/record/2665057>.
- [62] ATLAS Collaboration, *Search for non-resonant Higgs boson pair production in the $2b + 2\ell + E_T^{\text{miss}}$ final state in pp collisions at $\sqrt{s} = 13$ TeV with the ATLAS detector*, *JHEP* **02** (2024) 037, arXiv: [2310.11286 \[hep-ex\]](#).
- [63] A. Elagin, P. Murat, A. Pranko and A. Safonov, *A new mass reconstruction technique for resonances decaying to $\tau\tau$* , *Nucl. Instrum. Meth. A* **654** (2011) 481, arXiv: [1012.4686 \[hep-ex\]](#).
- [64] ATLAS Collaboration, *ATLAS flavour-tagging algorithms for the LHC Run 2 pp collision dataset*, *Eur. Phys. J. C* **83** (2023) 681, arXiv: [2211.16345 \[physics.data-an\]](#).
- [65] A. Hoecker et al., *TMVA - Toolkit for Multivariate Data Analysis*, 2009, arXiv: [physics/0703039 \[physics.data-an\]](#).
- [66] G. Cowan, K. Cranmer, E. Gross and O. Vitells, *Asymptotic formulae for likelihood-based tests of new physics*, *Eur. Phys. J. C* **71** (2011) 1554, arXiv: [1007.1727 \[physics.data-an\]](#), Erratum: *Eur. Phys. J. C* **73** (2013) 2501.
- [67] C. Bernaciak, M. S. A. Buschmann, A. Butter and T. Plehn, *Fox-Wolfram moments in Higgs physics*, *Phys. Rev. D* **87** (2013) 073014, arXiv: [1212.4436 \[hep-ph\]](#).
- [68] L. A. Spiller, *Modification of Fox-Wolfram moments for hadron colliders*, *JHEP* **03** (2016) 27, arXiv: [1508.03144 \[hep-ph\]](#).

- [69] C. G. Lester, *The transverse mass, M_{T2} , in special cases*, *JHEP* **05** (2011) 76, arXiv: [1103.5682 \[hep-ph\]](#).
- [70] M. L. Graesser and J. Shelton, *Hunting Mixed Top Squark Decays*, *Phys. Rev. Lett.* **111** (2013) 121802, arXiv: [1212.4495 \[hep-ph\]](#).
- [71] J. H. Kim, K. Kong, K. T. Matchev and M. Park, *Probing the Triple Higgs Self-Interaction at the Large Hadron Collider*, *Phys. Rev. Lett.* **122** (2019) 091801, arXiv: [1807.11498 \[hep-ph\]](#).
- [72] R. Barlow and C. Beeston, *Fitting using finite Monte Carlo samples*, *Comput. Phys. Commun.* **77** (1993) 219.
- [73] M. Bähr et al., *Herwig++ physics and manual*, *Eur. Phys. J. C* **58** (2008) 639, arXiv: [0803.0883 \[hep-ph\]](#).
- [74] J. Bellm et al., *Herwig 7.0/Herwig++ 3.0 release note*, *Eur. Phys. J. C* **76** (2016) 196, arXiv: [1512.01178 \[hep-ph\]](#).
- [75] R. Frederix and S. Frixione, *Merging meets matching in MC@NLO*, *JHEP* **12** (2012) 061, arXiv: [1209.6215 \[hep-ph\]](#).
- [76] S. Frixione, E. Laenen, P. Motylinski, C. White and B. R. Webber, *Single-top hadroproduction in association with a W boson*, *JHEP* **07** (2008) 029, arXiv: [0805.3067 \[hep-ph\]](#).
- [77] ATLAS Collaboration, *Measurements of inclusive and differential fiducial cross-sections of $t\bar{t}$ production with additional heavy-flavour jets in proton–proton collisions at $\sqrt{s} = 13$ TeV with the ATLAS detector*, *JHEP* **04** (2019) 046, arXiv: [1811.12113 \[hep-ex\]](#).
- [78] ATLAS Collaboration, *Measurement of the cross-section for W boson production in association with b-jets in pp collisions at $\sqrt{s} = 7$ TeV with the ATLAS detector*, *JHEP* **06** (2013) 084, arXiv: [1302.2929 \[hep-ex\]](#).
- [79] D. de Florian et al., *Handbook of LHC Higgs Cross Sections: 4. Deciphering the Nature of the Higgs Sector*, (2017), arXiv: [1610.07922 \[hep-ph\]](#).
- [80] A. L. Read, *Presentation of search results: the CL_S technique*, *J. Phys. G* **28** (2002) 2693.
- [81] G. Heinrich, J. Lang and L. Scyboz, *SMEFT predictions for $gg \rightarrow hh$ at full NLO QCD and truncation uncertainties*, *JHEP* **08** (2022) 079, arXiv: [2204.13045 \[hep-ph\]](#), Erratum: *JHEP* **10** (2023) 86.
- [82] E. Bagnaschi, G. Degrossi and R. Gröber, *Higgs boson pair production at NLO in the POWHEG approach and the top quark mass uncertainties*, *Eur. Phys. J. C* **83** (2023) 1054, arXiv: [2309.10525 \[hep-ph\]](#).
- [83] K. G. Hayes, M. L. Perl and B. Efron, *Application of the bootstrap statistical method to the tau-decay-mode problem*, *Phys. Rev. D* **39** (1989) 274.
- [84] ATLAS Collaboration, *Studies of new Higgs boson interactions through nonresonant HH production in the $b\bar{b}\gamma\gamma$ final state in pp collisions at $\sqrt{s} = 13$ TeV with the ATLAS detector*, *JHEP* **01** (2024) 066, arXiv: [2310.12301 \[hep-ex\]](#).

- [85] B. Grzadkowski, M. Iskrzyński, M. Misiak and J. Rosiek, *Dimension-six terms in the Standard Model Lagrangian*, *JHEP* **10** (2010) 085, arXiv: [1008.4884 \[hep-ph\]](#).
- [86] L. Alasfar et al., *Effective Field Theory descriptions of Higgs boson pair production*, LHCHWG-2022-004, 2023, arXiv: [2304.01968 \[hep-ph\]](#), URL: <https://cds.cern.ch/record/2843280>.
- [87] M. Capozzi and G. Heinrich, *Exploring anomalous couplings in Higgs boson pair production through shape analysis*, *JHEP* **03** (2020) 091, arXiv: [1908.08923 \[hep-ph\]](#).
- [88] ATLAS Collaboration, *Interpretations of the ATLAS measurements of Higgs boson production and decay rates and differential cross-sections in pp collisions at $\sqrt{s} = 13$ TeV*, (2024), arXiv: [2402.05742 \[hep-ex\]](#).
- [89] ATLAS Collaboration, *ATLAS Computing Acknowledgements*, ATL-SOFT-PUB-2023-001, 2023, URL: <https://cds.cern.ch/record/2869272>.

The ATLAS Collaboration

G. Aad ¹⁰³, E. Aakvaag ¹⁶, B. Abbott ¹²¹, K. Abeling ⁵⁵, N.J. Abicht ⁴⁹, S.H. Abidi ²⁹, M. Aboeela ⁴⁴, A. Aboulhorma ^{35e}, H. Abramowicz ¹⁵², H. Abreu ¹⁵¹, Y. Abulaiti ¹¹⁸, B.S. Acharya ^{69a,69b,1}, A. Ackermann ^{63a}, C. Adam Bourdarios ⁴, L. Adamczyk ^{86a}, S.V. Addepalli ²⁶, M.J. Addison ¹⁰², J. Adelman ¹¹⁶, A. Adiguzel ^{21c}, T. Adaye ¹³⁵, A.A. Affolder ¹³⁷, Y. Afik ³⁹, M.N. Agaras ¹³, J. Agarwala ^{73a,73b}, A. Aggarwal ¹⁰¹, C. Agheorghiesei ^{27c}, A. Ahmad ³⁶, F. Ahmadov ^{38,y}, W.S. Ahmed ¹⁰⁵, S. Ahuja ⁹⁶, X. Ai ^{62e}, G. Aielli ^{76a,76b}, A. Aikot ¹⁶⁴, M. Ait Tamlihat ^{35e}, B. Aitbenkhik ^{35a}, I. Aizenberg ¹⁷⁰, M. Akbiyik ¹⁰¹, T.P.A. Åkesson ⁹⁹, A.V. Akimov ³⁷, D. Akiyama ¹⁶⁹, N.N. Akolkar ²⁴, S. Aktas ^{21a}, K. Al Houry ⁴¹, G.L. Alberghi ^{23b}, J. Albert ¹⁶⁶, P. Albicocco ⁵³, G.L. Albouy ⁶⁰, S. Alderweireldt ⁵², Z.L. Alegria ¹²², M. Aleksa ³⁶, I.N. Aleksandrov ³⁸, C. Alexa ^{27b}, T. Alexopoulos ¹⁰, F. Alfonsi ^{23b}, M. Algren ⁵⁶, M. Alhroob ¹⁴², B. Ali ¹³³, H.M.J. Ali ⁹², S. Ali ¹⁴⁹, S.W. Alibocus ⁹³, M. Aliev ^{33c}, G. Alimonti ^{71a}, W. Alkakh ⁵⁵, C. Allaire ⁶⁶, B.M.M. Allbrooke ¹⁴⁷, J.F. Allen ⁵², C.A. Allendes Flores ^{138f}, P.P. Allport ²⁰, A. Aloisio ^{72a,72b}, F. Alonso ⁹¹, C. Alpigiani ¹³⁹, M. Alvarez Estevez ¹⁰⁰, A. Alvarez Fernandez ¹⁰¹, M. Alves Cardoso ⁵⁶, M.G. Alviggi ^{72a,72b}, M. Aly ¹⁰², Y. Amaral Coutinho ^{83b}, A. Ambler ¹⁰⁵, C. Amelung ³⁶, M. Amerl ¹⁰², C.G. Ames ¹¹⁰, D. Amidei ¹⁰⁷, K.J. Amirie ¹⁵⁶, S.P. Amor Dos Santos ^{131a}, K.R. Amos ¹⁶⁴, V. Ananiev ¹²⁶, C. Anastopoulos ¹⁴⁰, T. Andeen ¹¹, J.K. Anders ³⁶, S.Y. Andreat ^{47a,47b}, A. Andreatza ^{71a,71b}, S. Angelidakis ⁹, A. Angerami ^{41,aa}, A.V. Anisenkov ³⁷, A. Annovi ^{74a}, C. Antel ⁵⁶, M.T. Anthony ¹⁴⁰, E. Antipov ¹⁴⁶, M. Antonelli ⁵³, F. Anulli ^{75a}, M. Aoki ⁸⁴, T. Aoki ¹⁵⁴, J.A. Aparisi Pozo ¹⁶⁴, M.A. Aparo ¹⁴⁷, L. Aperio Bella ⁴⁸, C. Appelt ¹⁸, A. Apyan ²⁶, S.J. Arbiol Val ⁸⁷, C. Arcangeletti ⁵³, A.T.H. Arce ⁵¹, E. Arena ⁹³, J-F. Arguin ¹⁰⁹, S. Argyropoulos ⁵⁴, J.-H. Arling ⁴⁸, O. Arnaez ⁴, H. Arnold ¹¹⁵, G. Artoni ^{75a,75b}, H. Asada ¹¹², K. Asai ¹¹⁹, S. Asai ¹⁵⁴, N.A. Asbah ³⁶, K. Assamagan ²⁹, R. Astalos ^{28a}, S. Atashi ¹⁶⁰, R.J. Atkin ^{33a}, M. Atkinson ¹⁶³, H. Atmani ^{35f}, P.A. Atmasiddha ¹²⁹, K. Augsten ¹³³, S. Auricchio ^{72a,72b}, A.D. Aurio ²⁰, V.A. Austrup ¹⁰², G. Avolio ³⁶, K. Axiotis ⁵⁶, G. Azuelos ^{109,ae}, D. Babal ^{28b}, H. Bachacou ¹³⁶, K. Bachas ^{153,p}, A. Bachi ³⁴, F. Backman ^{47a,47b}, A. Badea ³⁹, T.M. Baer ¹⁰⁷, P. Bagnaia ^{75a,75b}, M. Bahmani ¹⁸, D. Bahner ⁵⁴, K. Bai ¹²⁴, A.J. Bailey ¹⁶⁴, J.T. Baines ¹³⁵, L. Baines ⁹⁵, O.K. Baker ¹⁷³, E. Bakos ¹⁵, D. Bakshi Gupta ⁸, V. Balakrishnan ¹²¹, R. Balasubramanian ¹¹⁵, E.M. Baldin ³⁷, P. Balek ^{86a}, E. Ballabene ^{23b,23a}, F. Balli ¹³⁶, L.M. Baltes ^{63a}, W.K. Balunas ³², J. Balz ¹⁰¹, E. Banas ⁸⁷, M. Bandieramonte ¹³⁰, A. Bandyopadhyay ²⁴, S. Bansal ²⁴, L. Barak ¹⁵², M. Barakat ⁴⁸, E.L. Barberio ¹⁰⁶, D. Barberis ^{57b,57a}, M. Barbero ¹⁰³, M.Z. Barel ¹¹⁵, K.N. Barends ^{33a}, T. Barillari ¹¹¹, M-S. Barisits ³⁶, T. Barklow ¹⁴⁴, P. Baron ¹²³, D.A. Baron Moreno ¹⁰², A. Baroncelli ^{62a}, G. Barone ²⁹, A.J. Barr ¹²⁷, J.D. Barr ⁹⁷, F. Barreiro ¹⁰⁰, J. Barreiro Guimarães da Costa ^{14a}, U. Barron ¹⁵², M.G. Barros Teixeira ^{131a}, S. Barsov ³⁷, F. Bartels ^{63a}, R. Bartoldus ¹⁴⁴, A.E. Barton ⁹², P. Bartos ^{28a}, A. Basan ¹⁰¹, M. Baselga ⁴⁹, A. Bassalat ^{66,b}, M.J. Basso ^{157a}, R.L. Bates ⁵⁹, S. Batlamous ^{35e}, B. Batool ¹⁴², M. Battaglia ¹³⁷, D. Battulga ¹⁸, M. Bauc ^{75a,75b}, M. Bauer ³⁶, P. Bauer ²⁴, L.T. Bazzano Hurrell ³⁰, J.B. Beacham ⁵¹, T. Beau ¹²⁸, J.Y. Beauchamp ⁹¹, P.H. Beauchemin ¹⁵⁹, P. Bechtel ²⁴, H.P. Beck ^{19,o}, K. Becker ¹⁶⁸, A.J. Beddall ⁸², V.A. Bednyakov ³⁸, C.P. Bee ¹⁴⁶, L.J. Beemster ¹⁵, T.A. Beermann ³⁶, M. Begalli ^{83d}, M. Biegel ²⁹, A. Behera ¹⁴⁶, J.K. Behr ⁴⁸, J.F. Beirer ³⁶, F. Beisiegel ²⁴, M. Belfkir ^{117b}, G. Bella ¹⁵², L. Bellagamba ^{23b}, A. Bellerive ³⁴, P. Bellos ²⁰, K. Beloborodov ³⁷, D. Benchechroun ^{35a}, F. Bendebba ^{35a}, Y. Benhammou ¹⁵², K.C. Benkendorfer ⁶¹, L. Beresford ⁴⁸, M. Beretta ⁵³, E. Bergeas Kuutmann ¹⁶², N. Berger ⁴,

B. Bergmann [id133](#), J. Beringer [id17a](#), G. Bernardi [id5](#), C. Bernius [id144](#), F.U. Bernlochner [id24](#),
 F. Bernon [id36,103](#), A. Berrocal Guardia [id13](#), T. Berry [id96](#), P. Berta [id134](#), A. Berthold [id50](#), S. Bethke [id111](#),
 A. Betti [id75a,75b](#), A.J. Bevan [id95](#), N.K. Bhalla [id54](#), M. Bhamjee [id33c](#), S. Bhatta [id146](#),
 D.S. Bhattacharya [id167](#), P. Bhattarai [id144](#), K.D. Bhide [id54](#), V.S. Bhopatkar [id122](#), R.M. Bianchi [id130](#),
 G. Bianco [id23b,23a](#), O. Biebel [id110](#), R. Bielski [id124](#), M. Biglietti [id77a](#), C.S. Billingsley [id44](#), M. Bindi [id55](#),
 A. Bingul [id21b](#), C. Bini [id75a,75b](#), A. Biondini [id93](#), C.J. Birch-sykes [id102](#), G.A. Bird [id32](#), M. Birman [id170](#),
 M. Biros [id134](#), S. Biryukov [id147](#), T. Bisanz [id49](#), E. Bisceglie [id43b,43a](#), J.P. Biswal [id135](#), D. Biswas [id142](#),
 K. Bjørke [id126](#), I. Bloch [id48](#), A. Blue [id59](#), U. Blumenschein [id95](#), J. Blumenthal [id101](#),
 V.S. Bobrovnikov [id37](#), M. Boehler [id54](#), B. Boehm [id167](#), D. Bogavac [id36](#), A.G. Bogdanchikov [id37](#),
 C. Bohm [id47a](#), V. Boisvert [id96](#), P. Bokan [id36](#), T. Bold [id36a](#), M. Bomben [id5](#), M. Bona [id95](#),
 M. Boonekamp [id136](#), C.D. Booth [id96](#), A.G. Borbély [id59](#), I.S. Bordulev [id37](#), H.M. Borecka-Bielska [id109](#),
 G. Borissov [id92](#), D. Bortoletto [id127](#), D. Boscherini [id23b](#), M. Bosman [id13](#), J.D. Bossio Sola [id36](#),
 K. Bouaouda [id35a](#), N. Bouchhar [id164](#), J. Boudreau [id130](#), E.V. Bouhova-Thacker [id92](#), D. Boumediene [id40](#),
 R. Bouquet [id57b,57a](#), A. Boveia [id120](#), J. Boyd [id36](#), D. Boye [id29](#), I.R. Boyko [id38](#), J. Bracinik [id20](#),
 N. Brahim [id4](#), G. Brandt [id172](#), O. Brandt [id32](#), F. Braren [id48](#), B. Brau [id104](#), J.E. Brau [id124](#),
 R. Brenner [id170](#), L. Brenner [id115](#), R. Brenner [id162](#), S. Bressler [id170](#), D. Britton [id59](#), D. Britzger [id111](#),
 I. Brock [id24](#), G. Brooijmans [id41](#), E. Brost [id29](#), L.M. Brown [id166](#), L.E. Bruce [id61](#), T.L. Bruckler [id127](#),
 P.A. Bruckman de Renstrom [id87](#), B. Brüers [id48](#), A. Bruni [id23b](#), G. Bruni [id23b](#), M. Bruschi [id23b](#),
 N. Brusino [id75a,75b](#), T. Buanes [id16](#), Q. Buat [id139](#), D. Buchin [id111](#), A.G. Buckley [id59](#), O. Bulekov [id37](#),
 B.A. Bullard [id144](#), S. Burdin [id93](#), C.D. Burgard [id49](#), A.M. Burger [id36](#), B. Burghgrave [id8](#),
 O. Burlayenko [id54](#), J.T.P. Burr [id32](#), C.D. Burton [id11](#), J.C. Burzynski [id143](#), E.L. Busch [id41](#),
 V. Büscher [id101](#), P.J. Bussey [id59](#), J.M. Butler [id25](#), C.M. Buttar [id59](#), J.M. Butterworth [id97](#),
 W. Buttinger [id135](#), C.J. Buxo Vazquez [id108](#), A.R. Buzykaev [id37](#), S. Cabrera Urbán [id164](#),
 L. Cadamuro [id66](#), D. Caforio [id58](#), H. Cai [id130](#), Y. Cai [id14a,14e](#), Y. Cai [id14c](#), V.M.M. Cairo [id36](#),
 O. Cakir [id3a](#), N. Calace [id36](#), P. Calafura [id17a](#), G. Calderini [id128](#), P. Calfayan [id68](#), G. Callea [id59](#),
 L.P. Caloba [id83b](#), D. Calvet [id40](#), S. Calvet [id40](#), M. Calvetti [id74a,74b](#), R. Camacho Toro [id128](#),
 S. Camarda [id36](#), D. Camarero Munoz [id26](#), P. Camarri [id76a,76b](#), M.T. Camerlingo [id72a,72b](#),
 D. Cameron [id36](#), C. Camincher [id166](#), M. Campanelli [id97](#), A. Camplani [id42](#), V. Canale [id72a,72b](#),
 A.C. Canbay [id3a](#), J. Cantero [id164](#), Y. Cao [id163](#), F. Capocasa [id26](#), M. Capua [id43b,43a](#), A. Carbone [id71a,71b](#),
 R. Cardarelli [id76a](#), J.C.J. Cardenas [id8](#), F. Cardillo [id164](#), G. Carducci [id43b,43a](#), T. Carli [id36](#),
 G. Carlino [id72a](#), J.I. Carlotto [id13](#), B.T. Carlson [id130,q](#), E.M. Carlson [id166,157a](#), L. Carminati [id71a,71b](#),
 A. Carnelli [id136](#), M. Carnesale [id75a,75b](#), S. Caron [id114](#), E. Carquin [id138f](#), S. Carrá [id71a](#),
 G. Carratta [id23b,23a](#), A.M. Carroll [id124](#), T.M. Carter [id52](#), M.P. Casado [id13,i](#), M. Caspar [id48](#),
 F.L. Castillo [id4](#), L. Castillo Garcia [id13](#), V. Castillo Gimenez [id164](#), N.F. Castro [id131a,131e](#),
 A. Catinaccio [id36](#), J.R. Catmore [id126](#), T. Cavaliere [id4](#), V. Cavaliere [id29](#), N. Cavalli [id23b,23a](#),
 Y.C. Cekmecelioglu [id48](#), E. Celebi [id21a](#), S. Cella [id36](#), F. Celli [id127](#), M.S. Centonze [id70a,70b](#),
 V. Cepaitis [id56](#), K. Cerny [id123](#), A.S. Cerqueira [id83a](#), A. Cerri [id147](#), L. Cerrito [id76a,76b](#), F. Cerutti [id17a](#),
 B. Cervato [id142](#), A. Cervelli [id23b](#), G. Cesarini [id53](#), S.A. Cetin [id82](#), D. Chakraborty [id116](#), J. Chan [id17a](#),
 W.Y. Chan [id154](#), J.D. Chapman [id32](#), E. Chapon [id136](#), B. Chargeishvili [id150b](#), D.G. Charlton [id20](#),
 M. Chatterjee [id19](#), C. Chauhan [id134](#), Y. Che [id14c](#), S. Chekanov [id6](#), S.V. Chekulaev [id157a](#),
 G.A. Chelkov [id38,a](#), A. Chen [id107](#), B. Chen [id152](#), B. Chen [id166](#), H. Chen [id14c](#), H. Chen [id29](#),
 J. Chen [id62c](#), J. Chen [id143](#), M. Chen [id127](#), S. Chen [id154](#), S.J. Chen [id14c](#), X. Chen [id62c,136](#),
 X. Chen [id14b,ad](#), Y. Chen [id62a](#), C.L. Cheng [id171](#), H.C. Cheng [id64a](#), S. Cheong [id144](#), A. Cheplakov [id38](#),
 E. Cheremushkina [id48](#), E. Cherepanova [id115](#), R. Cherkaoui El Moursli [id35e](#), E. Cheu [id7](#), K. Cheung [id65](#),
 L. Chevalier [id136](#), V. Chiarella [id53](#), G. Chiarelli [id74a](#), N. Chiedde [id103](#), G. Chiodini [id70a](#),
 A.S. Chisholm [id20](#), A. Chitan [id27b](#), M. Chitishvili [id164](#), M.V. Chizhov [id38](#), K. Choi [id11](#), Y. Chou [id139](#),
 E.Y.S. Chow [id114](#), K.L. Chu [id170](#), M.C. Chu [id64a](#), X. Chu [id14a,14e](#), J. Chudoba [id132](#),

J.J. Chwastowski ⁸⁷, D. Cieri ¹¹¹, K.M. Ciesla ^{86a}, V. Cindro ⁹⁴, A. Ciocio ^{17a}, F. Cirotto ^{72a,72b}, Z.H. Citron ¹⁷⁰, M. Citterio ^{71a}, D.A. Ciubotaru ^{27b}, A. Clark ⁵⁶, P.J. Clark ⁵², C. Clarry ¹⁵⁶, J.M. Clavijo Columbie ⁴⁸, S.E. Clawson ⁴⁸, C. Clement ^{47a,47b}, J. Clercx ⁴⁸, Y. Coadou ¹⁰³, M. Cobal ^{69a,69c}, A. Coccaro ^{57b}, R.F. Coelho Barrue ^{131a}, R. Coelho Lopes De Sa ¹⁰⁴, S. Coelli ^{71a}, B. Cole ⁴¹, J. Collot ⁶⁰, P. Conde Muiño ^{131a,131g}, M.P. Connell ^{33c}, S.H. Connell ^{33c}, E.I. Conroy ¹²⁷, F. Conventi ^{72a,af}, H.G. Cooke ²⁰, A.M. Cooper-Sarkar ¹²⁷, A. Cordeiro Oudot Choi ¹²⁸, L.D. Corpe ⁴⁰, M. Corradi ^{75a,75b}, F. Corriveau ^{105,w}, A. Cortes-Gonzalez ¹⁸, M.J. Costa ¹⁶⁴, F. Costanza ⁴, D. Costanzo ¹⁴⁰, B.M. Cote ¹²⁰, G. Cowan ⁹⁶, K. Cranmer ¹⁷¹, D. Cremonini ^{23b,23a}, S. Crépe-Renaudin ⁶⁰, F. Crescioli ¹²⁸, M. Cristinziani ¹⁴², M. Cristoforetti ^{78a,78b}, V. Croft ¹¹⁵, J.E. Crosby ¹²², G. Crosetti ^{43b,43a}, A. Cueto ¹⁰⁰, T. Cuhadar Donszelmann ¹⁶⁰, H. Cui ^{14a,14e}, Z. Cui ⁷, W.R. Cunningham ⁵⁹, F. Curcio ¹⁶⁴, J.R. Curran ⁵², P. Czodrowski ³⁶, M.M. Czurylo ³⁶, M.J. Da Cunha Sargedas De Sousa ^{57b,57a}, J.V. Da Fonseca Pinto ^{83b}, C. Da Via ¹⁰², W. Dabrowski ^{86a}, T. Dado ⁴⁹, S. Dahbi ¹⁴⁹, T. Dai ¹⁰⁷, D. Dal Santo ¹⁹, C. Dallapiccola ¹⁰⁴, M. Dam ⁴², G. D'amen ²⁹, V. D'Amico ¹¹⁰, J. Damp ¹⁰¹, J.R. Dandoy ³⁴, M. Danninger ¹⁴³, V. Dao ³⁶, G. Darbo ^{57b}, S. Darmora ⁶, S.J. Das ^{29,ag}, S. D'Auria ^{71a,71b}, A. D'Avanzo ^{72a,72b}, C. David ^{33a}, T. Davidek ¹³⁴, B. Davis-Purcell ³⁴, I. Dawson ⁹⁵, H.A. Day-hall ¹³³, K. De ⁸, R. De Asmundis ^{72a}, N. De Biase ⁴⁸, S. De Castro ^{23b,23a}, N. De Groot ¹¹⁴, P. de Jong ¹¹⁵, H. De la Torre ¹¹⁶, A. De Maria ^{14c}, A. De Salvo ^{75a}, U. De Sanctis ^{76a,76b}, F. De Santis ^{70a,70b}, A. De Santo ¹⁴⁷, J.B. De Vivie De Regie ⁶⁰, D.V. Dedovich ³⁸, J. Degens ⁹³, A.M. Deiana ⁴⁴, F. Del Corso ^{23b,23a}, J. Del Peso ¹⁰⁰, F. Del Rio ^{63a}, L. Delagrangé ¹²⁸, F. Deliot ¹³⁶, C.M. Delitzsch ⁴⁹, M. Della Pietra ^{72a,72b}, D. Della Volpe ⁵⁶, A. Dell'Acqua ³⁶, L. Dell'Asta ^{71a,71b}, M. Delmastro ⁴, P.A. Delsart ⁶⁰, S. Demers ¹⁷³, M. Demichev ³⁸, S.P. Denisov ³⁷, L. D'Eramo ⁴⁰, D. Derendarz ⁸⁷, F. Derue ¹²⁸, P. Dervan ⁹³, K. Desch ²⁴, C. Deutsch ²⁴, F.A. Di Bello ^{57b,57a}, A. Di Ciaccio ^{76a,76b}, L. Di Ciaccio ⁴, A. Di Domenico ^{75a,75b}, C. Di Donato ^{72a,72b}, A. Di Girolamo ³⁶, G. Di Gregorio ³⁶, A. Di Luca ^{78a,78b}, B. Di Micco ^{77a,77b}, R. Di Nardo ^{77a,77b}, M. Diamantopoulou ³⁴, F.A. Dias ¹¹⁵, T. Dias Do Vale ¹⁴³, M.A. Diaz ^{138a,138b}, F.G. Diaz Capriles ²⁴, M. Didenko ¹⁶⁴, E.B. Diehl ¹⁰⁷, S. Díez Cornell ⁴⁸, C. Diez Pardos ¹⁴², C. Dimitriadi ^{162,24}, A. Dimitrievska ^{17a}, J. Dingfelder ²⁴, I-M. Dinu ^{27b}, S.J. Dittmeier ^{63b}, F. Dittus ³⁶, M. Divisek ¹³⁴, F. Djama ¹⁰³, T. Djobava ^{150b}, C. Doglioni ^{102,99}, A. Dohnalova ^{28a}, J. Dolejsi ¹³⁴, Z. Dolezal ¹³⁴, K.M. Dona ³⁹, M. Donadelli ^{83c}, B. Dong ¹⁰⁸, J. Donini ⁴⁰, A. D'Onofrio ^{72a,72b}, M. D'Onofrio ⁹³, J. Dopke ¹³⁵, A. Doria ^{72a}, N. Dos Santos Fernandes ^{131a}, P. Dougan ¹⁰², M.T. Dova ⁹¹, A.T. Doyle ⁵⁹, M.A. Dragnet ¹²⁷, E. Dreyer ¹⁷⁰, I. Drivas-koulouris ¹⁰, M. Drnevich ¹¹⁸, M. Drozdova ⁵⁶, D. Du ^{62a}, T.A. du Pree ¹¹⁵, F. Dubinin ³⁷, M. Dubovsky ^{28a}, E. Duchovni ¹⁷⁰, G. Duckeck ¹¹⁰, O.A. Ducu ^{27b}, D. Duda ⁵², A. Dudarev ³⁶, E.R. Duden ²⁶, M. D'uffizi ¹⁰², L. Duflot ⁶⁶, M. Dührssen ³⁶, A.E. Dumitriu ^{27b}, M. Dunford ^{63a}, S. Dungs ⁴⁹, K. Dunne ^{47a,47b}, A. Duperrin ¹⁰³, H. Duran Yildiz ^{3a}, M. Düren ⁵⁸, A. Durglishvili ^{150b}, B.L. Dwyer ¹¹⁶, G.I. Dyckes ^{17a}, M. Dyndal ^{86a}, B.S. Dziedzic ⁸⁷, Z.O. Earnshaw ¹⁴⁷, G.H. Eberwein ¹²⁷, B. Eckerova ^{28a}, S. Eggebrecht ⁵⁵, E. Egidio Purcino De Souza ¹²⁸, L.F. Ehrke ⁵⁶, G. Eigen ¹⁶, K. Einsweiler ^{17a}, T. Ekelof ¹⁶², P.A. Ekman ⁹⁹, S. El Farkh ^{35b}, Y. El Ghazali ^{35b}, H. El Jarrari ³⁶, A. El Moussaouy ¹⁰⁹, V. Ellajosyula ¹⁶², M. Ellert ¹⁶², F. Ellinghaus ¹⁷², N. Ellis ³⁶, J. Elmsheuser ²⁹, M. Elsayy ^{117a}, M. Elsing ³⁶, D. Emelianov ¹³⁵, Y. Enari ¹⁵⁴, I. Ene ^{17a}, S. Epari ¹³, P.A. Erland ⁸⁷, M. Errenst ¹⁷², M. Escalier ⁶⁶, C. Escobar ¹⁶⁴, E. Etzion ¹⁵², G. Evans ^{131a}, H. Evans ⁶⁸, L.S. Evans ⁹⁶, A. Ezhilov ³⁷, S. Ezzarqtouni ^{35a}, F. Fabbri ^{23b,23a}, L. Fabbri ^{23b,23a}, G. Facini ⁹⁷, V. Fadeyev ¹³⁷, R.M. Fakhrutdinov ³⁷, D. Fakoudis ¹⁰¹, S. Falciano ^{75a}, L.F. Falda Ulhoa Coelho ³⁶, P.J. Falke ²⁴, J. Faltova ¹³⁴,

C. Fan ¹⁶³, Y. Fan ^{14a}, Y. Fang ^{14a,14e}, M. Fanti ^{71a,71b}, M. Faraj ^{69a,69b}, Z. Farazpay ⁹⁸, A. Farbin ⁸, A. Farilla ^{77a}, T. Farooque ¹⁰⁸, S.M. Farrington ⁵², F. Fassi ^{35e}, D. Fassouliotis ⁹, M. Faucci Giannelli ^{76a,76b}, W.J. Fawcett ³², L. Fayard ⁶⁶, P. Federic ¹³⁴, P. Federicova ¹³², O.L. Fedin ^{37,a}, M. Feickert ¹⁷¹, L. Feligioni ¹⁰³, D.E. Fellers ¹²⁴, C. Feng ^{62b}, M. Feng ^{14b}, Z. Feng ¹¹⁵, M.J. Fenton ¹⁶⁰, L. Ferencz ⁴⁸, R.A.M. Ferguson ⁹², S.I. Fernandez Luengo ^{138f}, P. Fernandez Martinez ¹³, M.J.V. Fernoux ¹⁰³, J. Ferrando ⁹², A. Ferrari ¹⁶², P. Ferrari ^{115,114}, R. Ferrari ^{73a}, D. Ferrere ⁵⁶, C. Ferretti ¹⁰⁷, F. Fiedler ¹⁰¹, P. Fiedler ¹³³, A. Filipčič ⁹⁴, E.K. Filmer ¹, F. Filthaut ¹¹⁴, M.C.N. Fiolhais ^{131a,131c,c}, L. Fiorini ¹⁶⁴, W.C. Fisher ¹⁰⁸, T. Fitschen ¹⁰², P.M. Fitzhugh ¹³⁶, I. Fleck ¹⁴², P. Fleischmann ¹⁰⁷, T. Flick ¹⁷², M. Flores ^{33d,ab}, L.R. Flores Castillo ^{64a}, L. Flores Sanz De Acedo ³⁶, F.M. Follega ^{78a,78b}, N. Fomin ¹⁶, J.H. Foo ¹⁵⁶, A. Formica ¹³⁶, A.C. Forti ¹⁰², E. Fortin ³⁶, A.W. Fortman ^{17a}, M.G. Foti ^{17a}, L. Fountas ^{9j}, D. Fournier ⁶⁶, H. Fox ⁹², P. Francavilla ^{74a,74b}, S. Francescato ⁶¹, S. Franchellucci ⁵⁶, M. Franchini ^{23b,23a}, S. Franchino ^{63a}, D. Francis ³⁶, L. Franco ¹¹⁴, V. Franco Lima ³⁶, L. Franconi ⁴⁸, M. Franklin ⁶¹, G. Frattari ²⁶, W.S. Freund ^{83b}, Y.Y. Frid ¹⁵², J. Friend ⁵⁹, N. Fritzsche ⁵⁰, A. Froch ⁵⁴, D. Froidevaux ³⁶, J.A. Frost ¹²⁷, Y. Fu ^{62a}, S. Fuenzalida Garrido ^{138f}, M. Fujimoto ¹⁰³, K.Y. Fung ^{64a}, E. Furtado De Simas Filho ^{83e}, M. Furukawa ¹⁵⁴, J. Fuster ¹⁶⁴, A. Gabrielli ^{23b,23a}, A. Gabrielli ¹⁵⁶, P. Gadow ³⁶, G. Gagliardi ^{57b,57a}, L.G. Gagnon ^{17a}, S. Galantzan ¹⁵², E.J. Gallas ¹²⁷, B.J. Gallop ¹³⁵, K.K. Gan ¹²⁰, S. Ganguly ¹⁵⁴, Y. Gao ⁵², F.M. Garay Walls ^{138a,138b}, B. Garcia ²⁹, C. García ¹⁶⁴, A. Garcia Alonso ¹¹⁵, A.G. Garcia Caffaro ¹⁷³, J.E. García Navarro ¹⁶⁴, M. Garcia-Sciveres ^{17a}, G.L. Gardner ¹²⁹, R.W. Gardner ³⁹, N. Garelli ¹⁵⁹, D. Garg ⁸⁰, R.B. Garg ^{144,m}, J.M. Gargan ⁵², C.A. Garner ¹⁵⁶, C.M. Garvey ^{33a}, P. Gaspar ^{83b}, V.K. Gassmann ¹⁵⁹, G. Gaudio ^{73a}, V. Gautam ¹³, P. Gauzzi ^{75a,75b}, I.L. Gavrilenko ³⁷, A. Gavrilyuk ³⁷, C. Gay ¹⁶⁵, G. Gaycken ⁴⁸, E.N. Gazis ¹⁰, A.A. Geanta ^{27b}, C.M. Gee ¹³⁷, A. Gekow ¹²⁰, C. Gemme ^{57b}, M.H. Genest ⁶⁰, A.D. Gentry ¹¹³, S. George ⁹⁶, W.F. George ²⁰, T. Gerialis ⁴⁶, P. Gessinger-Befurt ³⁶, M.E. Geyik ¹⁷², M. Ghani ¹⁶⁸, M. Ghneimat ¹⁴², K. Ghorbanian ⁹⁵, A. Ghosal ¹⁴², A. Ghosh ¹⁶⁰, A. Ghosh ⁷, B. Giacobbe ^{23b}, S. Giagu ^{75a,75b}, T. Giani ¹¹⁵, P. Giannetti ^{74a}, A. Giannini ^{62a}, S.M. Gibson ⁹⁶, M. Gignac ¹³⁷, D.T. Gil ^{86b}, A.K. Gilbert ^{86a}, B.J. Gilbert ⁴¹, D. Gillberg ³⁴, G. Gilles ¹¹⁵, L. Ginabat ¹²⁸, D.M. Gingrich ^{2,ae}, M.P. Giordani ^{69a,69c}, P.F. Giraud ¹³⁶, G. Giugliarelli ^{69a,69c}, D. Giugni ^{71a}, F. Giuli ³⁶, I. Gkialas ^{9j}, L.K. Gladilin ³⁷, C. Glasman ¹⁰⁰, G.R. Gledhill ¹²⁴, G. Glemža ⁴⁸, M. Glisic ¹²⁴, I. Gnesi ^{43b,f}, Y. Go ²⁹, M. Goblirsch-Kolb ³⁶, B. Gocke ⁴⁹, D. Godin ¹⁰⁹, B. Gokturk ^{21a}, S. Goldfarb ¹⁰⁶, T. Golling ⁵⁶, M.G.D. Gololo ^{33g}, D. Golubkov ³⁷, J.P. Gombas ¹⁰⁸, A. Gomes ^{131a,131b}, G. Gomes Da Silva ¹⁴², A.J. Gomez Delegido ¹⁶⁴, R. Gonçalves ^{131a,131c}, L. Gonella ²⁰, A. Gongadze ^{150c}, F. Gonnella ²⁰, J.L. Gonski ¹⁴⁴, R.Y. González Andana ⁵², S. González de la Hoz ¹⁶⁴, R. Gonzalez Lopez ⁹³, C. Gonzalez Renteria ^{17a}, M.V. Gonzalez Rodrigues ⁴⁸, R. Gonzalez Suarez ¹⁶², S. Gonzalez-Sevilla ⁵⁶, L. Goossens ³⁶, B. Gorini ³⁶, E. Gorini ^{70a,70b}, A. Gorišek ⁹⁴, T.C. Gosart ¹²⁹, A.T. Goshaw ⁵¹, M.I. Gostkin ³⁸, S. Goswami ¹²², C.A. Gottardo ³⁶, S.A. Gotz ¹¹⁰, M. Goughri ^{35b}, V. Goumarre ⁴⁸, A.G. Goussiou ¹³⁹, N. Govender ^{33c}, I. Grabowska-Bold ^{86a}, K. Graham ³⁴, E. Gramstad ¹²⁶, S. Grancagnolo ^{70a,70b}, C.M. Grant ^{1,136}, P.M. Gravila ^{27f}, F.G. Gravili ^{70a,70b}, H.M. Gray ^{17a}, M. Greco ^{70a,70b}, C. Grefe ²⁴, I.M. Gregor ⁴⁸, P. Grenier ¹⁴⁴, S.G. Grewe ¹¹¹, A.A. Grillo ¹³⁷, K. Grimm ³¹, S. Grinstein ^{13,s}, J.-F. Grivaz ⁶⁶, E. Gross ¹⁷⁰, J. Grosse-Knetter ⁵⁵, J.C. Grundy ¹²⁷, L. Guan ¹⁰⁷, C. Gubbels ¹⁶⁵, J.G.R. Guerrero Rojas ¹⁶⁴, G. Guerrieri ^{69a,69c}, F. Guescini ¹¹¹, R. Gugel ¹⁰¹, J.A.M. Guhit ¹⁰⁷, A. Guida ¹⁸, E. Guilloton ¹⁶⁸, S. Guindon ³⁶, F. Guo ^{14a,14e}, J. Guo ^{62c}, L. Guo ⁴⁸, Y. Guo ¹⁰⁷, R. Gupta ⁴⁸, R. Gupta ¹³⁰, S. Gurbuz ²⁴, S.S. Gurdasani ⁵⁴, G. Gustavino ³⁶, M. Guth ⁵⁶, P. Gutierrez ¹²¹, L.F. Gutierrez Zagazeta ¹²⁹, M. Gutsche ⁵⁰, C. Gutschow ⁹⁷, C. Gwenlan ¹²⁷,

C.B. Gwilliam [id⁹³](#), E.S. Haaland [id¹²⁶](#), A. Haas [id¹¹⁸](#), M. Habedank [id⁴⁸](#), C. Haber [id^{17a}](#),
 H.K. Hadavand [id⁸](#), A. Hadeef [id⁵⁰](#), S. Hadzic [id¹¹¹](#), A.I. Hagan [id⁹²](#), J.J. Hahn [id¹⁴²](#), E.H. Haines [id⁹⁷](#),
 M. Haleem [id¹⁶⁷](#), J. Haley [id¹²²](#), J.J. Hall [id¹⁴⁰](#), G.D. Hallelwell [id¹⁰³](#), L. Halser [id¹⁹](#), K. Hamano [id¹⁶⁶](#),
 M. Hamer [id²⁴](#), G.N. Hamity [id⁵²](#), E.J. Hampshire [id⁹⁶](#), J. Han [id^{62b}](#), K. Han [id^{62a}](#), L. Han [id^{14c}](#),
 L. Han [id^{62a}](#), S. Han [id^{17a}](#), Y.F. Han [id¹⁵⁶](#), K. Hanagaki [id⁸⁴](#), M. Hance [id¹³⁷](#), D.A. Hangal [id⁴¹](#),
 H. Hanif [id¹⁴³](#), M.D. Hank [id¹²⁹](#), J.B. Hansen [id⁴²](#), P.H. Hansen [id⁴²](#), K. Hara [id¹⁵⁸](#), D. Harada [id⁵⁶](#),
 T. Harenberg [id¹⁷²](#), S. Harkusha [id³⁷](#), M.L. Harris [id¹⁰⁴](#), Y.T. Harris [id¹²⁷](#), J. Harrison [id¹³](#),
 N.M. Harrison [id¹²⁰](#), P.F. Harrison [id¹⁶⁸](#), N.M. Hartman [id¹¹¹](#), N.M. Hartmann [id¹¹⁰](#), Y. Hasegawa [id¹⁴¹](#),
 F. Haslbeck [id¹²⁷](#), R. Hauser [id¹⁰⁸](#), C.M. Hawkes [id²⁰](#), R.J. Hawkings [id³⁶](#), Y. Hayashi [id¹⁵⁴](#),
 S. Hayashida [id¹¹²](#), D. Hayden [id¹⁰⁸](#), C. Hayes [id¹⁰⁷](#), R.L. Hayes [id¹¹⁵](#), C.P. Hays [id¹²⁷](#), J.M. Hays [id⁹⁵](#),
 H.S. Hayward [id⁹³](#), F. He [id^{62a}](#), M. He [id^{14a,14e}](#), Y. He [id¹⁵⁵](#), Y. He [id⁴⁸](#), Y. He [id⁹⁷](#), N.B. Heatley [id⁹⁵](#),
 V. Hedberg [id⁹⁹](#), A.L. Heggelund [id¹²⁶](#), N.D. Hehir [id^{95,*}](#), C. Heidegger [id⁵⁴](#), K.K. Heidegger [id⁵⁴](#),
 W.D. Heidorn [id⁸¹](#), J. Heilman [id³⁴](#), S. Heim [id⁴⁸](#), T. Heim [id^{17a}](#), J.G. Heinlein [id¹²⁹](#), J.J. Heinrich [id¹²⁴](#),
 L. Heinrich [id^{111,ac}](#), J. Hejbal [id¹³²](#), A. Held [id¹⁷¹](#), S. Hellesund [id¹⁶](#), C.M. Helling [id¹⁶⁵](#),
 S. Hellman [id^{47a,47b}](#), R.C.W. Henderson [id⁹²](#), L. Henkelmann [id³²](#), A.M. Henriques Correia [id³⁶](#), H. Herde [id⁹⁹](#),
 Y. Hernández Jiménez [id¹⁴⁶](#), L.M. Herrmann [id²⁴](#), T. Herrmann [id⁵⁰](#), G. Herten [id⁵⁴](#), R. Hertenberger [id¹¹⁰](#),
 L. Hervas [id³⁶](#), M.E. Hesping [id¹⁰¹](#), N.P. Hessey [id^{157a}](#), E. Hill [id¹⁵⁶](#), S.J. Hillier [id²⁰](#), J.R. Hinds [id¹⁰⁸](#),
 F. Hinterkeuser [id²⁴](#), M. Hirose [id¹²⁵](#), S. Hirose [id¹⁵⁸](#), D. Hirschbuehl [id¹⁷²](#), T.G. Hitchings [id¹⁰²](#),
 B. Hiti [id⁹⁴](#), J. Hobbs [id¹⁴⁶](#), R. Hobincu [id^{27e}](#), N. Hod [id¹⁷⁰](#), M.C. Hodgkinson [id¹⁴⁰](#),
 B.H. Hodgkinson [id¹²⁷](#), A. Hoecker [id³⁶](#), D.D. Hofer [id¹⁰⁷](#), J. Hofer [id⁴⁸](#), T. Holm [id²⁴](#), M. Holzbock [id¹¹¹](#),
 L.B.A.H. Hommels [id³²](#), B.P. Honan [id¹⁰²](#), J. Hong [id^{62c}](#), T.M. Hong [id¹³⁰](#), B.H. Hooberman [id¹⁶³](#),
 W.H. Hopkins [id⁶](#), Y. Horii [id¹¹²](#), S. Hou [id¹⁴⁹](#), A.S. Howard [id⁹⁴](#), J. Howarth [id⁵⁹](#), J. Hoya [id⁶](#),
 M. Hrabovsky [id¹²³](#), A. Hrynevich [id⁴⁸](#), T. Hryn'ova [id⁴](#), P.J. Hsu [id⁶⁵](#), S.-C. Hsu [id¹³⁹](#), Q. Hu [id^{62a}](#),
 S. Huang [id^{64b}](#), X. Huang [id^{14a,14e}](#), Y. Huang [id¹⁴⁰](#), Y. Huang [id^{14a}](#), Z. Huang [id¹⁰²](#), Z. Hubacek [id¹³³](#),
 M. Huebner [id²⁴](#), F. Huegging [id²⁴](#), T.B. Huffman [id¹²⁷](#), C.A. Hugli [id⁴⁸](#), M. Huhtinen [id³⁶](#),
 S.K. Huiberts [id¹⁶](#), R. Hulsken [id¹⁰⁵](#), N. Huseynov [id¹²](#), J. Huston [id¹⁰⁸](#), J. Huth [id⁶¹](#), R. Hyneman [id¹⁴⁴](#),
 G. Iacobucci [id⁵⁶](#), G. Iakovidis [id²⁹](#), I. Ibragimov [id¹⁴²](#), L. Iconomidou-Fayard [id⁶⁶](#), J.P. Iddon [id³⁶](#),
 P. Iengo [id^{72a,72b}](#), R. Iguchi [id¹⁵⁴](#), T. Iizawa [id¹²⁷](#), Y. Ikegami [id⁸⁴](#), N. Ilic [id¹⁵⁶](#), H. Imam [id^{35a}](#),
 M. Ince Lezki [id⁵⁶](#), T. Ingebretsen Carlson [id^{47a,47b}](#), G. Introzzi [id^{73a,73b}](#), M. Iodice [id^{77a}](#),
 V. Ippolito [id^{75a,75b}](#), R.K. Irwin [id⁹³](#), M. Ishino [id¹⁵⁴](#), W. Islam [id¹⁷¹](#), C. Issever [id^{18,48}](#), S. Istin [id^{21a,ai}](#),
 H. Ito [id¹⁶⁹](#), R. Iuppa [id^{78a,78b}](#), A. Ivina [id¹⁷⁰](#), J.M. Izen [id⁴⁵](#), V. Izzo [id^{72a}](#), P. Jacka [id^{132,133}](#), P. Jackson [id¹](#),
 B.P. Jaeger [id¹⁴³](#), C.S. Jagfeld [id¹¹⁰](#), G. Jain [id^{157a}](#), P. Jain [id⁵⁴](#), K. Jakobs [id⁵⁴](#), T. Jakoubek [id¹⁷⁰](#),
 J. Jamieson [id⁵⁹](#), K.W. Janas [id^{86a}](#), M. Javurkova [id¹⁰⁴](#), L. Jeanty [id¹²⁴](#), J. Jejelava [id^{150a,z}](#), P. Jenni [id^{54,g}](#),
 C.E. Jessiman [id³⁴](#), C. Jia [id^{62b}](#), J. Jia [id¹⁴⁶](#), X. Jia [id⁶¹](#), X. Jia [id^{14a,14e}](#), Z. Jia [id^{14c}](#), S. Jiggins [id⁴⁸](#),
 J. Jimenez Pena [id¹³](#), S. Jin [id^{14c}](#), A. Jinaru [id^{27b}](#), O. Jinnouchi [id¹⁵⁵](#), P. Johansson [id¹⁴⁰](#), K.A. Johns [id⁷](#),
 J.W. Johnson [id¹³⁷](#), D.M. Jones [id³²](#), E. Jones [id⁴⁸](#), P. Jones [id³²](#), R.W.L. Jones [id⁹²](#), T.J. Jones [id⁹³](#),
 H.L. Joos [id^{55,36}](#), R. Joshi [id¹²⁰](#), J. Jovicevic [id¹⁵](#), X. Ju [id^{17a}](#), J.J. Junggeburth [id¹⁰⁴](#), T. Junkermann [id^{63a}](#),
 A. Juste Rozas [id^{13,s}](#), M.K. Juzek [id⁸⁷](#), S. Kabana [id^{138e}](#), A. Kaczmarska [id⁸⁷](#), M. Kado [id¹¹¹](#),
 H. Kagan [id¹²⁰](#), M. Kagan [id¹⁴⁴](#), A. Kahn [id⁴¹](#), A. Kahn [id¹²⁹](#), C. Kahra [id¹⁰¹](#), T. Kaji [id¹⁵⁴](#),
 E. Kajomovitz [id¹⁵¹](#), N. Kakati [id¹⁷⁰](#), I. Kalaitzidou [id⁵⁴](#), C.W. Kalderon [id²⁹](#), N.J. Kang [id¹³⁷](#),
 D. Kar [id^{33g}](#), K. Karava [id¹²⁷](#), M.J. Kareem [id^{157b}](#), E. Karentzos [id⁵⁴](#), I. Karkanias [id¹⁵³](#), O. Karkout [id¹¹⁵](#),
 S.N. Karpov [id³⁸](#), Z.M. Karpova [id³⁸](#), V. Kartvelishvili [id⁹²](#), A.N. Karyukhin [id³⁷](#), E. Kasimi [id¹⁵³](#),
 J. Katzy [id⁴⁸](#), S. Kaur [id³⁴](#), K. Kawade [id¹⁴¹](#), M.P. Kawale [id¹²¹](#), C. Kawamoto [id⁸⁸](#), T. Kawamoto [id^{62a}](#),
 E.F. Kay [id³⁶](#), F.I. Kaya [id¹⁵⁹](#), S. Kazakos [id¹⁰⁸](#), V.F. Kazanin [id³⁷](#), Y. Ke [id¹⁴⁶](#), J.M. Keaveney [id^{33a}](#),
 R. Keeler [id¹⁶⁶](#), G.V. Kehris [id⁶¹](#), J.S. Keller [id³⁴](#), A.S. Kelly [id⁹⁷](#), J.J. Kempster [id¹⁴⁷](#), P.D. Kennedy [id¹⁰¹](#),
 O. Kepka [id¹³²](#), B.P. Kerridge [id¹³⁵](#), S. Kersten [id¹⁷²](#), B.P. Kerševan [id⁹⁴](#), L. Keszeghova [id^{28a}](#),
 S. Ketabchi Haghghat [id¹⁵⁶](#), R.A. Khan [id¹³⁰](#), A. Khanov [id¹²²](#), A.G. Kharlamov [id³⁷](#), T. Kharlamova [id³⁷](#),

E.E. Khoda [ID139](#), M. Kholodenko [ID37](#), T.J. Khoo [ID18](#), G. Khoriauli [ID167](#), J. Khubua [ID150b](#),
 Y.A.R. Khwaira [ID66](#), B. Kibirige [ID33g](#), A. Kilgallon [ID124](#), D.W. Kim [ID47a,47b](#), Y.K. Kim [ID39](#),
 N. Kimura [ID97](#), M.K. Kingston [ID55](#), A. Kirchhoff [ID55](#), C. Kirfel [ID24](#), F. Kirfel [ID24](#), J. Kirk [ID135](#),
 A.E. Kiryunin [ID111](#), C. Kitsaki [ID10](#), O. Kivernyk [ID24](#), M. Klassen [ID63a](#), C. Klein [ID34](#), L. Klein [ID167](#),
 M.H. Klein [ID44](#), S.B. Klein [ID56](#), U. Klein [ID93](#), P. Klimek [ID36](#), A. Klimentov [ID29](#), T. Klioutchnikova [ID36](#),
 P. Kluit [ID115](#), S. Kluth [ID111](#), E. Kneringer [ID79](#), T.M. Knight [ID156](#), A. Knue [ID49](#), R. Kobayashi [ID88](#),
 D. Kobylanskii [ID170](#), S.F. Koch [ID127](#), M. Kocian [ID144](#), P. Kodyš [ID134](#), D.M. Koeck [ID124](#),
 P.T. Koenig [ID24](#), T. Koffas [ID34](#), O. Kolay [ID50](#), I. Koletsou [ID4](#), T. Komarek [ID123](#), K. Köneke [ID54](#),
 A.X.Y. Kong [ID1](#), T. Kono [ID119](#), N. Konstantinidis [ID97](#), P. Kontaxakis [ID56](#), B. Konya [ID99](#),
 R. Kopeliansky [ID41](#), S. Koperny [ID86a](#), K. Korcyl [ID87](#), K. Kordas [ID153.e](#), A. Korn [ID97](#), S. Korn [ID55](#),
 I. Korolkov [ID13](#), N. Korotkova [ID37](#), B. Kortman [ID115](#), O. Kortner [ID111](#), S. Kortner [ID111](#),
 W.H. Kostecka [ID116](#), V.V. Kostyukhin [ID142](#), A. Kotsokechagia [ID136](#), A. Kotwal [ID51](#), A. Koulouris [ID36](#),
 A. Kourkoumeli-Charalampidi [ID73a,73b](#), C. Kourkoumelis [ID9](#), E. Kourlitis [ID111.ac](#), O. Kovanda [ID124](#),
 R. Kowalewski [ID166](#), W. Kozanecki [ID136](#), A.S. Kozhin [ID37](#), V.A. Kramarenko [ID37](#), G. Kramberger [ID94](#),
 P. Kramer [ID101](#), M.W. Krasny [ID128](#), A. Krasznahorkay [ID36](#), J.W. Kraus [ID172](#), J.A. Kremer [ID48](#),
 T. Kresse [ID50](#), J. Kretschmar [ID93](#), K. Kreul [ID18](#), P. Krieger [ID156](#), S. Krishnamurthy [ID104](#),
 M. Krivos [ID134](#), K. Krizka [ID20](#), K. Kroeninger [ID49](#), H. Kroha [ID111](#), J. Kroll [ID132](#), J. Kroll [ID129](#),
 K.S. Krowpman [ID108](#), U. Kruchonak [ID38](#), H. Krüger [ID24](#), N. Krumnack [ID81](#), M.C. Kruse [ID51](#),
 O. Kuchinskaia [ID37](#), S. Kuday [ID3a](#), S. Kuehn [ID36](#), R. Kuesters [ID54](#), T. Kuhl [ID48](#), V. Kukhtin [ID38](#),
 Y. Kulchitsky [ID37.a](#), S. Kuleshov [ID138d,138b](#), M. Kumar [ID33g](#), N. Kumari [ID48](#), P. Kumari [ID157b](#),
 A. Kupco [ID132](#), T. Kupfer [ID49](#), A. Kupich [ID37](#), O. Kuprash [ID54](#), H. Kurashige [ID85](#), L.L. Kurchaninov [ID157a](#),
 O. Kurdysh [ID66](#), Y.A. Kurochkin [ID37](#), A. Kurova [ID37](#), M. Kuze [ID155](#), A.K. Kvam [ID104](#), J. Kvita [ID123](#),
 T. Kwan [ID105](#), N.G. Kyriacou [ID107](#), L.A.O. Laatu [ID103](#), C. Lacasta [ID164](#), F. Lacava [ID75a,75b](#),
 H. Lacker [ID18](#), D. Lacour [ID128](#), N.N. Lad [ID97](#), E. Ladygin [ID38](#), A. Lafarge [ID40](#), B. Laforge [ID128](#),
 T. Lagouri [ID173](#), F.Z. Lahbabi [ID35a](#), S. Lai [ID55](#), I.K. Lakomic [ID86a](#), N. Lalloue [ID60](#), J.E. Lambert [ID166](#),
 S. Lammers [ID68](#), W. Lampl [ID7](#), C. Lampoudis [ID153.e](#), G. Lamprinoudis [ID101](#), A.N. Lancaster [ID116](#),
 E. Lançon [ID29](#), U. Landgraf [ID54](#), M.P.J. Landon [ID95](#), V.S. Lang [ID54](#), O.K.B. Langrekken [ID126](#),
 A.J. Lankford [ID160](#), F. Lanni [ID36](#), K. Lantzsch [ID24](#), A. Lanza [ID73a](#), A. Lapertosa [ID57b,57a](#),
 J.F. Laporte [ID136](#), T. Lari [ID71a](#), F. Lasagni Manghi [ID23b](#), M. Lassnig [ID36](#), V. Latonova [ID132](#),
 A. Laudrain [ID101](#), A. Laurier [ID151](#), S.D. Lawlor [ID140](#), Z. Lawrence [ID102](#), R. Lazaridou [ID168](#),
 M. Lazzaroni [ID71a,71b](#), B. Le [ID102](#), E.M. Le Boulicaut [ID51](#), B. Leban [ID23b,23a](#), A. Lebedev [ID81](#),
 M. LeBlanc [ID102](#), F. Ledroit-Guillon [ID60](#), A.C.A. Lee [ID97](#), S.C. Lee [ID149](#), S. Lee [ID47a,47b](#), T.F. Lee [ID93](#),
 L.L. Leeuw [ID33c](#), H.P. Lefebvre [ID96](#), M. Lefebvre [ID166](#), C. Leggett [ID17a](#), G. Lehmann Miotto [ID36](#),
 M. Leigh [ID56](#), W.A. Leight [ID104](#), W. Leinonen [ID114](#), A. Leisos [ID153.r](#), M.A.L. Leite [ID83c](#),
 C.E. Leitgeb [ID18](#), R. Leitner [ID134](#), K.J.C. Leney [ID44](#), T. Lenz [ID24](#), S. Leone [ID74a](#), C. Leonidopoulos [ID52](#),
 A. Leopold [ID145](#), C. Leroy [ID109](#), R. Les [ID108](#), C.G. Lester [ID32](#), M. Levchenko [ID37](#), J. Levêque [ID4](#),
 L.J. Levinson [ID170](#), G. Levrini [ID23b,23a](#), M.P. Lewicki [ID87](#), D.J. Lewis [ID4](#), A. Li [ID5](#), B. Li [ID62b](#), C. Li [ID62a](#),
 C-Q. Li [ID111](#), H. Li [ID62a](#), H. Li [ID62b](#), H. Li [ID14c](#), H. Li [ID14b](#), H. Li [ID62b](#), J. Li [ID62c](#), K. Li [ID139](#),
 L. Li [ID62c](#), M. Li [ID14a,14e](#), Q.Y. Li [ID62a](#), S. Li [ID14a,14e](#), S. Li [ID62d,62c,d](#), T. Li [ID5](#), X. Li [ID105](#), Z. Li [ID127](#),
 Z. Li [ID154](#), Z. Li [ID14a,14e](#), S. Liang [ID14a,14e](#), Z. Liang [ID14a](#), M. Liberatore [ID136](#), B. Liberti [ID76a](#), K. Lie [ID64c](#),
 J. Lieber Marin [ID83b](#), H. Lien [ID68](#), K. Lin [ID108](#), R.E. Lindley [ID7](#), J.H. Lindon [ID2](#), E. Lipeles [ID129](#),
 A. Lipniacka [ID16](#), A. Lister [ID165](#), J.D. Little [ID4](#), B. Liu [ID14a](#), B.X. Liu [ID143](#), D. Liu [ID62d,62c](#),
 E.H.L. Liu [ID20](#), J.B. Liu [ID62a](#), J.K.K. Liu [ID32](#), K. Liu [ID62d](#), K. Liu [ID62d,62c](#), M. Liu [ID62a](#), M.Y. Liu [ID62a](#),
 P. Liu [ID14a](#), Q. Liu [ID62d,139,62c](#), X. Liu [ID62a](#), X. Liu [ID62b](#), Y. Liu [ID14d,14e](#), Y.L. Liu [ID62b](#), Y.W. Liu [ID62a](#),
 J. Llorente Merino [ID143](#), S.L. Lloyd [ID95](#), E.M. Lobodzinska [ID48](#), P. Loch [ID7](#), T. Lohse [ID18](#),
 K. Lohwasser [ID140](#), E. Loiacono [ID48](#), M. Lokajicek [ID132,*](#), J.D. Lomas [ID20](#), J.D. Long [ID163](#),
 I. Longarini [ID160](#), L. Longo [ID70a,70b](#), R. Longo [ID163](#), I. Lopez Paz [ID67](#), A. Lopez Solis [ID48](#),

















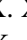



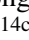
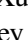


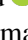

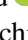


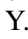


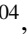

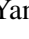
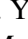
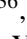
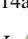
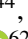
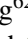
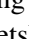
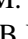

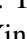
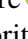

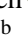









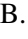
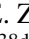

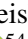
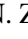


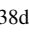
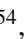



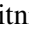
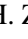

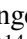
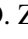


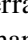
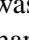

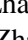
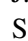
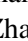
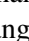


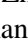


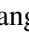



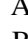


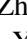
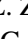
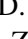







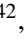
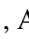
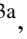
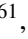



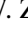
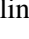



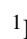

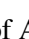




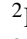
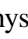
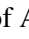
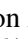
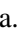


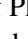
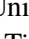
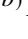
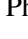
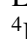
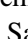
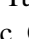
N. Lorenzo Martinez ^{id}4, A.M. Lory ^{id}110, G. Löschcke Centeno ^{id}147, O. Loseva ^{id}37, X. Lou ^{id}47a,47b, X. Lou ^{id}14a,14e, A. Lounis ^{id}66, P.A. Love ^{id}92, G. Lu ^{id}14a,14e, M. Lu ^{id}80, S. Lu ^{id}129, Y.J. Lu ^{id}65, H.J. Lubatti ^{id}139, C. Luci ^{id}75a,75b, F.L. Lucio Alves ^{id}14c, F. Luehring ^{id}68, I. Luise ^{id}146, O. Lukianchuk ^{id}66, O. Lundberg ^{id}145, B. Lund-Jensen ^{id}145, N.A. Luongo ^{id}6, M.S. Lutz ^{id}36, A.B. Lux ^{id}25, D. Lynn ^{id}29, R. Lysak ^{id}132, E. Lytken ^{id}99, V. Lyubushkin ^{id}38, T. Lyubushkina ^{id}38, M.M. Lyukova ^{id}146, H. Ma ^{id}29, K. Ma ^{id}62a, L.L. Ma ^{id}62b, W. Ma ^{id}62a, Y. Ma ^{id}122, D.M. Mac Donell ^{id}166, G. Maccarrone ^{id}53, J.C. MacDonald ^{id}101, P.C. Machado De Abreu Farias ^{id}83b, R. Madar ^{id}40, T. Madula ^{id}97, J. Maeda ^{id}85, T. Maeno ^{id}29, H. Maguire ^{id}140, V. Maiboroda ^{id}136, A. Maio ^{id}131a,131b,131d, K. Maj ^{id}86a, O. Majersky ^{id}48, S. Majewski ^{id}124, N. Makovec ^{id}66, V. Maksimovic ^{id}15, B. Malaescu ^{id}128, Pa. Malecki ^{id}87, V.P. Maleev ^{id}37, F. Malek ^{id}60,n, M. Mali ^{id}94, D. Malito ^{id}96, U. Mallik ^{id}80, S. Maltezos ^{id}10, S. Malyukov ^{id}38, J. Mamuzic ^{id}13, G. Mancini ^{id}53, M.N. Mancini ^{id}26, G. Manco ^{id}73a,73b, J.P. Mandalia ^{id}95, I. Mandić ^{id}94, L. Manhaes de Andrade Filho ^{id}83a, I.M. Maniatis ^{id}170, J. Manjarres Ramos ^{id}90, D.C. Mankad ^{id}170, A. Mann ^{id}110, S. Manzoni ^{id}36, L. Mao ^{id}62c, X. Mapekula ^{id}33c, A. Marantis ^{id}153,r, G. Marchiori ^{id}5, M. Marcisovsky ^{id}132, C. Marcon ^{id}71a, M. Marinescu ^{id}20, S. Marium ^{id}48, M. Marjanovic ^{id}121, M. Markovitch ^{id}66, E.J. Marshall ^{id}92, Z. Marshall ^{id}17a, S. Marti-Garcia ^{id}164, T.A. Martin ^{id}168, V.J. Martin ^{id}52, B. Martin dit Latour ^{id}16, L. Martinelli ^{id}75a,75b, M. Martinez ^{id}13,s, P. Martinez Agullo ^{id}164, V.I. Martinez Outschoorn ^{id}104, P. Martinez Suarez ^{id}13, S. Martin-Haugh ^{id}135, G. Martinovicova ^{id}134, V.S. Martoiu ^{id}27b, A.C. Martyniuk ^{id}97, A. Marzin ^{id}36, D. Mascione ^{id}78a,78b, L. Masetti ^{id}101, T. Mashimo ^{id}154, J. Masik ^{id}102, A.L. Maslennikov ^{id}37, P. Massarotti ^{id}72a,72b, P. Mastrandrea ^{id}74a,74b, A. Mastroberardino ^{id}43b,43a, T. Masubuchi ^{id}154, T. Mathisen ^{id}162, J. Matousek ^{id}134, N. Matsuzawa ^{id}154, J. Maurer ^{id}27b, A.J. Maury ^{id}66, B. Maček ^{id}94, D.A. Maximov ^{id}37, R. Mazini ^{id}149, I. Maznas ^{id}116, M. Mazza ^{id}108, S.M. Mazza ^{id}137, E. Mazzeo ^{id}71a,71b, C. Mc Ginn ^{id}29, J.P. Mc Gowan ^{id}166, S.P. Mc Kee ^{id}107, C.C. McCracken ^{id}165, E.F. McDonald ^{id}106, A.E. McDougall ^{id}115, J.A. Mcfayden ^{id}147, R.P. McGovern ^{id}129, G. Mchedlidze ^{id}150b, R.P. Mckenzie ^{id}33g, T.C. Mclachlan ^{id}48, D.J. Mclaughlin ^{id}97, S.J. McMahan ^{id}135, C.M. Mcpartland ^{id}93, R.A. McPherson ^{id}166,w, S. Mehlhase ^{id}110, A. Mehta ^{id}93, D. Melini ^{id}164, B.R. Mellado Garcia ^{id}33g, A.H. Melo ^{id}55, F. Meloni ^{id}48, A.M. Mendes Jacques Da Costa ^{id}102, H.Y. Meng ^{id}156, L. Meng ^{id}92, S. Menke ^{id}111, M. Mentink ^{id}36, E. Meoni ^{id}43b,43a, G. Mercado ^{id}116, C. Merlassino ^{id}69a,69c, L. Merola ^{id}72a,72b, C. Meroni ^{id}71a,71b, J. Metcalfe ^{id}6, A.S. Mete ^{id}6, C. Meyer ^{id}68, J-P. Meyer ^{id}136, R.P. Middleton ^{id}135, L. Mijović ^{id}52, G. Mikenberg ^{id}170, M. Migestikova ^{id}132, M. Mikuž ^{id}94, H. Mildner ^{id}101, A. Milic ^{id}36, D.W. Miller ^{id}39, E.H. Miller ^{id}144, L.S. Miller ^{id}34, A. Milov ^{id}170, D.A. Milstead ^{id}47a,47b, T. Min ^{id}14c, A.A. Minaenko ^{id}37, I.A. Minashvili ^{id}150b, L. Mince ^{id}59, A.I. Mincer ^{id}118, B. Mindur ^{id}86a, M. Mineev ^{id}38, Y. Mino ^{id}88, L.M. Mir ^{id}13, M. Miralles Lopez ^{id}59, M. Mironova ^{id}17a, A. Mishima ^{id}154, M.C. Missio ^{id}114, A. Mitra ^{id}168, V.A. Mitsou ^{id}164, Y. Mitsumori ^{id}112, O. Miu ^{id}156, P.S. Miyagawa ^{id}95, T. Mkrtchyan ^{id}63a, M. Mlinarevic ^{id}97, T. Mlinarevic ^{id}97, M. Mlynarikova ^{id}36, S. Mobius ^{id}19, P. Mogg ^{id}110, M.H. Mohamed Farook ^{id}113, A.F. Mohammed ^{id}14a,14e, S. Mohapatra ^{id}41, G. Mokgatitwane ^{id}33g, L. Moleri ^{id}170, B. Mondal ^{id}142, S. Mondal ^{id}133, K. Mönig ^{id}48, E. Monnier ^{id}103, L. Monsonis Romero ^{id}164, J. Montejo Berlingen ^{id}13, M. Montella ^{id}120, F. Montekali ^{id}77a,77b, F. Monticelli ^{id}91, S. Monzani ^{id}69a,69c, N. Morange ^{id}66, A.L. Moreira De Carvalho ^{id}131a, M. Moreno Llácer ^{id}164, C. Moreno Martinez ^{id}56, P. Morettini ^{id}57b, S. Morgenstern ^{id}36, M. Morii ^{id}61, M. Morinaga ^{id}154, F. Morodei ^{id}75a,75b, L. Morvaj ^{id}36, P. Moschovakos ^{id}36, B. Moser ^{id}36, M. Mosidze ^{id}150b, T. Moskalets ^{id}54, P. Moskvitina ^{id}114, J. Moss ^{id}31,k, A. Moussa ^{id}35d, E.J.W. Moyse ^{id}104, O. Mtintsilana ^{id}33g, S. Muanza ^{id}103, J. Mueller ^{id}130, D. Muenstermann ^{id}92, R. Müller ^{id}19, G.A. Mullier ^{id}162, A.J. Mullin ^{id}32, J.J. Mullin ^{id}129, D.P. Mungo ^{id}156, D. Munoz Perez ^{id}164, F.J. Munoz Sanchez ^{id}102, M. Murin ^{id}102, W.J. Murray ^{id}168,135,

M. Muškinja ⁹⁴, C. Mwewa ²⁹, A.G. Myagkov ^{37,a}, A.J. Myers ⁸, G. Myers ¹⁰⁷, M. Myska ¹³³,
B.P. Nachman ^{17a}, O. Nackenhorst ⁴⁹, K. Nagai ¹²⁷, K. Nagano ⁸⁴, J.L. Nagle ^{29,ag}, E. Nagy ¹⁰³,
A.M. Nairz ³⁶, Y. Nakahama ⁸⁴, K. Nakamura ⁸⁴, K. Nakkalil ⁵, H. Nanjo ¹²⁵, R. Narayan ⁴⁴,
E.A. Narayanan ¹¹³, I. Naryshkin ³⁷, M. Naseri ³⁴, S. Nasri ^{117b}, C. Nass ²⁴, G. Navarro ^{22a},
J. Navarro-Gonzalez ¹⁶⁴, R. Nayak ¹⁵², A. Nayaz ¹⁸, P.Y. Nechaeva ³⁷, F. Nechansky ⁴⁸,
L. Nedic ¹²⁷, T.J. Neep ²⁰, A. Negri ^{73a,73b}, M. Negrini ^{23b}, C. Nellist ¹¹⁵, C. Nelson ¹⁰⁵,
K. Nelson ¹⁰⁷, S. Nemecek ¹³², M. Nessi ^{36,h}, M.S. Neubauer ¹⁶³, F. Neuhaus ¹⁰¹,
J. Neundorff ⁴⁸, R. Newhouse ¹⁶⁵, P.R. Newman ²⁰, C.W. Ng ¹³⁰, Y.W.Y. Ng ⁴⁸, B. Ngair ^{117a},
H.D.N. Nguyen ¹⁰⁹, R.B. Nickerson ¹²⁷, R. Nicolaidou ¹³⁶, J. Nielsen ¹³⁷, M. Niemeyer ⁵⁵,
J. Niermann ⁵⁵, N. Nikiforou ³⁶, V. Nikolaenko ^{37,a}, I. Nikolic-Audit ¹²⁸, K. Nikolopoulos ²⁰,
P. Nilsson ²⁹, I. Ninca ⁴⁸, H.R. Nindhito ⁵⁶, G. Ninio ¹⁵², A. Nisati ^{75a}, N. Nishu ²,
R. Nisius ¹¹¹, J.-E. Nitschke ⁵⁰, E.K. Nkadimeng ^{33g}, T. Nobe ¹⁵⁴, D.L. Noel ³²,
T. Nommensen ¹⁴⁸, M.B. Norfolk ¹⁴⁰, R.R.B. Norisam ⁹⁷, B.J. Norman ³⁴, M. Noury ^{35a},
J. Novak ⁹⁴, T. Novak ⁴⁸, L. Novotny ¹³³, R. Novotny ¹¹³, L. Nozka ¹²³, K. Ntekas ¹⁶⁰,
N.M.J. Nunes De Moura Junior ^{83b}, J. Ocariz ¹²⁸, A. Ochi ⁸⁵, I. Ochoa ^{131a}, S. Oerdek ^{48,t},
J.T. Offermann ³⁹, A. Ogrodnik ¹³⁴, A. Oh ¹⁰², C.C. Ohm ¹⁴⁵, H. Oide ⁸⁴, R. Oishi ¹⁵⁴,
M.L. Ojeda ⁴⁸, Y. Okumura ¹⁵⁴, L.F. Oleiro Seabra ^{131a}, S.A. Olivares Pino ^{138d},
D. Oliveira Damazio ²⁹, D. Oliveira Goncalves ^{83a}, J.L. Oliver ¹⁶⁰, Ö.O. Öncel ⁵⁴,
A.P. O'Neill ¹⁹, A. Onofre ^{131a,131e}, P.U.E. Onyisi ¹¹, M.J. Oreglia ³⁹, G.E. Orellana ⁹¹,
D. Orestano ^{77a,77b}, N. Orlando ¹³, R.S. Orr ¹⁵⁶, V. O'Shea ⁵⁹, L.M. Osojnak ¹²⁹,
R. Ospanov ^{62a}, G. Otero y Garzon ³⁰, H. Otono ⁸⁹, P.S. Ott ^{63a}, G.J. Ottino ^{17a}, M. Ouchrif ^{35d},
F. Ould-Saada ¹²⁶, T. Ovsiannikova ¹³⁹, M. Owen ⁵⁹, R.E. Owen ¹³⁵, K.Y. Oyulmaz ^{21a},
V.E. Ozcan ^{21a}, F. Ozturk ⁸⁷, N. Ozturk ⁸, S. Ozturk ⁸², H.A. Pacey ¹²⁷, A. Pacheco Pages ¹³,
C. Padilla Aranda ¹³, G. Padovano ^{75a,75b}, S. Pagan Griso ^{17a}, G. Palacino ⁶⁸, A. Palazzo ^{70a,70b},
J. Pampel ²⁴, J. Pan ¹⁷³, T. Pan ^{64a}, D.K. Panchal ¹¹, C.E. Pandini ¹¹⁵, J.G. Panduro Vazquez ⁹⁶,
H.D. Pandya ¹, H. Pang ^{14b}, P. Pani ⁴⁸, G. Panizzo ^{69a,69c}, L. Panwar ¹²⁸, L. Paolozzi ⁵⁶,
S. Parajuli ¹⁶³, A. Paramonov ⁵, C. Paraskevopoulos ⁵³, D. Paredes Hernandez ^{64b},
A. Pareti ^{73a,73b}, K.R. Park ⁴¹, T.H. Park ¹⁵⁶, M.A. Parker ³², F. Parodi ^{57b,57a}, E.W. Parrish ¹¹⁶,
V.A. Parrish ⁵², J.A. Parsons ⁴¹, U. Parzefall ⁵⁴, B. Pascual Dias ¹⁰⁹, L. Pascual Dominguez ¹⁵²,
E. Pasqualucci ^{75a}, S. Passaggio ^{57b}, F. Pastore ⁹⁶, P. Patel ⁸⁷, U.M. Patel ⁵¹, J.R. Pater ¹⁰²,
T. Pauly ³⁶, C.I. Pazos ¹⁵⁹, J. Pearkes ¹⁴⁴, M. Pedersen ¹²⁶, R. Pedro ^{131a}, S.V. Peleganchuk ³⁷,
O. Penc ³⁶, E.A. Pender ⁵², G.D. Penn ¹⁷³, K.E. Penski ¹¹⁰, M. Penzin ³⁷, B.S. Peralva ^{83d},
A.P. Pereira Peixoto ¹³⁹, L. Pereira Sanchez ¹⁴⁴, D.V. Perepelitsa ^{29,ag}, E. Perez Codina ^{157a},
M. Perganti ¹⁰, H. Pernegger ³⁶, O. Perrin ⁴⁰, K. Peters ⁴⁸, R.F.Y. Peters ¹⁰², B.A. Petersen ³⁶,
T.C. Petersen ⁴², E. Petit ¹⁰³, V. Petousis ¹³³, C. Petridou ^{153,e}, T. Petru ¹³⁴, A. Petrukhin ¹⁴²,
M. Pettee ^{17a}, N.E. Pettersson ³⁶, A. Petukhov ³⁷, K. Petukhova ¹³⁴, R. Pezoa ^{138f},
L. Pezzotti ³⁶, G. Pezzullo ¹⁷³, T.M. Pham ¹⁷¹, T. Pham ¹⁰⁶, P.W. Phillips ¹³⁵, G. Piacquadio ¹⁴⁶,
E. Pianori ^{17a}, F. Piazza ¹²⁴, R. Piegaia ³⁰, D. Pietreanu ^{27b}, A.D. Pilkington ¹⁰²,
M. Pinamonti ^{69a,69c}, J.L. Pinfeld ², B.C. Pinheiro Pereira ^{131a}, A.E. Pinto Pinoargote ^{101,136},
L. Pintucci ^{69a,69c}, K.M. Piper ¹⁴⁷, A. Pirttikoski ⁵⁶, D.A. Pizzi ³⁴, L. Pizzimento ^{64b},
A. Pizzini ¹¹⁵, M.-A. Pleier ²⁹, V. Plesanovs ⁵⁴, V. Pleskot ¹³⁴, E. Plotnikova ³⁸, G. Poddar ⁹⁵,
R. Poettgen ⁹⁹, L. Poggioli ¹²⁸, I. Pokharel ⁵⁵, S. Polacek ¹³⁴, G. Polesello ^{73a}, A. Poley ^{143,157a},
A. Polini ^{23b}, C.S. Pollard ¹⁶⁸, Z.B. Pollock ¹²⁰, E. Pompa Pacchi ^{75a,75b}, D. Ponomarenko ¹¹⁴,
L. Pontecorvo ³⁶, S. Popa ^{27a}, G.A. Popeneciu ^{27d}, A. Poreba ³⁶, D.M. Portillo Quintero ^{157a},
S. Pospisil ¹³³, M.A. Postill ¹⁴⁰, P. Postolache ^{27c}, K. Potamianos ¹⁶⁸, P.A. Potepa ^{86a},
I.N. Potrap ³⁸, C.J. Potter ³², H. Potti ¹, J. Poveda ¹⁶⁴, M.E. Pozo Astigarraga ³⁶,
A. Prades Ibanez ¹⁶⁴, J. Pretel ⁵⁴, D. Price ¹⁰², M. Primavera ^{70a}, M.A. Principe Martin ¹⁰⁰,

R. Privara ¹²³, T. Procter ⁵⁹, M.L. Proffitt ¹³⁹, N. Proklova ¹²⁹, K. Prokofiev ^{64c}, G. Proto ¹¹¹, J. Proudfoot ⁶, M. Przybycien ^{36a}, W.W. Przygoda ^{86b}, A. Psallidas ⁴⁶, J.E. Puddefoot ¹⁴⁰, D. Pudzha ³⁷, D. Pyatiizbyantseva ³⁷, J. Qian ¹⁰⁷, D. Qichen ¹⁰², Y. Qin ¹³, T. Qiu ⁵², A. Quadt ⁵⁵, M. Queitsch-Maitland ¹⁰², G. Quetant ⁵⁶, R.P. Quinn ¹⁶⁵, G. Rabanal Bolanos ⁶¹, D. Rafanoharana ⁵⁴, F. Ragusa ^{71a,71b}, J.L. Rainbolt ³⁹, J.A. Raine ⁵⁶, S. Rajagopalan ²⁹, E. Ramakoti ³⁷, I.A. Ramirez-Berend ³⁴, K. Ran ^{48,14e}, N.P. Rapheeha ^{33g}, H. Rasheed ^{27b}, V. Raskina ¹²⁸, D.F. Rassloff ^{63a}, A. Rastogi ^{17a}, S. Rave ¹⁰¹, B. Ravina ⁵⁵, I. Ravinovich ¹⁷⁰, M. Raymond ³⁶, A.L. Read ¹²⁶, N.P. Readioff ¹⁴⁰, D.M. Rebutti ^{73a,73b}, G. Redlinger ²⁹, A.S. Reed ¹¹¹, K. Reeves ²⁶, J.A. Reidelsturz ¹⁷², D. Reikher ¹⁵², A. Rej ⁴⁹, C. Rembser ³⁶, M. Renda ^{27b}, M.B. Rendel ¹¹¹, F. Renner ⁴⁸, A.G. Rennie ¹⁶⁰, A.L. Rescia ⁴⁸, S. Resconi ^{71a}, M. Ressegotti ^{57b,57a}, S. Rettie ³⁶, J.G. Reyes Rivera ¹⁰⁸, E. Reynolds ^{17a}, O.L. Rezanova ³⁷, P. Reznicek ¹³⁴, H. Riani ^{35d}, N. Ribaric ⁹², E. Ricci ^{78a,78b}, R. Richter ¹¹¹, S. Richter ^{47a,47b}, E. Richter-Was ^{86b}, M. Ridel ¹²⁸, S. Ridouani ^{35d}, P. Rieck ¹¹⁸, P. Riedler ³⁶, E.M. Riefel ^{47a,47b}, J.O. Rieger ¹¹⁵, M. Rijssenbeek ¹⁴⁶, M. Rimoldi ³⁶, L. Rinaldi ^{23b,23a}, T.T. Rinn ²⁹, M.P. Rinnagel ¹¹⁰, G. Ripellino ¹⁶², I. Riu ¹³, J.C. Rivera Vergara ¹⁶⁶, F. Rizatdinova ¹²², E. Rizvi ⁹⁵, B.R. Roberts ^{17a}, S.H. Robertson ^{105,w}, D. Robinson ³², C.M. Robles Gajardo ^{138f}, M. Robles Manzano ¹⁰¹, A. Robson ⁵⁹, A. Rocchi ^{76a,76b}, C. Roda ^{74a,74b}, S. Rodriguez Bosca ³⁶, Y. Rodriguez Garcia ^{22a}, A. Rodriguez Rodriguez ⁵⁴, A.M. Rodríguez Vera ¹¹⁶, S. Roe ³⁶, J.T. Roemer ¹⁶⁰, A.R. Roepe-Gier ¹³⁷, J. Roggel ¹⁷², O. Røhne ¹²⁶, R.A. Rojas ¹⁰⁴, C.P.A. Roland ¹²⁸, J. Roloff ²⁹, A. Romaniouk ³⁷, E. Romano ^{73a,73b}, M. Romano ^{23b}, A.C. Romero Hernandez ¹⁶³, N. Rompotis ⁹³, L. Roos ¹²⁸, S. Rosati ^{75a}, B.J. Rosser ³⁹, E. Rossi ¹²⁷, E. Rossi ^{72a,72b}, L.P. Rossi ⁶¹, L. Rossini ⁵⁴, R. Rosten ¹²⁰, M. Rotaru ^{27b}, B. Rottler ⁵⁴, C. Rougier ⁹⁰, D. Rousseau ⁶⁶, D. Rousso ³², A. Roy ¹⁶³, S. Roy-Garand ¹⁵⁶, A. Rozanov ¹⁰³, Z.M.A. Rozario ⁵⁹, Y. Rozen ¹⁵¹, A. Rubio Jimenez ¹⁶⁴, A.J. Ruby ⁹³, V.H. Ruelas Rivera ¹⁸, T.A. Ruggeri ¹, A. Ruggiero ¹²⁷, A. Ruiz-Martinez ¹⁶⁴, A. Rummeler ³⁶, Z. Rurikova ⁵⁴, N.A. Rusakovich ³⁸, H.L. Russell ¹⁶⁶, G. Russo ^{75a,75b}, J.P. Rutherford ⁷, S. Rutherford Colmenares ³², K. Rybacki ⁹², M. Rybar ¹³⁴, E.B. Rye ¹²⁶, A. Ryzhov ⁴⁴, J.A. Sabater Iglesias ⁵⁶, P. Sabatini ¹⁶⁴, H.F.W. Sadrozinski ¹³⁷, F. Safai Tehrani ^{75a}, B. Safarzadeh Samani ¹³⁵, M. Safdari ¹⁴⁴, S. Saha ¹, M. Sahinsoy ¹¹¹, A. Saibel ¹⁶⁴, M. Saimpert ¹³⁶, M. Saito ¹⁵⁴, T. Saito ¹⁵⁴, D. Salamani ³⁶, A. Salnikov ¹⁴⁴, J. Salt ¹⁶⁴, A. Salvador Salas ¹⁵², D. Salvatore ^{43b,43a}, F. Salvatore ¹⁴⁷, A. Salzburger ³⁶, D. Sammel ⁵⁴, E. Sampson ⁹², D. Sampsonidis ^{153,e}, D. Sampsonidou ¹²⁴, J. Sánchez ¹⁶⁴, V. Sanchez Sebastian ¹⁶⁴, H. Sandaker ¹²⁶, C.O. Sander ⁴⁸, J.A. Sandesara ¹⁰⁴, M. Sandhoff ¹⁷², C. Sandoval ^{22b}, D.P.C. Sankey ¹³⁵, T. Sano ⁸⁸, A. Sansoni ⁵³, L. Santi ^{75a,75b}, C. Santoni ⁴⁰, H. Santos ^{131a,131b}, A. Santra ¹⁷⁰, K.A. Saoucha ¹⁶¹, J.G. Saraiva ^{131a,131d}, J. Sardain ⁷, O. Sasaki ⁸⁴, K. Sato ¹⁵⁸, C. Sauer ^{63b}, F. Sauerburger ⁵⁴, E. Sauvan ⁴, P. Savard ^{156,ae}, R. Sawada ¹⁵⁴, C. Sawyer ¹³⁵, L. Sawyer ⁹⁸, I. Sayago Galvan ¹⁶⁴, C. Sbarra ^{23b}, A. Sbrizzi ^{23b,23a}, T. Scanlon ⁹⁷, J. Schaarschmidt ¹³⁹, U. Schäfer ¹⁰¹, A.C. Schaffer ^{66,44}, D. Schaile ¹¹⁰, R.D. Schamberger ¹⁴⁶, C. Scharf ¹⁸, M.M. Schefer ¹⁹, V.A. Schegelsky ³⁷, D. Scheirich ¹³⁴, F. Schenck ¹⁸, M. Schernau ¹⁶⁰, C. Scheulen ⁵⁵, C. Schiavi ^{57b,57a}, M. Schioppa ^{43b,43a}, B. Schlag ^{144,m}, K.E. Schleicher ⁵⁴, S. Schlenker ³⁶, J. Schmeing ¹⁷², M.A. Schmidt ¹⁷², K. Schmieden ¹⁰¹, C. Schmitt ¹⁰¹, N. Schmitt ¹⁰¹, S. Schmitt ⁴⁸, L. Schoeffel ¹³⁶, A. Schoening ^{63b}, P.G. Scholer ³⁴, E. Schopf ¹²⁷, M. Schott ¹⁰¹, J. Schovancova ³⁶, S. Schramm ⁵⁶, T. Schroer ⁵⁶, H-C. Schultz-Coulon ^{63a}, M. Schumacher ⁵⁴, B.A. Schumm ¹³⁷, Ph. Schune ¹³⁶, A.J. Schuy ¹³⁹, H.R. Schwartz ¹³⁷, A. Schwartzman ¹⁴⁴, T.A. Schwarz ¹⁰⁷, Ph. Schwemling ¹³⁶, R. Schvienhorst ¹⁰⁸, A. Sciandra ¹³⁷, G. Sciolla ²⁶, F. Scuri ^{74a}, C.D. Sebastiani ⁹³, K. Sedlaczek ¹¹⁶, P. Seema ¹⁸, S.C. Seidel ¹¹³, A. Seiden ¹³⁷,

B.D. Seidlitz ⁴¹, C. Seitz ⁴⁸, J.M. Seixas ^{83b}, G. Sekhniaidze ^{72a}, L. Selem ⁶⁰,
 N. Semprini-Cesari ^{23b,23a}, D. Sengupta ⁵⁶, V. Senthilkumar ¹⁶⁴, L. Serin ⁶⁶, L. Serkin ^{69a,69b},
 M. Sessa ^{76a,76b}, H. Severini ¹²¹, F. Sforza ^{57b,57a}, A. Sfyrla ⁵⁶, Q. Sha ^{14a}, E. Shabalina ⁵⁵,
 R. Shaheen ¹⁴⁵, J.D. Shahinian ¹²⁹, D. Shaked Renous ¹⁷⁰, L.Y. Shan ^{14a}, M. Shapiro ^{17a},
 A. Sharma ³⁶, A.S. Sharma ¹⁶⁵, P. Sharma ⁸⁰, P.B. Shatalov ³⁷, K. Shaw ¹⁴⁷, S.M. Shaw ¹⁰²,
 A. Shcherbakova ³⁷, Q. Shen ^{62c,5}, D.J. Sheppard ¹⁴³, P. Sherwood ⁹⁷, L. Shi ⁹⁷, X. Shi ^{14a},
 C.O. Shimmin ¹⁷³, J.D. Shinner ⁹⁶, I.P.J. Shipsey ¹²⁷, S. Shirabe ⁸⁹, M. Shiyakova ^{38,u},
 J. Shlomi ¹⁷⁰, M.J. Shochet ³⁹, J. Shojaii ¹⁰⁶, D.R. Shope ¹²⁶, B. Shrestha ¹²¹, S. Shrestha ^{120,ah},
 E.M. Shrif ^{33g}, M.J. Shroff ¹⁶⁶, P. Sicho ¹³², A.M. Sickles ¹⁶³, E. Sideras Haddad ^{33g},
 A. Sidoti ^{23b}, F. Siegert ⁵⁰, Dj. Sijacki ¹⁵, F. Sili ⁹¹, J.M. Silva ⁵², M.V. Silva Oliveira ²⁹,
 S.B. Silverstein ^{47a}, S. Simion ⁶⁶, R. Simoniello ³⁶, E.L. Simpson ⁵⁹, H. Simpson ¹⁴⁷,
 L.R. Simpson ¹⁰⁷, N.D. Simpson ⁹⁹, S. Simsek ⁸², S. Sindhu ⁵⁵, P. Sinervo ¹⁵⁶, S. Singh ¹⁵⁶,
 S. Sinha ⁴⁸, S. Sinha ¹⁰², M. Sioli ^{23b,23a}, I. Siral ³⁶, E. Sitnikova ⁴⁸, J. Sjölin ^{47a,47b},
 A. Skaf ⁵⁵, E. Skorda ²⁰, P. Skubic ¹²¹, M. Slawinska ⁸⁷, V. Smakhtin ¹⁷⁰, B.H. Smart ¹³⁵,
 S.Yu. Smirnov ³⁷, Y. Smirnov ³⁷, L.N. Smirnova ^{37,a}, O. Smirnova ⁹⁹, A.C. Smith ⁴¹,
 E.A. Smith ³⁹, H.A. Smith ¹²⁷, J.L. Smith ¹⁰², R. Smith ¹⁴⁴, M. Smizanska ⁹², K. Smolek ¹³³,
 A.A. Snesarev ³⁷, S.R. Snider ¹⁵⁶, H.L. Snoek ¹¹⁵, S. Snyder ²⁹, R. Sobie ^{166,w}, A. Soffer ¹⁵²,
 C.A. Solans Sanchez ³⁶, E.Yu. Soldatov ³⁷, U. Soldevila ¹⁶⁴, A.A. Solodkov ³⁷, S. Solomon ²⁶,
 A. Soloshenko ³⁸, K. Solovieva ⁵⁴, O.V. Solovyanov ⁴⁰, V. Solovyev ³⁷, P. Sommer ³⁶,
 A. Sonay ¹³, W.Y. Song ^{157b}, A. Sopczak ¹³³, A.L. Sopio ⁹⁷, F. Sopkova ^{28b}, J.D. Sorenson ¹¹³,
 I.R. Sotarriva Alvarez ¹⁵⁵, V. Sothilingam ^{63a}, O.J. Soto Sandoval ^{138c,138b}, S. Sottocornola ⁶⁸,
 R. Soualah ¹⁶¹, Z. Soumami ^{35e}, D. South ⁴⁸, N. Soybelman ¹⁷⁰, S. Spagnolo ^{70a,70b},
 M. Spalla ¹¹¹, D. Sperlich ⁵⁴, G. Spigo ³⁶, S. Spinali ⁹², D.P. Spiteri ⁵⁹, M. Spousta ¹³⁴,
 E.J. Staats ³⁴, R. Stamen ^{63a}, A. Stampeki ²⁰, M. Standke ²⁴, E. Stanecka ⁸⁷, M.V. Stange ⁵⁰,
 B. Stanislaus ^{17a}, M.M. Stanitzki ⁴⁸, B. Stapf ⁴⁸, E.A. Starchenko ³⁷, G.H. Stark ¹³⁷, J. Stark ⁹⁰,
 P. Staroba ¹³², P. Starovoitov ^{63a}, S. Stärz ¹⁰⁵, R. Staszewski ⁸⁷, G. Stavropoulos ⁴⁶,
 J. Steentoft ¹⁶², P. Steinberg ²⁹, B. Stelzer ^{143,157a}, H.J. Stelzer ¹³⁰, O. Stelzer-Chilton ^{157a},
 H. Stenzel ⁵⁸, T.J. Stevenson ¹⁴⁷, G.A. Stewart ³⁶, J.R. Stewart ¹²², M.C. Stockton ³⁶,
 G. Stoicea ^{27b}, M. Stolarski ^{131a}, S. Stonjek ¹¹¹, A. Straessner ⁵⁰, J. Strandberg ¹⁴⁵,
 S. Strandberg ^{47a,47b}, M. Stratmann ¹⁷², M. Strauss ¹²¹, T. Strebler ¹⁰³, P. Strizenec ^{28b},
 R. Ströhmer ¹⁶⁷, D.M. Strom ¹²⁴, R. Stroynowski ⁴⁴, A. Strubig ^{47a,47b}, S.A. Stucci ²⁹,
 B. Stugu ¹⁶, J. Stupak ¹²¹, N.A. Styles ⁴⁸, D. Su ¹⁴⁴, S. Su ^{62a}, W. Su ^{62d}, X. Su ^{62a},
 D. Suchy ^{28a}, K. Sugizaki ¹⁵⁴, V.V. Sulin ³⁷, M.J. Sullivan ⁹³, D.M.S. Sultan ¹²⁷,
 L. Sultanaliyeva ³⁷, S. Sultansoy ^{3b}, T. Sumida ⁸⁸, S. Sun ¹⁰⁷, S. Sun ¹⁷¹,
 O. Sunneborn Gudnadottir ¹⁶², N. Sur ¹⁰³, M.R. Sutton ¹⁴⁷, H. Suzuki ¹⁵⁸, M. Svatos ¹³²,
 M. Swiatlowski ^{157a}, T. Swirski ¹⁶⁷, I. Sykora ^{28a}, M. Sykora ¹³⁴, T. Sykora ¹³⁴, D. Ta ¹⁰¹,
 K. Tackmann ^{48,t}, A. Taffard ¹⁶⁰, R. Tafirout ^{157a}, J.S. Tafoya Vargas ⁶⁶, Y. Takubo ⁸⁴,
 M. Talby ¹⁰³, A.A. Talyshv ³⁷, K.C. Tam ^{64b}, N.M. Tamir ¹⁵², A. Tanaka ¹⁵⁴, J. Tanaka ¹⁵⁴,
 R. Tanaka ⁶⁶, M. Tanasini ^{57b,57a}, Z. Tao ¹⁶⁵, S. Tapia Araya ^{138f}, S. Tapprogge ¹⁰¹,
 A. Tarek Abouelfadl Mohamed ¹⁰⁸, S. Tarem ¹⁵¹, K. Tariq ^{14a}, G. Tarna ^{103,27b}, G.F. Tartarelli ^{71a},
 P. Tas ¹³⁴, M. Tasevsky ¹³², E. Tassi ^{43b,43a}, A.C. Tate ¹⁶³, G. Tateno ¹⁵⁴, Y. Tayalati ^{35e,v},
 G.N. Taylor ¹⁰⁶, W. Taylor ^{157b}, A.S. Tee ¹⁷¹, R. Teixeira De Lima ¹⁴⁴, P. Teixeira-Dias ⁹⁶,
 J.J. Teoh ¹⁵⁶, K. Terashi ¹⁵⁴, J. Terron ¹⁰⁰, S. Terzo ¹³, M. Testa ⁵³, R.J. Teuscher ^{156,w},
 A. Thaler ⁷⁹, O. Theiner ⁵⁶, N. Themistokleous ⁵², T. Theveneaux-Pelzer ¹⁰³, O. Thielmann ¹⁷²,
 D.W. Thomas ⁹⁶, J.P. Thomas ²⁰, E.A. Thompson ^{17a}, P.D. Thompson ²⁰, E. Thomson ¹²⁹,
 R.E. Thornberry ⁴⁴, Y. Tian ⁵⁵, V. Tikhomirov ^{37,a}, Yu.A. Tikhonov ³⁷, S. Timoshenko ³⁷,
 D. Timoshyn ¹³⁴, E.X.L. Ting ¹, P. Tipton ¹⁷³, S.H. Tlou ^{33g}, K. Todome ¹⁵⁵,

S. Todorova-Nova ¹³⁴, S. Todt⁵⁰, M. Togawa ⁸⁴, J. Tojo ⁸⁹, S. Tokár ^{28a}, K. Tokushuku ⁸⁴,
 O. Toldaiev ⁶⁸, R. Tombs ³², M. Tomoto ^{84,112}, L. Tompkins ^{144,m}, K.W. Topolnicki ^{86b},
 E. Torrence ¹²⁴, H. Torres ⁹⁰, E. Torró Pastor ¹⁶⁴, M. Toscani ³⁰, C. Tosciri ³⁹, M. Tost ¹¹,
 D.R. Tovey ¹⁴⁰, A. Traeet¹⁶, I.S. Trandafir ^{27b}, T. Trefzger ¹⁶⁷, A. Tricoli ²⁹, I.M. Trigger ^{157a},
 S. Trincaz-Duvoid ¹²⁸, D.A. Trischuk ²⁶, B. Trocmé ⁶⁰, L. Truong ^{33c}, M. Trzebinski ⁸⁷,
 A. Trzupiek ⁸⁷, F. Tsai ¹⁴⁶, M. Tsai ¹⁰⁷, A. Tsiamis ^{153,e}, P.V. Tsiareshka³⁷, S. Tsigaridas ^{157a},
 A. Tsirigotis ^{153,r}, V. Tsiskaridze ¹⁵⁶, E.G. Tskhadadze ^{150a}, M. Tsopoulou ¹⁵³, Y. Tsujikawa ⁸⁸,
 I.I. Tsukerman ³⁷, V. Tsulaia ^{17a}, S. Tsuno ⁸⁴, K. Tsuru ¹¹⁹, D. Tsybychev ¹⁴⁶, Y. Tu ^{64b},
 A. Tudorache ^{27b}, V. Tudorache ^{27b}, A.N. Tuna ⁶¹, S. Turchikhin ^{57b,57a}, I. Turk Cakir ^{3a},
 R. Turra ^{71a}, T. Turtuvshin ^{38,x}, P.M. Tuts ⁴¹, S. Tzamarias ^{153,e}, E. Tzovara ¹⁰¹, F. Ukegawa ¹⁵⁸,
 P.A. Ulloa Poblete ^{138c,138b}, E.N. Umaka ²⁹, G. Unal ³⁶, A. Undrus ²⁹, G. Unel ¹⁶⁰, J. Urban ^{28b},
 P. Urquijo ¹⁰⁶, P. Urrejola ^{138a}, G. Usai ⁸, R. Ushioda ¹⁵⁵, M. Usman ¹⁰⁹, Z. Uysal ⁸²,
 V. Vacek ¹³³, B. Vachon ¹⁰⁵, K.O.H. Vadla ¹²⁶, T. Vafeiadis ³⁶, A. Vaitkus ⁹⁷, C. Valderanis ¹¹⁰,
 E. Valdes Santurio ^{47a,47b}, M. Valente ^{157a}, S. Valentinetti ^{23b,23a}, A. Valero ¹⁶⁴,
 E. Valiente Moreno ¹⁶⁴, A. Vallier ⁹⁰, J.A. Valls Ferrer ¹⁶⁴, D.R. Van Arneman ¹¹⁵,
 T.R. Van Daalen ¹³⁹, A. Van Der Graaf ⁴⁹, P. Van Gemmeren ⁶, M. Van Rijnbach ¹²⁶,
 S. Van Stroud ⁹⁷, I. Van Vulpen ¹¹⁵, P. Vana ¹³⁴, M. Vanadia ^{76a,76b}, W. Vandelli ³⁶,
 E.R. Vandewall ¹²², D. Vannicola ¹⁵², L. Vannoli ⁵³, R. Vari ^{75a}, E.W. Varnes ⁷, C. Varni ^{17b},
 T. Varol ¹⁴⁹, D. Varouchas ⁶⁶, L. Varriale ¹⁶⁴, K.E. Varvell ¹⁴⁸, M.E. Vasile ^{27b}, L. Vaslin⁸⁴,
 G.A. Vazquez ¹⁶⁶, A. Vasyukov ³⁸, R. Vavricka¹⁰¹, F. Vazeille ⁴⁰, T. Vazquez Schroeder ³⁶,
 J. Veatch ³¹, V. Vecchio ¹⁰², M.J. Veen ¹⁰⁴, I. Veliscek ²⁹, L.M. Veloce ¹⁵⁶, F. Veloso ^{131a,131c},
 S. Veneziano ^{75a}, A. Ventura ^{70a,70b}, S. Ventura Gonzalez ¹³⁶, A. Verbytskyi ¹¹¹,
 M. Verducci ^{74a,74b}, C. Vergis ²⁴, M. Verissimo De Araujo ^{83b}, W. Verkerke ¹¹⁵,
 J.C. Vermeulen ¹¹⁵, C. Vernieri ¹⁴⁴, M. Vessella ¹⁰⁴, M.C. Vetterli ^{143,ae}, A. Vgenopoulos ^{153,e},
 N. Viaux Maira ^{138f}, T. Vickey ¹⁴⁰, O.E. Vickey Boeriu ¹⁴⁰, G.H.A. Viehhauser ¹²⁷, L. Vignani ^{63b},
 M. Villa ^{23b,23a}, M. Villaplana Perez ¹⁶⁴, E.M. Villhauer⁵², E. Vilucchi ⁵³, M.G. Vinciter ³⁴,
 G.S. Virdee ²⁰, A. Vishwakarma ⁵², A. Visibile¹¹⁵, C. Vittori ³⁶, I. Vivarelli ^{23b,23a},
 E. Voevodina ¹¹¹, F. Vogel ¹¹⁰, J.C. Voigt ⁵⁰, P. Vokac ¹³³, Yu. Volkotrub ^{86b}, J. Von Ahnen ⁴⁸,
 E. Von Toerne ²⁴, B. Vormwald ³⁶, V. Vorobel ¹³⁴, K. Vorobev ³⁷, M. Vos ¹⁶⁴, K. Voss ¹⁴²,
 M. Vozak ¹¹⁵, L. Vozdecky ¹²¹, N. Vranjes ¹⁵, M. Vranjes Milosavljevic ¹⁵, M. Vreeswijk ¹¹⁵,
 N.K. Vu ^{62d,62c}, R. Vuillermet ³⁶, O. Vujanovic ¹⁰¹, I. Vukotic ³⁹, S. Wada ¹⁵⁸, C. Wagner¹⁰⁴,
 J.M. Wagner ^{17a}, W. Wagner ¹⁷², S. Wahdan ¹⁷², H. Wahlberg ⁹¹, M. Wakida ¹¹², J. Walder ¹³⁵,
 R. Walker ¹¹⁰, W. Walkowiak ¹⁴², A. Wall ¹²⁹, E.J. Wallin ⁹⁹, T. Wamorkar ⁶, A.Z. Wang ¹³⁷,
 C. Wang ¹⁰¹, C. Wang ¹¹, H. Wang ^{17a}, J. Wang ^{64c}, R.-J. Wang ¹⁰¹, R. Wang ⁶¹, R. Wang ⁶,
 S.M. Wang ¹⁴⁹, S. Wang ^{62b}, T. Wang ^{62a}, W.T. Wang ⁸⁰, W. Wang ^{14a}, X. Wang ^{14c},
 X. Wang ¹⁶³, X. Wang ^{62c}, Y. Wang ^{62d}, Y. Wang ^{14c}, Z. Wang ¹⁰⁷, Z. Wang ^{62d,51,62c},
 Z. Wang ¹⁰⁷, A. Warburton ¹⁰⁵, R.J. Ward ²⁰, N. Warrack ⁵⁹, S. Waterhouse ⁹⁶, A.T. Watson ²⁰,
 H. Watson ⁵⁹, M.F. Watson ²⁰, E. Watton ^{59,135}, G. Watts ¹³⁹, B.M. Waugh ⁹⁷, C. Weber ²⁹,
 H.A. Weber ¹⁸, M.S. Weber ¹⁹, S.M. Weber ^{63a}, C. Wei ^{62a}, Y. Wei ¹²⁷, A.R. Weidberg ¹²⁷,
 E.J. Weik ¹¹⁸, J. Weingarten ⁴⁹, M. Weirich ¹⁰¹, C. Weiser ⁵⁴, C.J. Wells ⁴⁸, T. Wenaus ²⁹,
 B. Wendland ⁴⁹, T. Wengler ³⁶, N.S. Wenke¹¹¹, N. Wermes ²⁴, M. Wessels ^{63a}, A.M. Wharton ⁹²,
 A.S. White ⁶¹, A. White ⁸, M.J. White ¹, D. Whiteson ¹⁶⁰, L. Wickremasinghe ¹²⁵,
 W. Wiedenmann ¹⁷¹, M. Wielers ¹³⁵, C. Wigglesworth ⁴², D.J. Wilbern¹²¹, H.G. Wilkens ³⁶,
 D.M. Williams ⁴¹, H.H. Williams¹²⁹, S. Williams ³², S. Willocq ¹⁰⁴, B.J. Wilson ¹⁰²,
 P.J. Windischhofer ³⁹, F.I. Winkel ³⁰, F. Winklmeier ¹²⁴, B.T. Winter ⁵⁴, J.K. Winter ¹⁰²,
 M. Wittgen¹⁴⁴, M. Wobisch ⁹⁸, Z. Wolffs ¹¹⁵, J. Wollrath¹⁶⁰, M.W. Wolter ⁸⁷, H. Wolters ^{131a,131c},
 M.C. Wong¹³⁷, E.L. Woodward ⁴¹, S.D. Worm ⁴⁸, B.K. Wosiek ⁸⁷, K.W. Woźniak ⁸⁷,

S. Wozniowski ⁵⁵, K. Wraight ⁵⁹, C. Wu ²⁰, M. Wu ^{14d}, M. Wu ¹¹⁴, S.L. Wu ¹⁷¹, X. Wu ⁵⁶, Y. Wu ^{62a}, Z. Wu ⁴, J. Wuerzinger ^{111,ac}, T.R. Wyatt ¹⁰², B.M. Wynne ⁵², S. Xella ⁴², L. Xia ^{14c}, M. Xia ^{14b}, J. Xiang ^{64c}, M. Xie ^{62a}, X. Xie ^{62a}, S. Xin ^{14a,14e}, A. Xiong ¹²⁴, J. Xiong ^{17a}, D. Xu ^{14a}, H. Xu ^{62a}, L. Xu ^{62a}, R. Xu ¹²⁹, T. Xu ¹⁰⁷, Y. Xu ^{14b}, Z. Xu ⁵², Z. Xu ^{14c}, B. Yabsley ¹⁴⁸, S. Yacoob ^{33a}, Y. Yamaguchi ¹⁵⁵, E. Yamashita ¹⁵⁴, H. Yamauchi ¹⁵⁸, T. Yamazaki ^{17a}, Y. Yamazaki ⁸⁵, J. Yan ^{62c}, S. Yan ⁵⁹, Z. Yan ¹⁰⁴, H.J. Yang ^{62c,62d}, H.T. Yang ^{62a}, S. Yang ^{62a}, T. Yang ^{64c}, X. Yang ³⁶, X. Yang ^{14a}, Y. Yang ⁴⁴, Y. Yang ^{62a}, Z. Yang ^{62a}, W.-M. Yao ^{17a}, H. Ye ^{14c}, H. Ye ⁵⁵, J. Ye ^{14a}, S. Ye ²⁹, X. Ye ^{62a}, Y. Yeh ⁹⁷, I. Yeletskikh ³⁸, B.K. Yeo ^{17b}, M.R. Yexley ⁹⁷, P. Yin ⁴¹, K. Yorita ¹⁶⁹, S. Younas ^{27b}, C.J.S. Young ³⁶, C. Young ¹⁴⁴, C. Yu ^{14a,14e}, Y. Yu ^{62a}, M. Yuan ¹⁰⁷, R. Yuan ^{62b}, L. Yue ⁹⁷, M. Zaazoua ^{62a}, B. Zabinski ⁸⁷, E. Zaid ⁵², Z.K. Zak ⁸⁷, T. Zakareishvili ¹⁶⁴, N. Zakharchuk ³⁴, S. Zambito ⁵⁶, J.A. Zamora Saa ^{138d,138b}, J. Zang ¹⁵⁴, D. Zanzi ⁵⁴, O. Zaplatilek ¹³³, C. Zeitnitz ¹⁷², H. Zeng ^{14a}, J.C. Zeng ¹⁶³, D.T. Zenger Jr ²⁶, O. Zenin ³⁷, T. Ženiš ^{28a}, S. Zenz ⁹⁵, S. Zerradi ^{35a}, D. Zerwas ⁶⁶, M. Zhai ^{14a,14e}, D.F. Zhang ¹⁴⁰, J. Zhang ^{62b}, J. Zhang ⁶, K. Zhang ^{14a,14e}, L. Zhang ^{14c}, P. Zhang ^{14a,14e}, R. Zhang ¹⁷¹, S. Zhang ¹⁰⁷, S. Zhang ⁴⁴, T. Zhang ¹⁵⁴, X. Zhang ^{62c}, X. Zhang ^{62b}, Y. Zhang ^{62c,5}, Y. Zhang ⁹⁷, Y. Zhang ^{14c}, Z. Zhang ^{17a}, Z. Zhang ⁶⁶, H. Zhao ¹³⁹, T. Zhao ^{62b}, Y. Zhao ¹³⁷, Z. Zhao ^{62a}, A. Zhemchugov ³⁸, J. Zheng ^{14c}, K. Zheng ¹⁶³, X. Zheng ^{62a}, Z. Zheng ¹⁴⁴, D. Zhong ¹⁶³, B. Zhou ¹⁰⁷, H. Zhou ⁷, N. Zhou ^{62c}, Y. Zhou ^{14c}, Y. Zhou ⁷, C.G. Zhu ^{62b}, J. Zhu ¹⁰⁷, Y. Zhu ^{62c}, Y. Zhu ^{62a}, X. Zhuang ^{14a}, K. Zhukov ³⁷, N.I. Zimine ³⁸, J. Zinsser ^{63b}, M. Ziolkowski ¹⁴², L. Živković ¹⁵, A. Zoccoli ^{23b,23a}, K. Zoch ⁶¹, T.G. Zorbas ¹⁴⁰, O. Zormpa ⁴⁶, W. Zou ⁴¹, L. Zwalinski ³⁶.

¹Department of Physics, University of Adelaide, Adelaide; Australia.

²Department of Physics, University of Alberta, Edmonton AB; Canada.

³(^a)Department of Physics, Ankara University, Ankara; (^b)Division of Physics, TOBB University of Economics and Technology, Ankara; Türkiye.

⁴LAPP, Université Savoie Mont Blanc, CNRS/IN2P3, Annecy; France.

⁵APC, Université Paris Cité, CNRS/IN2P3, Paris; France.

⁶High Energy Physics Division, Argonne National Laboratory, Argonne IL; United States of America.

⁷Department of Physics, University of Arizona, Tucson AZ; United States of America.

⁸Department of Physics, University of Texas at Arlington, Arlington TX; United States of America.

⁹Physics Department, National and Kapodistrian University of Athens, Athens; Greece.

¹⁰Physics Department, National Technical University of Athens, Zografou; Greece.

¹¹Department of Physics, University of Texas at Austin, Austin TX; United States of America.

¹²Institute of Physics, Azerbaijan Academy of Sciences, Baku; Azerbaijan.

¹³Institut de Física d'Altes Energies (IFAE), Barcelona Institute of Science and Technology, Barcelona; Spain.

¹⁴(^a)Institute of High Energy Physics, Chinese Academy of Sciences, Beijing; (^b)Physics Department, Tsinghua University, Beijing; (^c)Department of Physics, Nanjing University, Nanjing; (^d)School of Science, Shenzhen Campus of Sun Yat-sen University; (^e)University of Chinese Academy of Science (UCAS), Beijing; China.

¹⁵Institute of Physics, University of Belgrade, Belgrade; Serbia.

¹⁶Department for Physics and Technology, University of Bergen, Bergen; Norway.

¹⁷(^a)Physics Division, Lawrence Berkeley National Laboratory, Berkeley CA; (^b)University of California, Berkeley CA; United States of America.

¹⁸Institut für Physik, Humboldt Universität zu Berlin, Berlin; Germany.

- ¹⁹Albert Einstein Center for Fundamental Physics and Laboratory for High Energy Physics, University of Bern, Bern; Switzerland.
- ²⁰School of Physics and Astronomy, University of Birmingham, Birmingham; United Kingdom.
- ²¹(^a)Department of Physics, Bogazici University, Istanbul; (^b)Department of Physics Engineering, Gaziantep University, Gaziantep; (^c)Department of Physics, Istanbul University, Istanbul; Türkiye.
- ²²(^a)Facultad de Ciencias y Centro de Investigaciones, Universidad Antonio Nariño, Bogotá; (^b)Departamento de Física, Universidad Nacional de Colombia, Bogotá; Colombia.
- ²³(^a)Dipartimento di Fisica e Astronomia A. Righi, Università di Bologna, Bologna; (^b)INFN Sezione di Bologna; Italy.
- ²⁴Physikalisches Institut, Universität Bonn, Bonn; Germany.
- ²⁵Department of Physics, Boston University, Boston MA; United States of America.
- ²⁶Department of Physics, Brandeis University, Waltham MA; United States of America.
- ²⁷(^a)Transilvania University of Brasov, Brasov; (^b)Horia Hulubei National Institute of Physics and Nuclear Engineering, Bucharest; (^c)Department of Physics, Alexandru Ioan Cuza University of Iasi, Iasi; (^d)National Institute for Research and Development of Isotopic and Molecular Technologies, Physics Department, Cluj-Napoca; (^e)National University of Science and Technology Politehnica, Bucharest; (^f)West University in Timisoara, Timisoara; (^g)Faculty of Physics, University of Bucharest, Bucharest; Romania.
- ²⁸(^a)Faculty of Mathematics, Physics and Informatics, Comenius University, Bratislava; (^b)Department of Subnuclear Physics, Institute of Experimental Physics of the Slovak Academy of Sciences, Kosice; Slovak Republic.
- ²⁹Physics Department, Brookhaven National Laboratory, Upton NY; United States of America.
- ³⁰Universidad de Buenos Aires, Facultad de Ciencias Exactas y Naturales, Departamento de Física, y CONICET, Instituto de Física de Buenos Aires (IFIBA), Buenos Aires; Argentina.
- ³¹California State University, CA; United States of America.
- ³²Cavendish Laboratory, University of Cambridge, Cambridge; United Kingdom.
- ³³(^a)Department of Physics, University of Cape Town, Cape Town; (^b)iThemba Labs, Western Cape; (^c)Department of Mechanical Engineering Science, University of Johannesburg, Johannesburg; (^d)National Institute of Physics, University of the Philippines Diliman (Philippines); (^e)University of South Africa, Department of Physics, Pretoria; (^f)University of Zululand, KwaDlangezwa; (^g)School of Physics, University of the Witwatersrand, Johannesburg; South Africa.
- ³⁴Department of Physics, Carleton University, Ottawa ON; Canada.
- ³⁵(^a)Faculté des Sciences Ain Chock, Réseau Universitaire de Physique des Hautes Energies - Université Hassan II, Casablanca; (^b)Faculté des Sciences, Université Ibn-Tofail, Kénitra; (^c)Faculté des Sciences Semlalia, Université Cadi Ayyad, LPHEA-Marrakech; (^d)LPMR, Faculté des Sciences, Université Mohamed Premier, Oujda; (^e)Faculté des sciences, Université Mohammed V, Rabat; (^f)Institute of Applied Physics, Mohammed VI Polytechnic University, Ben Guerir; Morocco.
- ³⁶CERN, Geneva; Switzerland.
- ³⁷Affiliated with an institute covered by a cooperation agreement with CERN.
- ³⁸Affiliated with an international laboratory covered by a cooperation agreement with CERN.
- ³⁹Enrico Fermi Institute, University of Chicago, Chicago IL; United States of America.
- ⁴⁰LPC, Université Clermont Auvergne, CNRS/IN2P3, Clermont-Ferrand; France.
- ⁴¹Nevis Laboratory, Columbia University, Irvington NY; United States of America.
- ⁴²Niels Bohr Institute, University of Copenhagen, Copenhagen; Denmark.
- ⁴³(^a)Dipartimento di Fisica, Università della Calabria, Rende; (^b)INFN Gruppo Collegato di Cosenza, Laboratori Nazionali di Frascati; Italy.
- ⁴⁴Physics Department, Southern Methodist University, Dallas TX; United States of America.
- ⁴⁵Physics Department, University of Texas at Dallas, Richardson TX; United States of America.

- ⁴⁶National Centre for Scientific Research "Demokritos", Agia Paraskevi; Greece.
- ⁴⁷(^a)Department of Physics, Stockholm University;(^b)Oskar Klein Centre, Stockholm; Sweden.
- ⁴⁸Deutsches Elektronen-Synchrotron DESY, Hamburg and Zeuthen; Germany.
- ⁴⁹Fakultät Physik , Technische Universität Dortmund, Dortmund; Germany.
- ⁵⁰Institut für Kern- und Teilchenphysik, Technische Universität Dresden, Dresden; Germany.
- ⁵¹Department of Physics, Duke University, Durham NC; United States of America.
- ⁵²SUPA - School of Physics and Astronomy, University of Edinburgh, Edinburgh; United Kingdom.
- ⁵³INFN e Laboratori Nazionali di Frascati, Frascati; Italy.
- ⁵⁴Physikalisches Institut, Albert-Ludwigs-Universität Freiburg, Freiburg; Germany.
- ⁵⁵II. Physikalisches Institut, Georg-August-Universität Göttingen, Göttingen; Germany.
- ⁵⁶Département de Physique Nucléaire et Corpusculaire, Université de Genève, Genève; Switzerland.
- ⁵⁷(^a)Dipartimento di Fisica, Università di Genova, Genova;(^b)INFN Sezione di Genova; Italy.
- ⁵⁸II. Physikalisches Institut, Justus-Liebig-Universität Giessen, Giessen; Germany.
- ⁵⁹SUPA - School of Physics and Astronomy, University of Glasgow, Glasgow; United Kingdom.
- ⁶⁰LPSC, Université Grenoble Alpes, CNRS/IN2P3, Grenoble INP, Grenoble; France.
- ⁶¹Laboratory for Particle Physics and Cosmology, Harvard University, Cambridge MA; United States of America.
- ⁶²(^a)Department of Modern Physics and State Key Laboratory of Particle Detection and Electronics, University of Science and Technology of China, Hefei;(^b)Institute of Frontier and Interdisciplinary Science and Key Laboratory of Particle Physics and Particle Irradiation (MOE), Shandong University, Qingdao;(^c)School of Physics and Astronomy, Shanghai Jiao Tong University, Key Laboratory for Particle Astrophysics and Cosmology (MOE), SKLPPC, Shanghai;(^d)Tsung-Dao Lee Institute, Shanghai;(^e)School of Physics and Microelectronics, Zhengzhou University; China.
- ⁶³(^a)Kirchhoff-Institut für Physik, Ruprecht-Karls-Universität Heidelberg, Heidelberg;(^b)Physikalisches Institut, Ruprecht-Karls-Universität Heidelberg, Heidelberg; Germany.
- ⁶⁴(^a)Department of Physics, Chinese University of Hong Kong, Shatin, N.T., Hong Kong;(^b)Department of Physics, University of Hong Kong, Hong Kong;(^c)Department of Physics and Institute for Advanced Study, Hong Kong University of Science and Technology, Clear Water Bay, Kowloon, Hong Kong; China.
- ⁶⁵Department of Physics, National Tsing Hua University, Hsinchu; Taiwan.
- ⁶⁶IJCLab, Université Paris-Saclay, CNRS/IN2P3, 91405, Orsay; France.
- ⁶⁷Centro Nacional de Microelectrónica (IMB-CNM-CSIC), Barcelona; Spain.
- ⁶⁸Department of Physics, Indiana University, Bloomington IN; United States of America.
- ⁶⁹(^a)INFN Gruppo Collegato di Udine, Sezione di Trieste, Udine;(^b)ICTP, Trieste;(^c)Dipartimento Politecnico di Ingegneria e Architettura, Università di Udine, Udine; Italy.
- ⁷⁰(^a)INFN Sezione di Lecce;(^b)Dipartimento di Matematica e Fisica, Università del Salento, Lecce; Italy.
- ⁷¹(^a)INFN Sezione di Milano;(^b)Dipartimento di Fisica, Università di Milano, Milano; Italy.
- ⁷²(^a)INFN Sezione di Napoli;(^b)Dipartimento di Fisica, Università di Napoli, Napoli; Italy.
- ⁷³(^a)INFN Sezione di Pavia;(^b)Dipartimento di Fisica, Università di Pavia, Pavia; Italy.
- ⁷⁴(^a)INFN Sezione di Pisa;(^b)Dipartimento di Fisica E. Fermi, Università di Pisa, Pisa; Italy.
- ⁷⁵(^a)INFN Sezione di Roma;(^b)Dipartimento di Fisica, Sapienza Università di Roma, Roma; Italy.
- ⁷⁶(^a)INFN Sezione di Roma Tor Vergata;(^b)Dipartimento di Fisica, Università di Roma Tor Vergata, Roma; Italy.
- ⁷⁷(^a)INFN Sezione di Roma Tre;(^b)Dipartimento di Matematica e Fisica, Università Roma Tre, Roma; Italy.
- ⁷⁸(^a)INFN-TIFPA;(^b)Università degli Studi di Trento, Trento; Italy.
- ⁷⁹Universität Innsbruck, Department of Astro and Particle Physics, Innsbruck; Austria.
- ⁸⁰University of Iowa, Iowa City IA; United States of America.

- ⁸¹Department of Physics and Astronomy, Iowa State University, Ames IA; United States of America.
- ⁸²Istinye University, Sariyer, Istanbul; Türkiye.
- ⁸³(^a) Departamento de Engenharia Elétrica, Universidade Federal de Juiz de Fora (UFJF), Juiz de Fora; (^b) Universidade Federal do Rio De Janeiro COPPE/EE/IF, Rio de Janeiro; (^c) Instituto de Física, Universidade de São Paulo, São Paulo; (^d) Rio de Janeiro State University, Rio de Janeiro; (^e) Federal University of Bahia, Bahia; Brazil.
- ⁸⁴KEK, High Energy Accelerator Research Organization, Tsukuba; Japan.
- ⁸⁵Graduate School of Science, Kobe University, Kobe; Japan.
- ⁸⁶(^a) AGH University of Krakow, Faculty of Physics and Applied Computer Science, Krakow; (^b) Marian Smoluchowski Institute of Physics, Jagiellonian University, Krakow; Poland.
- ⁸⁷Institute of Nuclear Physics Polish Academy of Sciences, Krakow; Poland.
- ⁸⁸Faculty of Science, Kyoto University, Kyoto; Japan.
- ⁸⁹Research Center for Advanced Particle Physics and Department of Physics, Kyushu University, Fukuoka ; Japan.
- ⁹⁰L2IT, Université de Toulouse, CNRS/IN2P3, UPS, Toulouse; France.
- ⁹¹Instituto de Física La Plata, Universidad Nacional de La Plata and CONICET, La Plata; Argentina.
- ⁹²Physics Department, Lancaster University, Lancaster; United Kingdom.
- ⁹³Oliver Lodge Laboratory, University of Liverpool, Liverpool; United Kingdom.
- ⁹⁴Department of Experimental Particle Physics, Jožef Stefan Institute and Department of Physics, University of Ljubljana, Ljubljana; Slovenia.
- ⁹⁵School of Physics and Astronomy, Queen Mary University of London, London; United Kingdom.
- ⁹⁶Department of Physics, Royal Holloway University of London, Egham; United Kingdom.
- ⁹⁷Department of Physics and Astronomy, University College London, London; United Kingdom.
- ⁹⁸Louisiana Tech University, Ruston LA; United States of America.
- ⁹⁹Fysiska institutionen, Lunds universitet, Lund; Sweden.
- ¹⁰⁰Departamento de Física Teórica C-15 and CIAFF, Universidad Autónoma de Madrid, Madrid; Spain.
- ¹⁰¹Institut für Physik, Universität Mainz, Mainz; Germany.
- ¹⁰²School of Physics and Astronomy, University of Manchester, Manchester; United Kingdom.
- ¹⁰³CPPM, Aix-Marseille Université, CNRS/IN2P3, Marseille; France.
- ¹⁰⁴Department of Physics, University of Massachusetts, Amherst MA; United States of America.
- ¹⁰⁵Department of Physics, McGill University, Montreal QC; Canada.
- ¹⁰⁶School of Physics, University of Melbourne, Victoria; Australia.
- ¹⁰⁷Department of Physics, University of Michigan, Ann Arbor MI; United States of America.
- ¹⁰⁸Department of Physics and Astronomy, Michigan State University, East Lansing MI; United States of America.
- ¹⁰⁹Group of Particle Physics, University of Montreal, Montreal QC; Canada.
- ¹¹⁰Fakultät für Physik, Ludwig-Maximilians-Universität München, München; Germany.
- ¹¹¹Max-Planck-Institut für Physik (Werner-Heisenberg-Institut), München; Germany.
- ¹¹²Graduate School of Science and Kobayashi-Maskawa Institute, Nagoya University, Nagoya; Japan.
- ¹¹³Department of Physics and Astronomy, University of New Mexico, Albuquerque NM; United States of America.
- ¹¹⁴Institute for Mathematics, Astrophysics and Particle Physics, Radboud University/Nikhef, Nijmegen; Netherlands.
- ¹¹⁵Nikhef National Institute for Subatomic Physics and University of Amsterdam, Amsterdam; Netherlands.
- ¹¹⁶Department of Physics, Northern Illinois University, DeKalb IL; United States of America.
- ¹¹⁷(^a) New York University Abu Dhabi, Abu Dhabi; (^b) United Arab Emirates University, Al Ain; United

Arab Emirates.

¹¹⁸Department of Physics, New York University, New York NY; United States of America.

¹¹⁹Ochanomizu University, Otsuka, Bunkyo-ku, Tokyo; Japan.

¹²⁰Ohio State University, Columbus OH; United States of America.

¹²¹Homer L. Dodge Department of Physics and Astronomy, University of Oklahoma, Norman OK; United States of America.

¹²²Department of Physics, Oklahoma State University, Stillwater OK; United States of America.

¹²³Palacký University, Joint Laboratory of Optics, Olomouc; Czech Republic.

¹²⁴Institute for Fundamental Science, University of Oregon, Eugene, OR; United States of America.

¹²⁵Graduate School of Science, Osaka University, Osaka; Japan.

¹²⁶Department of Physics, University of Oslo, Oslo; Norway.

¹²⁷Department of Physics, Oxford University, Oxford; United Kingdom.

¹²⁸LPNHE, Sorbonne Université, Université Paris Cité, CNRS/IN2P3, Paris; France.

¹²⁹Department of Physics, University of Pennsylvania, Philadelphia PA; United States of America.

¹³⁰Department of Physics and Astronomy, University of Pittsburgh, Pittsburgh PA; United States of America.

¹³¹(^a)Laboratório de Instrumentação e Física Experimental de Partículas - LIP, Lisboa; (^b)Departamento de Física, Faculdade de Ciências, Universidade de Lisboa, Lisboa; (^c)Departamento de Física, Universidade de Coimbra, Coimbra; (^d)Centro de Física Nuclear da Universidade de Lisboa, Lisboa; (^e)Departamento de Física, Universidade do Minho, Braga; (^f)Departamento de Física Teórica y del Cosmos, Universidad de Granada, Granada (Spain); (^g)Departamento de Física, Instituto Superior Técnico, Universidade de Lisboa, Lisboa; Portugal.

¹³²Institute of Physics of the Czech Academy of Sciences, Prague; Czech Republic.

¹³³Czech Technical University in Prague, Prague; Czech Republic.

¹³⁴Charles University, Faculty of Mathematics and Physics, Prague; Czech Republic.

¹³⁵Particle Physics Department, Rutherford Appleton Laboratory, Didcot; United Kingdom.

¹³⁶IRFU, CEA, Université Paris-Saclay, Gif-sur-Yvette; France.

¹³⁷Santa Cruz Institute for Particle Physics, University of California Santa Cruz, Santa Cruz CA; United States of America.

¹³⁸(^a)Departamento de Física, Pontificia Universidad Católica de Chile, Santiago; (^b)Millennium Institute for Subatomic physics at high energy frontier (SAPHIR), Santiago; (^c)Instituto de Investigación Multidisciplinario en Ciencia y Tecnología, y Departamento de Física, Universidad de La Serena; (^d)Universidad Andres Bello, Department of Physics, Santiago; (^e)Instituto de Alta Investigación, Universidad de Tarapacá, Arica; (^f)Departamento de Física, Universidad Técnica Federico Santa María, Valparaíso; Chile.

¹³⁹Department of Physics, University of Washington, Seattle WA; United States of America.

¹⁴⁰Department of Physics and Astronomy, University of Sheffield, Sheffield; United Kingdom.

¹⁴¹Department of Physics, Shinshu University, Nagano; Japan.

¹⁴²Department Physik, Universität Siegen, Siegen; Germany.

¹⁴³Department of Physics, Simon Fraser University, Burnaby BC; Canada.

¹⁴⁴SLAC National Accelerator Laboratory, Stanford CA; United States of America.

¹⁴⁵Department of Physics, Royal Institute of Technology, Stockholm; Sweden.

¹⁴⁶Departments of Physics and Astronomy, Stony Brook University, Stony Brook NY; United States of America.

¹⁴⁷Department of Physics and Astronomy, University of Sussex, Brighton; United Kingdom.

¹⁴⁸School of Physics, University of Sydney, Sydney; Australia.

¹⁴⁹Institute of Physics, Academia Sinica, Taipei; Taiwan.

- ¹⁵⁰(*a*) E. Andronikashvili Institute of Physics, Iv. Javakhishvili Tbilisi State University, Tbilisi; (*b*) High Energy Physics Institute, Tbilisi State University, Tbilisi; (*c*) University of Georgia, Tbilisi; Georgia.
- ¹⁵¹ Department of Physics, Technion, Israel Institute of Technology, Haifa; Israel.
- ¹⁵² Raymond and Beverly Sackler School of Physics and Astronomy, Tel Aviv University, Tel Aviv; Israel.
- ¹⁵³ Department of Physics, Aristotle University of Thessaloniki, Thessaloniki; Greece.
- ¹⁵⁴ International Center for Elementary Particle Physics and Department of Physics, University of Tokyo, Tokyo; Japan.
- ¹⁵⁵ Department of Physics, Tokyo Institute of Technology, Tokyo; Japan.
- ¹⁵⁶ Department of Physics, University of Toronto, Toronto ON; Canada.
- ¹⁵⁷(*a*) TRIUMF, Vancouver BC; (*b*) Department of Physics and Astronomy, York University, Toronto ON; Canada.
- ¹⁵⁸ Division of Physics and Tomonaga Center for the History of the Universe, Faculty of Pure and Applied Sciences, University of Tsukuba, Tsukuba; Japan.
- ¹⁵⁹ Department of Physics and Astronomy, Tufts University, Medford MA; United States of America.
- ¹⁶⁰ Department of Physics and Astronomy, University of California Irvine, Irvine CA; United States of America.
- ¹⁶¹ University of Sharjah, Sharjah; United Arab Emirates.
- ¹⁶² Department of Physics and Astronomy, University of Uppsala, Uppsala; Sweden.
- ¹⁶³ Department of Physics, University of Illinois, Urbana IL; United States of America.
- ¹⁶⁴ Instituto de Física Corpuscular (IFIC), Centro Mixto Universidad de Valencia - CSIC, Valencia; Spain.
- ¹⁶⁵ Department of Physics, University of British Columbia, Vancouver BC; Canada.
- ¹⁶⁶ Department of Physics and Astronomy, University of Victoria, Victoria BC; Canada.
- ¹⁶⁷ Fakultät für Physik und Astronomie, Julius-Maximilians-Universität Würzburg, Würzburg; Germany.
- ¹⁶⁸ Department of Physics, University of Warwick, Coventry; United Kingdom.
- ¹⁶⁹ Waseda University, Tokyo; Japan.
- ¹⁷⁰ Department of Particle Physics and Astrophysics, Weizmann Institute of Science, Rehovot; Israel.
- ¹⁷¹ Department of Physics, University of Wisconsin, Madison WI; United States of America.
- ¹⁷² Fakultät für Mathematik und Naturwissenschaften, Fachgruppe Physik, Bergische Universität Wuppertal, Wuppertal; Germany.
- ¹⁷³ Department of Physics, Yale University, New Haven CT; United States of America.
- a* Also Affiliated with an institute covered by a cooperation agreement with CERN.
- b* Also at An-Najah National University, Nablus; Palestine.
- c* Also at Borough of Manhattan Community College, City University of New York, New York NY; United States of America.
- d* Also at Center for High Energy Physics, Peking University; China.
- e* Also at Center for Interdisciplinary Research and Innovation (CIRI-AUTH), Thessaloniki; Greece.
- f* Also at Centro Studi e Ricerche Enrico Fermi; Italy.
- g* Also at CERN, Geneva; Switzerland.
- h* Also at Département de Physique Nucléaire et Corpusculaire, Université de Genève, Genève; Switzerland.
- i* Also at Departament de Física de la Universitat Autònoma de Barcelona, Barcelona; Spain.
- j* Also at Department of Financial and Management Engineering, University of the Aegean, Chios; Greece.
- k* Also at Department of Physics, California State University, Sacramento; United States of America.
- l* Also at Department of Physics, King's College London, London; United Kingdom.
- m* Also at Department of Physics, Stanford University, Stanford CA; United States of America.
- n* Also at Department of Physics, Stellenbosch University; South Africa.
- o* Also at Department of Physics, University of Fribourg, Fribourg; Switzerland.

- p* Also at Department of Physics, University of Thessaly; Greece.
- q* Also at Department of Physics, Westmont College, Santa Barbara; United States of America.
- r* Also at Hellenic Open University, Patras; Greece.
- s* Also at Institutio Catalana de Recerca i Estudis Avancats, ICREA, Barcelona; Spain.
- t* Also at Institut für Experimentalphysik, Universität Hamburg, Hamburg; Germany.
- u* Also at Institute for Nuclear Research and Nuclear Energy (INRNE) of the Bulgarian Academy of Sciences, Sofia; Bulgaria.
- v* Also at Institute of Applied Physics, Mohammed VI Polytechnic University, Ben Guerir; Morocco.
- w* Also at Institute of Particle Physics (IPP); Canada.
- x* Also at Institute of Physics and Technology, Mongolian Academy of Sciences, Ulaanbaatar; Mongolia.
- y* Also at Institute of Physics, Azerbaijan Academy of Sciences, Baku; Azerbaijan.
- z* Also at Institute of Theoretical Physics, Ilia State University, Tbilisi; Georgia.
- aa* Also at Lawrence Livermore National Laboratory, Livermore; United States of America.
- ab* Also at National Institute of Physics, University of the Philippines Diliman (Philippines); Philippines.
- ac* Also at Technical University of Munich, Munich; Germany.
- ad* Also at The Collaborative Innovation Center of Quantum Matter (CICQM), Beijing; China.
- ae* Also at TRIUMF, Vancouver BC; Canada.
- af* Also at Università di Napoli Parthenope, Napoli; Italy.
- ag* Also at University of Colorado Boulder, Department of Physics, Colorado; United States of America.
- ah* Also at Washington College, Chestertown, MD; United States of America.
- ai* Also at Yeditepe University, Physics Department, Istanbul; Türkiye.
- * Deceased